Western&Graduate&PostdoctoralStudies

Electronic Thesis and Dissertation Repository

2-21-2020 10:00 AM

Mitogen Inducible Gene-6 in Joint Health and Osteoarthritis

Melina Rodrigues Bellini, *The University of Western Ontario*

Supervisor: Beier, Frank., *The University of Western Ontario*
A thesis submitted in partial fulfillment of the requirements for the Doctor of Philosophy degree in Physiology and Pharmacology
© Melina Rodrigues Bellini 2020

Follow this and additional works at: https://ir.lib.uwo.ca/etd

Recommended Citation

Abstract

Osteoarthritis (OA) is the most common type of arthritis or degenerative disease and leads to chronic and functional disability affecting a patient's quality of life. The etiology of OA is a heterogeneous multifactorial disease, with inflammatory, metabolic, and mechanical causes. Therefore, OA commonly affects a heterogeneous population, ranging widely from the middle-aged and elderly populations, although younger people may be affected as a result of injury or overuse. Moreover, OA is characterized by loss of articular cartilage, changes in subchondral bone, synovium and supporting structures that ultimately affect all the tissues necessary for joint function. Despite an increasing awareness of OA as a medical problem, there is a surprising absence of effective medical treatments beyond pain control and surgery. The progressive understanding of the pathophysiology of OA leads to the perception that the disease is not purely mechanical or aging, and clarification of the signalling pathways and molecular mechanisms is necessary to the clinical application.

Our lab has demonstrated the importance of Epidermal Growth Factor Receptor/Mitogen Inducible Gene 6 (EGFR/Mig-6) for joint development. I hypothesized that Mig-6 regulates cartilage homeostasis. We first started investigating the role of Mig-6 in cartilage using cartilage-specific (Col2) overexpression of Mig-6 in a mouse model. Using histopathological assessment, histological and imaging techniques, we concluded that these animals showed significantly greater cartilage breakdown with aging, while younger *Mig-6$^{over/over}$* mice resulted in healthy articular cartilage. Moreover, μCT analysis showed small but significant reductions in the size of long bones of *Mig-6$^{over/over}$* mice compared to control group (wild type).

To further analyze the *in vivo* animal model, we subsequently assessed Mig-6 in cartilage using skeleton (Prx1)-specific overexpression. I again evaluated the morphology of articular cartilage using histological techniques and long bones of these mice and concluded similar results from the previous study, I found that mice overexpressing Mig-6 displayed significantly cartilage damage.

Subsequently, we compared the disease progression between mice with cartilage-specific (Col2) overexpression of Mig-6 and controls after destabilization of medial meniscus surgery (DMM) to induce post-traumatic osteoarthritis (PTOA). *Mig-6$^{over/over}$* mice exhibited behavioural changes

(vertical activity count) and appeared to show accelerated cartilage breakdown in surgically induced OA. Collectively, these data demonstrate that Mig-6 plays an important mediating role in articular cartilage homeostasis and development of osteoarthritis. Overexpression of this protein compromises the joint's homeostatic mechanisms, predisposing them to accelerated degeneration.

Keywords

Summary for Lay Audience

Osteoarthritis (OA) is a slowly progressive degenerative joint disease characterized by loss of articular cartilage. Our current understanding of the pathophysiology of OA suggests that the disease is not purely caused by mechanical factors or aging, and clarification of the biochemical and inflammatory pathways involved is necessary to develop new therapies. The economic and social impact of OA due to direct medical costs, loss of work time and quality of life are considerable.

Currently, there are no treatment options available to slow, stop or reverse the course of OA, and the etiology of the disease is poorly understood. Thus, additional work to reveal the underlying pathobiology is required if treatment options are to be developed. Therefore, our laboratory has focused on elucidating the molecular mechanism relevant to OA using animal models, cell and organ culture, and biochemical techniques.

We have identified that the epidermal growth factor receptor (EGFR) signaling pathway is involved in regulating the health of cartilage and other joint structures. In particular, we are interested in a gene called mitogen-inducible gene 6 (Mig-6) that regulates EGFR signaling, and loss of this protein has been shown to lead to severe joint dysfunction in mice. Using genetically modified mice lacking Mig-6 in critical joint tissues our laboratory showed that deletion of Mig-6 resulted in thicker articular cartilage with extra, abnormal cartilage surrounding the knee. My project focuses on whether overexpression of Mig-6 is enough to cause OA.

Indeed, my work shows that higher levels of Mig-6 in cartilage and other joint tissues leads to faster and more severe OA both during aging and after injury. Altogether, these studies may indicate Mig-6 and EGFR as potential therapeutic targets in the treatment of osteoarthritis and similar diseases.

Epigraph

*"**Gratitude** makes sense of our past, brings peace for today, and creates a vision for tomorrow."*

— Melody Beattie

Co-Authorship Statement

Chapter 2 is adapted from: Bellini M. Pest, MA, Miranda-Rodrigues, M, Qin, Ling, Jeong JW, Beier F. Overexpression of Mig-6 in cartilage induces an osteoarthritis-like phenotype in mice. *BioRxiv https://doi.org/10.1101/764142*. MB performed most experiments and contributed to study design and manuscript writing. MAP contributed with OARSI scoring and contributed to study design. MRM performed real-time quantitative polymerase chain reaction. JWJ provided *Mig-6$^{over/over}$* transgenic mice essential for this study. FB contributed to study conception and design, and edited the manuscript. All authors read and approved the submitted version of the manuscript.

Chapter 3 is adapted from: Bellini M. Pest, MA, Jeong JW, Beier F. Overexpression of Mig-6 in Limb Mesenchyme Leads to Accelerated Osteoarthritis in Mice. *BioRxiv https://doi.org/10.1101/871350.* MB performed the experiments and contributed to study design and manuscript writing. MAP contributed to OARSI scoring and study design. JWJ provided *Mig-6$^{over/over}$* transgenic mice essential for this study. FB contributed to study conception and design, and edited the manuscript. All authors read and approved the submitted version of the manuscript.

Chapter 4 MB performed the experiments, sectioning, scoring and contributed to study design and manuscript writing. MAP contributed to OARSI scoring and study design. SB performed surgeries. JWJ provided *Mig-6$^{over/over}$* transgenic mice essential for this study. FB contributed to study conception and design, and edited the chapter. These data have not yet been published but will be submitted in for publication in 2020.

Acknowledgments

of people surrounding you. In these past years you have helped me to become a more creative, open-minded, and resilient person, I thank-you for listening to me and having such a great impact on my life, as well as other peoples' lives, and also being an extraordinary person who goes the extra mile for those around him. This is the best quote that express how grateful I am: "*If I have seen further than others, it is by standing upon the shoulders of giants*" (Isaac Newton).

I would like to express my gratitude to the Science without Borders scholarship committee, as well as the CIHR, without whom, quite simply, our research would not have been possible. If you had not supported me and my pursuit for knowledge, I would not be addressing you today.In addition, I would like to thank my committee members, *Drs. Cheryle Séguin, Dean Betts, and Marco Prado* for your academic insight, scientific guidance, and boundless encouragement. I truly appreciate all of you, and hope you acknowledge your role as being an instrumental part of my graduate career and scientific advances.

During my time at Western I have had opportunity to encounter a number of brilliant scientists. These include, but are definitely not limited to, *Dr. Jeff Dixon*, for whom I would like to thank his positive thinking and kindness; I will never forget how much I enjoyed your last class in Physiology 4530B. *Drs. Wataru Inoue, Rithwik Ramachandran, and Trevor Birmingham* for being part of my Ph.D. Comprehensive Exam; your patience and knowledge are truly appreciated. Additionally, I would like to say how much I appreciated working at the "Lower Ground" (LG) floor, because all the supervisors-particularly those who are members of Musculoskeletal Health Research-kept their office doors open and greatly nourished my academic journey. Again: thank you!

Thank you for my present and past members of the *Beier Lab* who have made my lab journey more enjoyable and special! I would like to thank the following people: Dawn and Holly, I still remember when Frank first introduced me to you: Dawn had a big smile and Holly had a great (unique) look at me, I'm enormous thankful for ALL your help at the lab! *Holly* (Jolly), you have the best humour ever, such as a clever person and you have admirable qualities: adventurous and loyalty and I love having a chance to work with you as well as our chance to go for conference together! I appreciate your "lab manager skills" in our lab, thank you for all your contributions over these years. You are very special to me because I admire you. By the way, I will miss the

"birthday cakes" stories. *Dawn*, if you had a website, I would be the one following your posts and (likely) sharing most of them.Actually if I had a superpower, I would put more "Dawn's" personality in this world. Thank you for your all the time that you answer my question in the most generous way ever! I'll always remember you with a smile on my face, I really mean that. Obrigada (thank you).

Mikeee! I know you are a very hard-worker person and you are very precise and have valuable scientific questions and thank you for being my second-mentor! Thank you for putting so much efforts and for having "PEST" as your last name and it is part of "Gene 33/Mig-6", you also "own" this project. I'll always recognize you as an intelligent person who can see further and find solutions whenever life takes you!

Anusha, thank you for company at the lab, you are one of the smartest people that I've ever met. I can see you will have a great future, you will always shine and I'll be here to applaud you; thank you for your friendship. I have collected great memories and tasted good food, even those that included (surprisingly) bacon with you. *Margaret*, I do not have enough words to describe how much you've helped me. You are such a wonderful person, with a BIG heart, you deserve this world! Thank you for explaining different experiments to me and for being at the lab on Sunday evenings. We have absolutely great memories, and our friendship means a lot to me. I feel blessed for meeting you and I'm sure your future patients will feel the same! *Kristyn*, thank you for being such a great friend, I'll never forget that you were the first person that Frank introduced to me and I love having coffee/tea with you over a great conversation. *Katie*, you were one of the people from the lab who shared solutions with me, actually I think in the first week, you shared some important documents that helped me to understand more about our Grad program at Western. Too bad our time overlapping at the lab was too short, but I know how smart and special you are! *Paxton*, thank you for always being willing to answer my questions and for your time! I hope life brings you a lot of good experiences, also a lot of patients because I believe that they will be in good hands, so enjoy your journey!

Supinder (Supi), since 2016 when we first met I could see that you are a very strong person who is always seeking your bliss, dreams and achievement-focuses – I really like that. Thank you for all the insights and ideas, I very much appreciated it. Also thank you for your contributions to the

third section in this thesis and for all your knowledge in our lab, with all my heart I wish you success in life, as you have demonstrated over all these years, go girl! *Ayten*, you are one of the sweetest people that I've met in Canada, you are very determined and kind person. Thank you for being "always there" for me, I wish you all the wisdom and strength in life, you will always rock it, sis! *Carina* (Cariniiiii), I truly appreciate your hard work and the early-bird person you are! Thank you for all your patience with me and our amazing conversations that I'll never forget. Plus all the great memories from this strong German girl and her "leidenschaft" for science and discovery. I respect the commitment you have for your work, keeping following your passion, girl! *Manuela* (Manu), first of all, thank you for sticking with me through "the good, the bad, and the ugly." Secondly, you don't need me to write words down to explain how much you mean to me. I embrace our friendship and I hope (and wish) your desires, dreams and goals come true and your universe will open doors for you 'wherever you will go'; you have a superpower! I will love and cherish all the amazing memories we've had together, and look forward to many more years learning with you. *Obrigada* Manu!

Ermina, thank you very much for all your help at our lab plus sharing lab bench with me! I will not forget our wonderful/intense conversations about PCR tubes – I would like to keep my word that I do not mind sharing them with you. I hope you keep enjoying doing the science and get a lot of good results, I really wish you an amazing future, because you deserve it a lot. *Bethia*, I'm really proud of you! You will get your master's degree so soon and I'm sure you will continue to achieve all your wishes in your life; you are persistent and very strong! You've got it girl and I'm also happy for meeting you, we have collected great memories with popcorn at 11:30pm at the lab (wow!). *Julia*, thank you so much for your friendship and for "always being there", you are my coffee buddy! I'm so glad our paths have crossed, for it was a pleasure meeting you. I encourage you to follow your bliss because you will no doubt have a bright future! *Amanda*, you are one of the most distinguished and notable people that I know, thank you for always listening to me and for taking me to Toronto to get create memories with you! I'll be with you whenever you go there in the future.

I would also like to thank members of *Appleton's Lab*: *Garth Blackler, Gaelle Wambiekele Kiyeko, Yue Lai-Zhao, Holly Philpott* and *Dr. Tom Appleton*: you guys are talented and work great together as a team. I appreciate all your effort, contributing to "synovial translational biology lab in OA".

Table of Contents

List of Figures

Appendices

List of Abbreviations

ACL   Anterior cruciate ligament

ADAM   A disintegrin and metalloproteinase

ADAMTS   A disintegrin and metalloproteinase with thrombospondin motifs

Agc1   Aggrecan gene

Alp   Alkaline phosphatase gene

AR   Amphiregulin

BTC   Betacellulin

BMP   Bone morphogenetic protein

BMU   Basic multicellular unit

CCAC   Canadian Council on Animal Care

CD   Campomelic dysplasia

cDNA   Complimentary DNA

DAB   Diaminobenzidine

ΔΔCT   Delta-delta cycle threshold

DIPEN   Matrix metalloproteinase mediated aggrecan cleavage neoepitope

E15.5   Embryonic day 15.5

ECM   Extracellular matrix

GAG   Glycosaminoglycan

Gapdh   Glyceraldehyde-3-phosphate gene

Gdf5	Growth differentiation factor-5 gene
ECM	Extracellular matrix
EDTA	Ethylene diaminetetraacetic acid
EGF	Epidermal growth factor
EGFR	Epidermal growth factor receptor
EO	Endochondral ossification
EPGN	Epigen
EREG	Epiregulin
ERK	Extracellular signal-regulated kinase
ERRFI1	ERBB receptor feedback inhibitor 1
Errfi1	Mig-6 gene
FGF	Fibroblast growth factor
FGFR	Fibroblast growth factor receptor
GAG	Glycosaminoglycan
GDF5	Growth/differentiation factor 5
Gdf5	Growth/differentiation factor 5 gene
GWAS	Genome wide association study
HB-EGF	Heparin-binding epidermal growth factor-like growth factor
HS	Heparan sulphate
HSPG	Heparan sulphate proteoglycans

IHH	Indian hedgehog
IL-1β	Interleukin 1 beta
IGF-1	Insulin like growth factor 1
IGF-1R	Insulin like growth factor 1 receptor
IO	Intramembranous ossification
JAK-STAT	Janus kinase- signal transducer and activator of transcription
KO	Knockout
LFC	Lateral femoral condyle
LPS	Lipopolysaccharides
LTP	Lateral tibial plateau
MAPK	Mitogen activated protein kinase
M-CSF	Macrophage colony stimulating factor
MEK	Mitogen-activated protein kinase
MFC	Medial femoral condyle
MIA	Monoiodoacetate
microCT	Micro computed tomography
Mig-6	Mitogen-inducible gene 6
Mig-6	Mig-6 gene (*Errfi1* encodes Mig-6, *Mig-6* notation used for simplicity)
MKP1	MAP (mitogen activated protein) kinase phosphatase 1
MMP	Matrix metalloproteinase

Mmp13	Matrix metalloproteinase 13 gene
MRI	Magnetic resonance imaging
MTP	Medial tibial plateau
OA	Osteoarthritis
OPG	Osteoprotegerin
OARSI	Osteoarthritis Research Society International
PBS	Phosphate buffered saline
PCK	Posterior cruciate ligament
PI3K	Phosphatidylinositol-3-kinase
PKC	Protein kinase C
Prg4	Lubricin gene
Ptgs2	COX2 gene
Ptpn11	SHP2 gene
PTHrP	Parathyroid hormone-related protein
PTOA	Post-traumatic Osteoarthritis
RAGE	Advanced glycation end product receptor
RANK	Receptor activator of nuclear factor kappa B
RANKL	Receptor activator of nuclear factor kappa B ligand
RFP	Red fluorescent protein
RUNX2	Runt-related transcription factor 2

Runx2	Runt-related transcription factor 2 gene
SHP2	Src-homology 2 domain-containing phosphatase
SOX5	SRY (sex determining region Y)-box 5
SOX6	SRY (sex determining region Y)-box 6
SOX9	SRY (sex determining region Y)-box 9
Sox9	SRY (sex determining region Y)-box 9 gene
TEGE	aggrecanase mediated aggrecan cleavage neoepitope
TGFα	Transforming growth factor alpha
Tgfa	Transforming growth factor alpha gene
TGFβ	Transforming growth factor beta
TIMP	Tissue inhibitor of metalloproteinases
TNFα	Tumor necrosis factor alpha
VEGF	Vascular endothelial growth factor
WT	Wild type

Chapter 1

1 Literature Review

1.1 The Development of the Skeleton

The skeletal system consists of approximately 206 bones in the adult human, including long bones (ex. femur), short bones (ex. carpal bone of the wrist), flat bones (ex. skull) and irregular bones (ex. vertebrae) (1). Bones are responsible for different functions such as: providing support for muscle, ligament and tendons, permitting them to attach and allowing for free movement; protection of soft tissues such as brain, spinal cord, heart and lungs from insult and absorbing shock related to locomotion; and harboring of hematopoietic red bone marrow within the skeleton (2). Moreover, as an endocrine organ, bone plays a role in energy metabolism and mineral ion homeostasis due its function as reservoir for calcium and phosphate storage. Importantly, bones contain two types of skeletal tissue: cortical and trabecular bone. Roughly 80% of the bone is composed of the cortical compartment which can be found on the outermost surface at the diaphysis and metaphysis of long bones, as well as the outer surface of the irregular, short and flat bones. Cortical bone presents hard and dense tissue and is responsible for the strength of the skeleton. Trabecular bone comprises 20% of the bone mass, exhibits a spongy appearance and is situated at the end of long bones and in the inner vertebral space (3). Different cell lineages contribute to the skeleton during development (4). The onset of skeletogenesis begins with condensation of mesenchymal cells that either differentiate into osteoblasts to generate bone or differentiate into chondrocytes to form cartilage templates (anlagen) of future bones (5). Mature bone is highly mineralized, with a composition of 70% calcium phosphate crystals (mostly hydroxyapatite [$Ca_{10}(PO_4)_6(OH)_2$]), 25% of collagenous proteins, cells and other macromolecules, and 5% of water (6). During embryogenesis, bone tissue is formed via intramembranous bone formation or endochondral ossification. Intramembranous ossification occurs directly from precursor cells, when these cells differentiate into osteoblasts that synthesize bone without the cartilage phase. This process forms parts of the craniofacial skeleton and clavicle (7). In endochondral ossification, precursor cells differentiate into chondrocytes and produce cartilage matrix, before replacement of cartilage by bone tissue. This process guides the formation of the

appendicular and axial skeleton (8,9). Recent studies have shown that proper skeletal development relies on a variety of cells types and multiple signalling pathways influence bone homeostasis (10–12). Bone is a highly organized and dynamic connective tissue which is constantly remodelled throughout life by two processes: bone formation and bone resorption (13). Some bones such as the flat bones of the skull, shoulder, scapula, pelvis and sesamoid bones are formed by intramembranous ossification (IO). Mesenchymal cells differentiate into osteoblasts in a process involving transcription factors such as runt-related transcription factor 2 (RUNX2), Osterix (Osx) and ATF4 that are essential for osteoblast differentiation and maturation (10). The osteoblasts produce and secrete collagen type I and proteoglycans to synthesize an osteoid matrix, which is then calcified to form bone. Ultimately, the osteoblasts differentiate into osteocytes and become embedded within the formed bone matrix (14). Many different growth factors play a role in intramembranous ossifications, most notably members of the bone morphogenetic protein family (such as BMP2, BMP4, and BMP7).

1.1.1   Endochondral Ossification

The majority of our mammalian skeleton consists of bones originating from a cartilage template intermediate that is then replaced by bone (7,15). Endochondral ossification is initiated during embryogenesis, and continues until the end of puberty. During this process, condensation of embryonic mesenchymal stem cells forms the primary template of bone. After condensation, progenitor cells differentiate to immature chondrocytes that express the transcription factor SRY (sex determining region Y)-box 9 (SOX9), which is essential for chondrogenesis (16,17). Sox9 has been extensively studied and works with two other members of the Sox family, Sox5 and Sox6, to constitute the "Sox Trio"(16,18). The Sox Trio activates the expression of aggrecan (*Agc1*) and collagen II (*Col2a1*) genes and thereby controls the synthesis of cartilage extracellular matrix (ECM) rich in aggrecan and collagen II (19,20). Following mesenchymal condensation and chondrocyte differentiation, the cells located at the periphery of the cartilage anlagen starts to flatten and elongate to form the perichondrium (21,22). Ultimately, the chondrocytes in the center region of the cartilage exit the cell cycle and terminally differentiate into hypertrophic chondrocytes (23,24). This event occurs around embryonic day 14.5 in mice (e.g., in the tibia). These hypertrophic cells increase their volume and express type X collagen and the transcription factor Runx2. Terminal hypertrophic chondrocytes also express molecular markers such as

metalloproteinase 13 (MMP13), vascular endothelial growth factor (VEGF) and secreted phosphoprotein 1 (osteopoitin) (25–27). Some of the cells in the perichondrium start to express osteoblastic genes such as *type I collagen (Col1), alkaline phosphatase (Alp), Runx2,* among others, and ECM secreted by these preosteoblast cells initiates ossification adjacent to the hypertrophic chondrocytes to form a collar of compact bone around the diaphysis of the cartilage (28,29). In addition, MMP9 is produced by osteoclasts which are activated by RANKL (receptor activator of NF-kB ligand) produced by hypertrophic chondrocytes (30,31).

During the transition from hypertrophic cartilage to bone, a sequence of events occurs including mineralization of the cartilage matrix, hypertrophic chondrocyte apoptosis and/or transdifferentiation to osteoblasts, and the invasion of blood vessels that bring osteoblast, hematopoietic cells and osteoclasts. Collectively, these processes remove the mineralized cartilage matrix and replace it with bone tissue (32). This results in the formation of primary ossification center (POC) of endochondral bone. Eventually, the production and maturation of chondrocytes is restricted to the end of the cartilage (epiphyses) at the growth plate, which is responsible for longitudinal bone growth in the body (33). At approximately postnatal day 5-7, the secondary ossification centers appear within the epiphysis in mice, separating the growth plate from the distal ends of the long bones (34).

1.1.2   Epiphyseal growth plate development

The growth plate forms during fetal developmental and the closure of the epiphyseal growth plate occurs in late puberty in humans, under the influence of of estrogen in both sexes (35–37). The elongation of the long bone is the main function of the growth plate (38). The growth plate is a thin layer composed of highly organized chondrocytes and can be divided into four distinct zones: proliferative, resting (reserve), hypertrophic and prehypertrophic chondrocytes is also shown in **figure 1.1**.

Figure 1.1 Schematic representation of the growth plate. The endochondral growth plate is composed of distinct cell zones of resting, proliferative, pre-hypertrophic and hypertrophic cells. A series of cellular differentiation stages occurs from resting cells to hypertrophy, resulting in longitudinal bone growth, largely because of the proliferation and enlargement of chondrocytes.
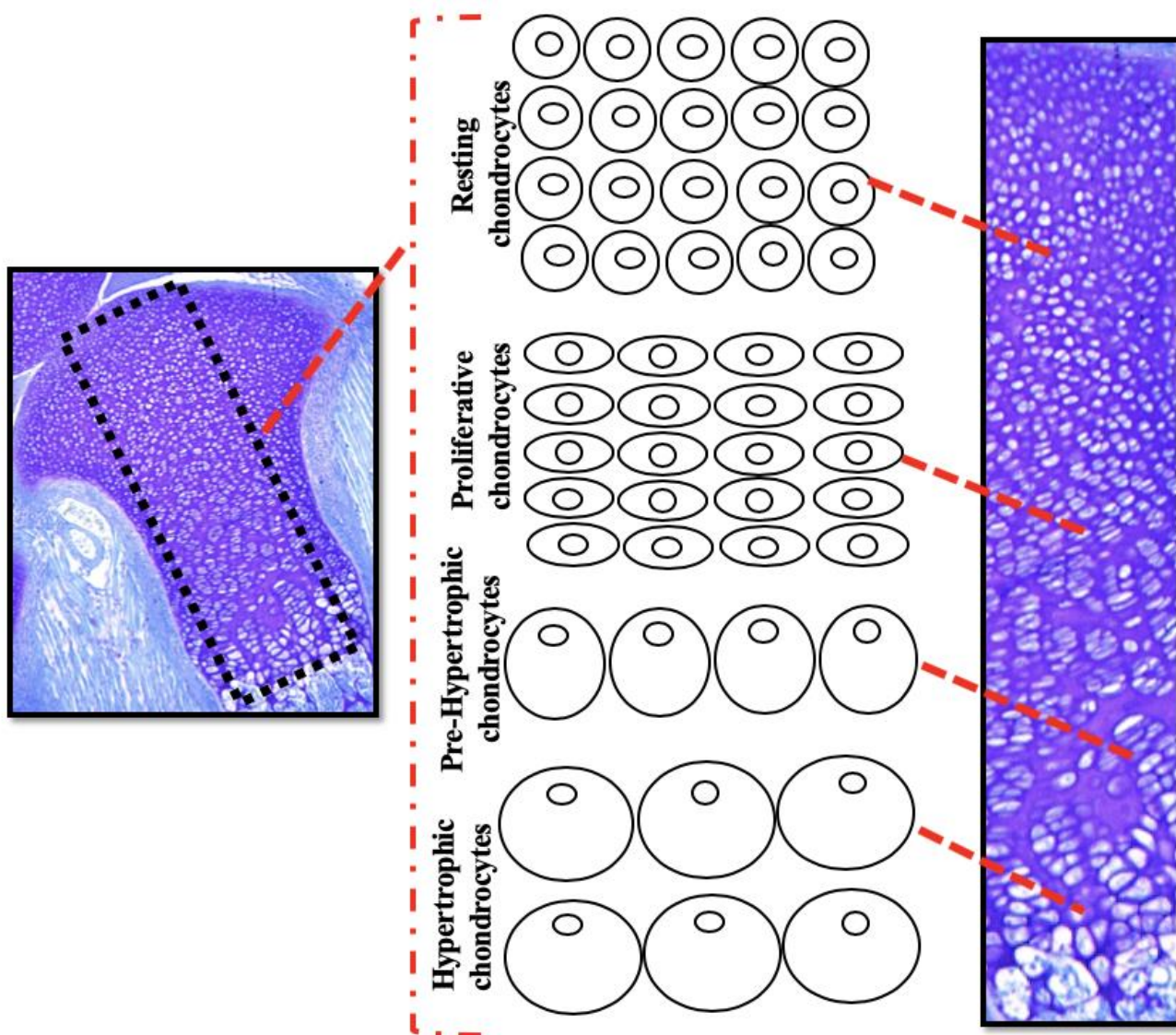
Figure 1.1 The Growth Plate

The resting or reserve zone contains small and round cells, with high volume of extracellular matrix but low metabolic activity (39,40). Moreover, a recent study has shown that the resting zone includes stem-like cells that will generate proliferative chondrocytes; deletion of resting chondrocytes leads to growth plate senescence (41,42). The proliferative zone is composed of columnar chondrocytes which undergo rapid cellular division in direction towards the diaphysis which leads to longitudinal bone growth. These cells express *Col2a1* and *Aggrecan* genes to synthesize the cartilage-specific matrix (43). When chondrocytes exit from the cell cycle, they start to increase their cell volume and enter first the prehypertrophic zone, and then the hypertrophic zone. Hypertrophic chondrocytes express collagen, type X (*Col10a1*) (44). Late hypertrophic chondrocytes initiate expression of MMP13, VEGF, and alkaline phosphatase (45). Growth plate chondrocyte proliferation and maturation is regulated by systemic and local factors that include different hormones, growth factors, and multiple signaling pathways. For example, growth hormone (GH) induces the production of insulin-like growth factor I (IGF-1) which promotes chondrocyte proliferation and initiates chondrocyte hypertrophy (46). IGF-1 signaling also interacts with the Indian hedgehog (Ihh), parathyroid hormone related peptide (PTHrP), and Wnt/β-catenin pathways that are crucial during skeletal development (47–49). In addition, some studies have shown that thyroid hormone is essential for skeletal growth and that hypothyroidism leads to bone growth retardation, delayed bone age, and short stature (50,51). Taken together, a number of transcription factors and signaling pathways mediate the epiphyseal growth plate through the fascinating interaction between cell types which can help to elucidated human skeletal dysplasia's involvement in this process.

1.1.3   Secondary Ossification Center

During early postnatal development the secondary ossification center (SOC) is formed and separates the growth plate from the articular cartilage (52,53). Differently from the POC, SOC formation is not preceded by the formation of hypertrophy and mineralization of cartilage or of a bony collar (54,55). The first event in secondary ossification is the vascular invasion of uncalcified hyaline cartilage of the epiphysis (perichondrium), enabling the infiltration of osteoclast and osteoblast cells (56,57). Studies have identified high expression levels of MMPs around forming blood vessels and at the borders of the marrow cavity, allowing for remodeling of the extracellular

matrix, which is necessary for ossification of the epiphysis (58). Accordingly, it has been also reported that VEGF is required for neovascularization of hypertrophic cartilage to enhance the vascular ingrowth of growth plate in this region (55). Interestingly, the last phase of the endochondral ossification is the mineralization process. Following the calcification of the extracellular matrix by hypertrophic chondrocytes and vascular invasion, osteoclasts break down cartilage (28). At the same time, osteoprogenitor cells are recruited and differentiate into osteoblasts that secrete osteoid, which forms the bone trabecula within the growth plate resulting in mature secondary ossification centers (59,60). Many signaling pathways interact with each other to regulate this process, such as WNT/ β-catenin signaling (61,62) and epidermal growth factor (EGFR) to fine tune bone development (63).

1.1.4   Synovial Joint Development

Joints are structures where adjacent bones are held together by connective tissue. Synarthroses (*syn*= together + *arthrosis* = articulation) can be divided into: 1) fibrous joints, in which skull bones from children and young adults are connected by layers of connective tissue; for example, sutures; 2) cartilaginous joints are found between bones that articulate against each other with a pad of fibrocartilage; for example, the intervertebral discs of the spinal column; 3) synovial joints, where the adjacent bones are in contact with each other within a sealed joint cavity that contains synovial fluid; for example, joints of knees, elbows or ankles (64,65). Synovial joints from mice are formed through a series of steps between E12.5 and E13.5 days. Growth/Differentiation factor 5 (GDF5) is important in defining the interzone between adjacent cartilages (66,67). The interzone zone originates from condensed mesenchymal cells that express the "*Sox trio*", *Col2a1*, and *Agc1* but also *Wnt9a, Wnt4* and *Noggin* which are important anti-chondrogenic factors (19,68–73). The exact balance of these pro- and anti-chondrogenic factors is crucial for the formation of articular cartilage and non-cartilaginous joint structures (such as ligaments, synovial lining) (73). Cell apoptosis also contributes to formation of the joint area. The joints from mice are completely formed by E16.5 days. Interestingly, mechanical stimuli through the movement of muscle contraction is an important factor for joint progenitor cells (74). Previous studies have shown that mechanical forces can contribute to the development of joint formation as well as endochondral ossification (75).

Anatomically, the synovial joint is comprised of different tissues including articular cartilage, synovial membrane, subchondral bone, ligaments, tendons and meniscus (Fig. 1.2). Altogether theses tissues play a role in maintaining the homeostasis of the joint (76,77). The main function of articular cartilage is to minimize friction upon joint movement and to distribute loads (78). The collagen network of the hyaline articular cartilage enables even distribution of the forces generated by mechanical compression (79). The joint cavity is enclosed by a specialized fibrous connective tissue including the synovial membrane that extends folds and villi into the joint cavity and secretes the lubricating synovial fluid (80). Synovial fluid is derived from blood plasm, but with a high concentration of hyaluronan (HA) produced by cells of the synovial membrane. Cells of the synovial membrane include macrophage-like synovial cells (type A cells) and fibroblastic synovial cells (type B cells) (81–83). Subchondral bone is the zone of epiphyseal bone underneath the articular cartilage and its main role is to form the "osteochondral junction", which is related to biomechanical and biochemical cross-talk between articular cartilage and underlying bone (84,85). Another supporting structure in the knee joint is the meniscus, which is a C-shaped fibrocartilaginous tissue between the tibia and femur. Knee meniscus is important to allow smooth load transfer from femur to tibia and for joint stability (86,87).

Subchondral bone consists of two distinct structure: subchondral bone plate (SBP) and subchondral trabecular bone (STB), which form a unit that separates the articular cartilage from the bone marrow (88). The main functions of the subchondral bone are to dissipate forces and provide elasticity for shock absorption caused by repetitive loading such as locomotion. Furthermore, subchondral bone has an extensive local response to repetitive loading though the bone remodeling process (89). It has since been shown the subchondral bone is a highly vascularized, innervated and dynamic tissue which provides a connection between the uncalcified cartilage and the bone marrow space (90). In fact, many signaling mechanisms facilitate the communication between articular chondrocytes and subchondral bone cells (osteoblast, osteoclasts and osteocytes) (91). Another important function of subchondral bone is to deliver nutrition and oxygen supply to cartilage through the medullary cavity via channels that connect subchondral bone and cartilage (92).

Moreover, synovial joints are reinforced by a number of extracapsular ligaments that are made from bands of dense regular connective tissue that connect bones to other bones (93). Skeletal

muscle mediates movement/locomotion and also helps to stabilize the joint. Every joint has nervous innervations related to nociception and neurogenic inflammation; sympathetic and sensory nerve fibers are present in synovium, subchondral bone, and periosteum (94,95).

1.2 Cartilage

1.2.1 Composition of Cartilage

Cartilage is an avascular, aneural and alymphatic tissue that mainly consists of ECM and water, comprising more than 95% of tissue volume (96,97). There are three major types of cartilage: elastic cartilage, fibrocartilage and hyaline cartilage. Elastic cartilage is found in the epiglottis (part of the larynx) and the pinnae (external part of ear flaps) and is composed of collagen fibers and elastin protein (98,99). Fibrocartilage is found in the pubic symphysis, the annulus fibrosus of intervertebral discs, menisci and the temporal mandibular joint. Fibrocartilage is also largely composed by type I collagen (100,101). Hyaline cartilage can be found on many joints surfaces (ex. articular surfaces of long bones) as well as at the epiphyseal plate (growth plate) (102), as previously discussed. Histologically distinguishable from the other types of cartilage, the ECM of hyaline cartilage is mainly composed of collagen type II, proteoglycan, water and lesser amounts of other non-collagenous proteins and glycoproteins (103). More specifically, these proteoglycans consist of core protein (210-250 kDa), mostly aggrecan, that is the most abundant by weight and largest in size in the ECM of cartilage. Aggrecan has many glycosaminoglycan (GAG) side-chains and binds to hyaluronic acid (HA) polymers to form a large complex with negative charges, which contributes to its function (104). The GAG chains are composed of chondroitin-sulfate and keratan sulphate with a high water-binding capacity and provide osmotic properties to cartilage, which will ultimately contribute to retain water within the ECM (105,106). Moreover, the principal collagen in the ECM of articular cartilage is the type II collagen. Articular cartilage, collagen type II, provide tensile strength and physical properties of the mature matrix. Also, collagens IX and XI are responsible to stabilize and help in the organization of the collagen network.

Together, these components and structures provide the cartilage function as a very resilient and highly specialized tissue that forms the smooth gliding surface of synovial joints, as well as, shear strength and self-lubrication (107). Articular cartilage has limited self-repairing capacity; the amount of cartilage ECM decreases with age and this has been attributed mainly to diminished

anabolic activity of cartilage cells (108). The cellular component of cartilage is made up by only one cell type, the chondrocytes which occupy about 2% of the volume of human cartilage (109). In healthy cartilage, chondrocytes produce proteolytic enzymes that act on collagen and proteoglycans, promoting localized and controlled tissue turnover and repair. The half-life of collagen is from several decades to up to 400 years for human femoral head cartilage, however, the average half-life of aggrecan is 25 years (110). The homeostasis of matrix turnover in articular cartilage will be explained later in this chapter but involves a dynamic equilibrium involving biochemical mediators including hormones, growth factors and cytokines as well as mechanical forces (111).

1.2.2 Zones of Articular Cartilage

Articular cartilage is composed of four different zones: superficial zone, middle zone, deep zone, and calcified zone. Within each zone, 3 different regions can be identified: the pericellular region, the territorial region, and the interterritorial region. The superficial zone (SZP) is the outermost layer of articular cartilage, protects deeper layers from shear stress, and makes up roughly 10% to 20% of articular cartilage thickness (112). Collagen type II is aligned parallel to the articular surface, but there is less aggrecan in the SZP (113). This zone is in contact with synovial fluid and is responsible for most of the tensile and compressive stiffness of cartilage to resist shear forces during joint movement (114).

In the superficial zone, the chondrocytes are smaller and flattened in morphology and have a greater density (115). Interestingly, mesenchymal stem cell markers have also been detected in the superficial zone of adult articular cartilage, suggesting a potential role in endogenous repair or cell-based therapy for treating some diseases such as osteoarthritis (OA) (116). However, more research is needed to elucidate the activity of these progenitor cells and the involvement of signalling pathways that regulate their functions. Importantly, the chondrocytes in this zone express several molecules such as superficial zone protein (SZP), also known as lubricin (PGR4) (117). Likewise, hyaluronan and surface-active phospholipids (SAPL) are involved as key boundary lubricants in cartilage (118). The middle (transitional) zone (MZ) is the largest zone that represents 40% to 60% of the total cartilage volume and acts as a first barrier in resisting the compressive loads between the superficial and deep zone, due to collagen fibrils organized obliquely from articular surface to subchondral bone (112,119). Recent studies have shown the

importance of the middle zone for the biomechanical resilience. MZ chondrocytes are spherical and large cells, with a column-like stacked arrangement (119). Below the MZ is the deep zone (DZ) that comprises 30% of cartilage volume and also contributes to its compressive strength. The DZ is characterized by vertical and columnar type II collagen fibers and proteoglycan organized perpendicular to the articular surface (120). In this layer, the chondrocytes are rounded and arranged as vertical columns of cells (121,122). The final layer is the calcified zone of cartilage (CZC), the deepest zone characterized by a calcified cartilage matrix which ultimately contributes to dissipating shock absorbance and confers structural integrity between the tissues of cartilage and bone during loading. Moreover, the calcified zone contacts the underlying subchondral cortical bone, known as the articular cartilage end plate (123). The cells in this layer are hypertrophic chondrocytes producing type X collagen, and the cell density is relatively low compared to the other zones (124). The deep zone is separated from the other zones by an irregular thin cement line known as tidemark (125).

1.2.3 Extracellular matrix and chondrocyte interaction

The cartilage ECM contains proteoglycans, collagens, cell binding glycoproteins, non-collagen ECM proteins, and lipids (126,127). The ECM can be divided into different regions such as: pericellular, territorial and interterritorial. The chondrocyte and its PCM environment is termed as chondron, which is surrounded by the territorial matrix including type XVI collagen (127). Type XVI collagen organize the ECM by anchoring and stabilizing collagen fibrils and sustaining microfibrils, intercepting intracellular signalling involved in proliferation and cell adhesion. The territorial matrix is made up of fine collagen fibrils containing types II and XI collagen is involved in the protection of chondrocytes from mechanical load and may facilitate the resiliency of articular cartilage to load bearing (126,128). The largest region is the interterritorial region that is composed mostly of proteoglycans and randomly oriented collagen fibrils which contribute to the biomechanical properties of articular cartilage (129).

1.2.4 Cartilage Molecular Mechanism of Cartilage Homeostasis: Catabolic and Anabolic Factors

Joint movement and dynamic loading of articular cartilage play crucial roles in the joint homeostasis and the pathogenesis of OA. The process by which chondrocytes convert mechanical signals into biochemical responses is called chondrocyte mechanotransduction (130). During joint loading, the compression of cartilage results in altered matrix water content and osmotic pressure, complex changes in calcium concentration, and fluid shear stress (131). Moreover, excessive mechanical loading can also influence the physiological balance between catabolism and anabolism factors, resulting in the development of diseases such as OA (132). Many candidate mechanoreceptors have been identified in chondrocytes including integrins, stretch-activated or stretch-sensitive ion channel (SACs), connexins, and primary cilia (133). These mechanoreceptors initiate intracellular signaling cascades leading to articular cartilage remodeling (134). Under physiological loading, chondrocytes maintain homeostasis. Unphysiological stimulation, however, can lead to changes in the chondrocyte phenotype, such as de- differentiation to a fibroblast-like cell and decrease of production of cartilage specific makers including type II collagen and aggrecan, or the induction of chondrocyte hypertrophy and apoptosis (135).

Healthy joint tissue under mechanical loading conditions has appropriate anabolic responses to antagonize the process of catabolic cytokines. One of the most important anabolic factors for articular cartilage, insulin-like growth factor-I (IGF-I), has been implicated in proteoglycan production. Many studies have demonstrated that IGF-I plays a role in chondrogenesis by enhancing proliferation and stimulating expression of collagen II and Sox9 (136). Furthermore, the TGF-β family members such as: bone morphogenetic proteins (BMPs), GDF5 and TGFβ itself (137). Members of the FGF family including FGF-10 and FGF-18 have anabolic effects on cartilage tissue at early stages of development (138). Interestingly, FGF-18 induces cartilage matrix production by activating the FGF receptor 3 (FGFR3) (139). As stated above, during life time, chondrocytes are responsible for the maintenance of the articular cartilage by regulating matrix metalloproteinases (MMPs) and A Disintegrin and Metalloproteinase with Thrombospondin Motif (ADAMTSs), collagen II and aggrecan networks surrounding them (140).

In summary, a variety of stimuli (chemical, inflammatory, growth factors and other signalling factors) can contribute to the anabolic and catabolic balance on cartilage and OA pathogenesis. Catabolic event is marked by cartilage matrix degradation markers, such as proinflammatory cytokines including interleukin-1-beta (IL-1β) and tumor necrosis factor-alpha (TNFα) (141). Evidence from *in vitro* and *in vivo* studies have demonstrated that TNFα and IL-1β contribute to ECM destruction and induce chondrocyte apoptosis (142). In addition, IL-1β can enhance expression of MMP-1, MMP-3 and MMP-13(143). Other inflammatory cytokines such as IL-4 have been reported as well in human articular cartilage, and IL-1, -6, -8 are increased in the osteoarthritic synovial lining (144). ADAMTS proteins are proteases that target aggrecan. IL-1β and TNF-α stimulate the production of ADAMTS-4 (145) through activation of the transcription factor NF-κB, as well as p38 and c-Jun N-terminal kinase (JNK) MAP kinases (146).

1.3 Osteoarthritis

Currently, there are more than 100 different forms of arthritis, and the most common form is osteoarthritis (OA). It has been estimated that currently 250 million people are affected by OA worldwide (147). The burden of OA is increasing substantially in Canada and the United States, including direct and indirect economic costs. More research is needed to enable a better understanding of the pathophysiology of OA, and clarification of the underlying signalling pathways and molecular mechanisms is necessary to direct the clinical approaches to disease management.

1.3.1 Etiology of Osteoarthritis

OA is a heterogeneous pathology characterized by many different factors involving metabolic, inflammatory, and mechanical causes. The classification of OA has traditionally been subcategorized into idiopathic (ie, primary) in nature, with no known specific cause, and secondary OA (148). Both primary and secondary OA involve the deterioration of cartilage in joints, and bones begin to rub against one another. However, primary and secondary OA have different triggers. For example, primary OA is affected by several factors including obesity, gender, age, and genetic factors that can lead to the development of OA (149). Contrarily, secondary OA or posttraumatic OA, is caused by trauma that directly damages joint tissues and destabilizes the joint

(i.e. meniscectomy or anterior cruciate ligament (ACL) tears). Abnormal anatomical stress such as femoroacetabular impingement (FAI), or malalignment of the tibia and femur of the knee resulting in 'knock-kneed' or 'bow-legged' (valgus and varus, respectively) can contribute to OA susceptibility (150,151).

1.3.2 Non-Modifiable Risk Factors For OA

Although the cause of OA is still unclear, there are non-modifiable and modifiable risk factors for OA. *Age* is one of the greatest non-modifiable risk factors for the development of OA as a result of many biological age-related changes in the joint structures. In fact, 70% of women and 60% of men over the age of 65 years were diagnosed with radiographic signs of OA in one or more joints (108,152). Moreover, several studies have demonstrated that senescent chondrocytes are found in degenerated cartilage tissue and cartilage tissue from OA patients undergoing joint replacement surgery (153). Senescence of chondrocytes is associated with development or progression of OA, since the senescent cells show increased production of MMPs and catabolic degradation of type II collagen (154). Several pathways such as p38 MAPK and PI3K/Akt are involved in the senescence-associated secretory phenotype (SASP) (155). Furthermore, OA chondrocytes display more production of reactive oxygen species (ROS) due the mitochondrial dysfunction, which may increase inflammation and catabolic responses mediated by NF-kB pathways (156). *In vivo* studies have also demonstrated that mechanical injury to cartilage can lead to senescence in the superficial zone in young animals and throughout cartilage in aged animals (157). In addition, with age, changes in other tissues such as subchondral bone changes, loss of muscle mass (sarcopenia), synovium and ligament changes, can contribute to the onset of OA development (158–160).

According to World Health Organization (WHO) the prevalence of OA is higher in *women* (18%) than in men (9.8%), particularly in those above 60 years of age. Some studies have shown anatomic differences between women and men, with women showing significantly tibiofemoral cartilage defects and tibial and patella cartilage loss (161). Moreover, a study comparing the kinematic differences between male and female athletes demonstrated that women exhibited greater anterior and posterior shear forces, knee extension and valgus moments, which may also play a role in the development of knee OA in women (162,163). *In vivo* studies have suggested that sex hormone deficiency influence joint structure as shown in orchiectomized (ORX) male and ovariectomized

(OVX) female mice (164). As a result, intact male mice had more accelerated OA development than ORX male, however, OVX female mice had more severe OA than intact female. But the direct actions of estrogen or testosterone on cartilage are still unclear (165). A large number of studies have shown the contribution of *genetics and epigenetics* in OA, which is estimated to be between 40% and 80%, and higher in hand and hips than for knee OA (166). An inherited predisposition to OA has been evidenced for many years from twin and sibling studies (167). The past decade has identified a great number of candidate genes that confer susceptibility for OA disease. Previous findings using genome-wide associated studies (GWAS) have identified *GDF5*, *COL2A1*, *TGFB1*, Matrilin 3 (MATN3), *IL1*, and I*L4R* as contributors to OA risk in different joints (168–170).

1.3.3   Modifiable Risk Factors For OA

The most significant modifiable risk factor in OA is obesity, since weight loss in OA can benefit patient pain significantly and slow down progression of joint structural damage. *Obesity* affects the weight-bearing joint by altering joint kinematics and increasing ambulatory load (173). Interesting, there also is evidence that obese people are at increased risk for developing hand OA due the metabolic association between adipose tissue and OA (174). Adipokines such as leptin have been identified in articular cartilage and synovial fluid from knee or hip OA patients (175). Moreover, the systemic inflammatory effect of increased adipose tissue leads to "metainflammation" (inflammatory and metabolically active) involving proinflammatory cytokines that have a role in joint structural change and in the perception of pain, altogether contributing to a positive feedback loop of obesity and OA (176).

Different tissue in the joint can be affected due to either a single episode of trauma or repetitive overuse. Studies have shown structural damage resulting from mechanical forces from high-impact exercise on cartilage tissue, which can lead to the incidence of secondary OA(177). Meniscal or anterior cruciate ligament (ACL) injury arise frequently from joint trauma (sports injuries, falls, occupational activity) and present a risk factor for OA (178). Joint trauma induces to a complex metabolic response that involves cell death, matrix degradation, release of oxidants and inflammatory cytokines, potentially causing further joint damage (179). A synovial inflammatory response is a regular consequence following injury. Moreover, mechanical

instability often results from joint injury (e.g. ACL rupture), leading to an unbalanced load distribution and cartilage degeneration (180). Thus, direct trauma to joint structures, an inflammatory response, and mechanical instability all contribute to the risk of post-traumatic OA.

1.3.4   Pathobiology of Osteoarthritis

OA is characterized by failure of the synovial joint organ as a result of dysfunction of one or more joint structure (as shown in **Figure 1.2**), resulting in joint pain and increasing disability. Indeed, subchondral bone, synovium, supportive ligaments and articular cartilage all play a role in progression of OA pathology.

Figure 1.2 Synovial joints in health and OA knees. The articular surfaces of bones within synovial joints are covered with a thin layer of hyaline cartilage that provides a smooth surface and reduces friction during movement. Moreover, articular cartilage enables the subchondral bone to absorb and dissipate impact energy during weight bearing. The fluid-filled joint cavity is enclosed by a fibrous joint capsule. The synovium (synovial membrane) lines the joint cavity and produces synovial fluid which provides nutrition and lubrication to the cartilage surfaces. In addition, other structures such as ligaments, tendons and muscle support stability and alignment of the joint. Menisci are responsible for the distribution of mechanical loading in the femorotibial joint. Figure courtesy of Ermina Hadzic.
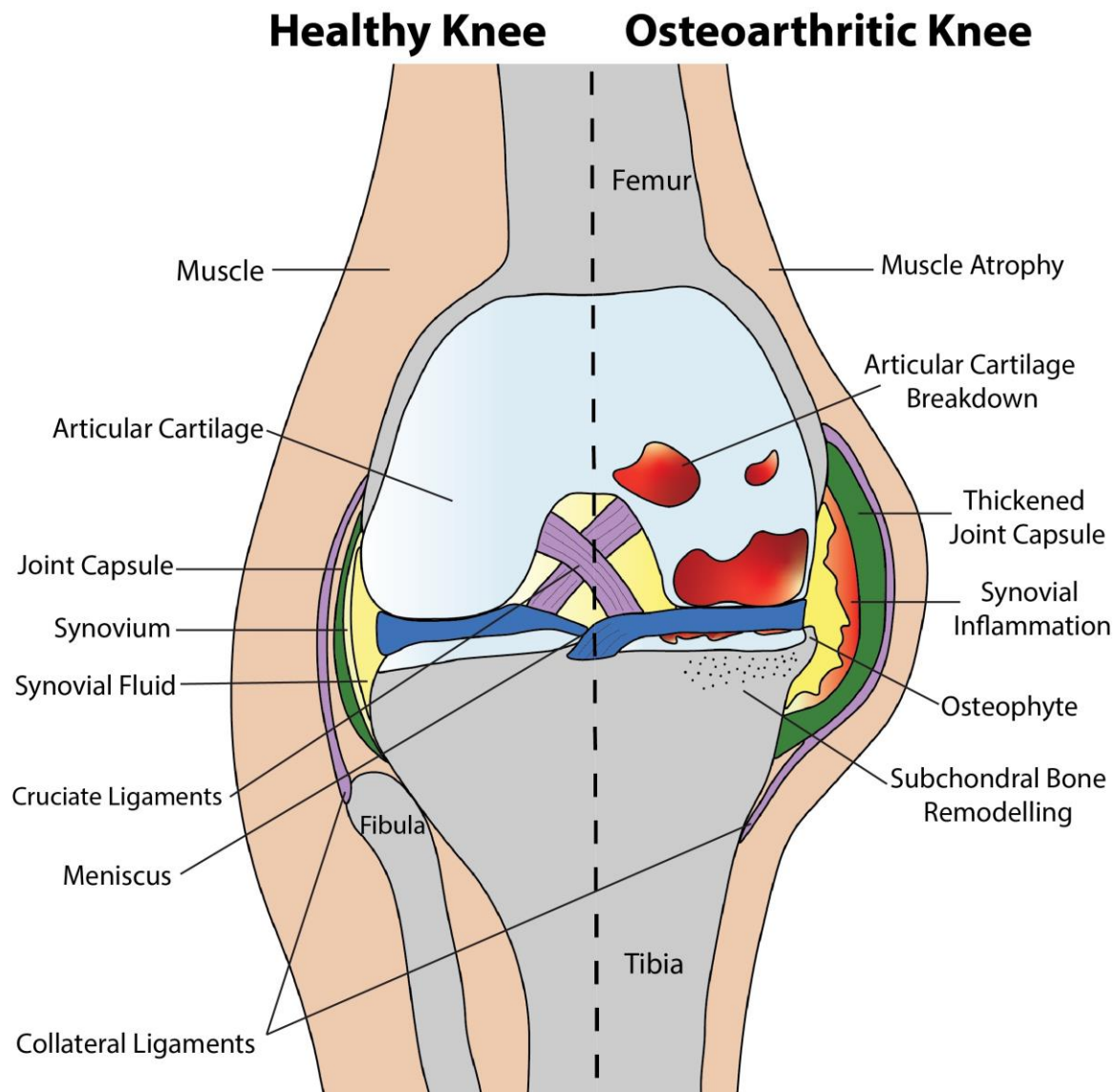
Figure 1.2 Synovial joints in health and OA knees.

1.3.5   Cartilage Breakdown in OA

As mentioned before, OA is not simply a disease of cartilage it is, rather, the irreversible destruction of cartilage which is attributed to OA. At the early stage of OA, articular cartilage loses its structure and composition due to decreasing proteoglycan content. Once collagen is degraded, it appears that a state is reached that cannot be reversed (149). Early degenerative changes happen in the SZP of articular cartilage after successive loads and contribute to the progressive cartilage destruction (181). Articular cartilage progressively undergoes fibrillation and erosion towards the calcified cartilage and extends into the mid and deep zone of cartilage (182). The continued deterioration of articular cartilage eventually exposes the underlying subchondral bone, resulting in a decrease in joint motion and increase of pain (183). During OA, changes in chondrocyte behaviour with disease advancement can be seen. Chondrocyte responses and expression profiles are altered during OA, for example, increased expression of degenerative enzymes (such as MMP13 and ADAMTS-5) (184). Overall, the alteration in chondrocyte phenotype leads to an imbalance in anabolic and catabolic processes in articular cartilage and ultimately in the progression of the disease.

1.3.6   Subchondral Bone in Osteoarthritis

As the disease progresses, not only articular cartilage is deteriorated, but changes in the underlying subchondral bone also play an important role in the onset of OA (185). The subchondral bone tissue is a biphasic material and is designed to support axial loads and respond to stresses placed across the joint structure. Mechanical properties can be associated with bone thickening, increased porosity, reduced density/elasticity and reduced capacity for shock absorption (89). Current evidence suggests that subchondral bone disease is part of OA pathogenesis. For example, patients with hip OA pathology showed an increased volume of trabecular bone as well as higher bone mineral density (BMD) (186). Moreover, using magnetic resonance imaging (MRI) bone marrow lesions (BML) (also called bone marrow edema or bone bruises) have been associated with knee malalignment and knee pain (187). BMLs are strongly associated with pain and related to the occurrence of subchondral microfractures (188). In order to compensate the mechanical instability of the joint, osteophytes are formed at joint margins in a process similar to endochondral ossification, regulated by the actions of TGFβ and BMP2 (189,190). Subchondral bone sclerosis,

subchondral bone cysts formation, osteophytes, subluxation, narrowing of the joint space and intra-articular or periarticular calcification are commonly seen radiographically in more chronic cases of OA (191).

1.3.7   Changes in the Synovium

Mounting evidence suggests that the synovium plays an important role as a driver of the OA process at early and late stages. Synovitis is a complex process and can be induced by release of fragments from degraded hyaline cartilage as well bone (detritus) structures into the synovial cavity, which ultimately initiate synovial inflammation (192). Several studies have shown that synoviocytes produce pro-inflammatory factors that attract immune cells and inflammatory mediators such as macrophages and T-cell lymphocytes into the OA synovium (78). Cytokines and chemokines as well as their downstream signalling pathways have been extensively studied in the synovium, including TNFα, IL-1β, IL-6, IL-15, IL-17, and IL-18 that are up-regulated in OA synovial fluid and synovial membrane (SM) (193). Moreover, Toll-like receptors (TLRs) are expressed by macrophages found in SM in both OA and rheumatoid arthritis (RA) (194). TLRs activate nuclear-factor κB (NF-κB), resulting in the production of chemokines and cytokines such as IL-8, CCL5, and IL-6 and stimulation of macrophages, granulocytes, and lymphocytes (195). Aspects of synovitis in knee OA include thickened synovium, villous hyperplasia, increased synovial vascularity and vascular flow, infiltration of lymphocytes and macrophages, and fibrosis (196).

1.3.8   Mechanism of OA Pain

The perception of pain is the predominant and most disabling symptom of OA patients and those affected by pain usually report pain-related psychological distress, swelling, fatigue and morning stiffness (197). Peripheral mechanism can increase chronic pain and also contribute to hyperalgesia (enhanced pain response) or allodynia (pain in response to non-noxious stimuli) (198). Nociceptors (pain-sensing afferent neurons) and proprioceptors (afferent receptors for motor control) are present in tissues that are compromised by OA, including the periosteum and subchondral bone, soft tissues including ligament insertions, menisci, and synovium that ultimately leads to the feeling of joint pain (199). Therefore, OA pain is a complex process that involves nociceptive input

from the joint as well as in the peripheral and central nervous system. Under disease conditions, many inflammatory mediators are released within the joint to elicit pain (200). Synovium in OA patients has "macroscopic" inflammation that can corroborate to the pain within the joint, since cartilage debris can be phagocytosed by cells lining the synovium (201). Articular cartilage is anural and avascular, however, the degeneration in cartilage that leads to subchondral bone plate exposure is associated with prevalent and incident knee pain in patients with knee OA (202). Furthermore, there are many signaling pathways contributing to the mechanism underlying OA pain. Chemotactic cytokine ligand 2 (CCL2) signalling has been identified as nociceptive stimulator in the development of pain in mice (203). Clinical and animal studies have targeted nerve growth factor (NGF) and inhibition of its receptor, tropomyosin receptor kinase A (TrkA), in OA pain. Interesting results have shown the efficacy of targeting NGF on reducing OA pain, as seen in patients that had treatment with the anti-NGF antibody tanezumab (204). However, more clinical and animal studies are required for understanding the role of the NGF/ TrkA pathway in OA to optimize therapeutic strategies for OA.

1.3.9 Diagnosis and Treatments for OA

OA commonly affects multiple joints such as hands, knee, hips and spine, and plain radiograph (x-rays) or advanced imaging techniques including MRI or computed tomography (CT) can be also used for diagnosis of OA pathology (205). Radiography enables the visualization of marginal osteophytes, subchondral sclerosis and cysts, cortical alterations and alignment of the joint. Other joint structures such as articular cartilage, crucial or collateral ligaments, and menisci are more easily visualized by MRI (206). Furthermore, (CT arthrography (CTA) and MR-arthrography (MRA) can also identity articular cartilage, synovial inflammation, and osteophytes with high anatomic resolution (206). Additional guidelines to diagnose OA include: pain is enhanced with activity of daily living; morning stiffness with duration of less than 30 minutes; range of motion becomes limited with joint locking or joint instability; and patients older than 45 years (207,208). The treatment for OA patients is focused on relief of pain, and improvement/maintenance of quality of life. OA treatment can be divided in three categories: nonpharmacologic, pharmacologic and surgical management (207). In order to control pain, the use of nonsteroidal anti-inflammatory drugs (NSAIDs) is recommended, such as acetaminophen or cyclooxygenase-2 (COX-2) inhibitors (209). Moreover, intra-articular therapies can also be used for acute pain, such as

hyaluronic acid (HA) or corticosteroid (CSs) injections; however, variable and controversial results have been reported in clinical trials and meta-analysis (210,211). Non-pharmacological management includes weight reduction and targeted exercise; for example, low-impact activities have shown improvements in pain and physical performance for OA patients (212,213). The last option for OA treatment is total joint replacement; however, it is not a final resolution for OA disease, since most of the joint prostheses will function well for 15 to 20 years, not a life time (214). Complications post-surgery are not uncommon (215).

Clearly there is a need for new OA treatments, in particular disease-modifying drugs that can slow stop, or reverse OA progression. For example, strategies aimed at synovial fluid (targeting activated macrophages), C reactive protein, cytokines and adipokines/hormones are under research for OA treatment (320,321). However, a more detailed understanding of the molecular mechanisms driving OA might identify more drug targets.

1.4   Signaling Pathways in Osteoarthritis

1.4.1   Receptor Tyrosine Kinase Signaling in Osteoarthritis

Many different signal proteins act via receptor tyrosine kinases (RTK), such as epidermal growth factor (EGF) receptor, insulin receptor, insulin-like growth factor (IGF1) receptor, nerve growth factor receptor, vascular endothelial growth factor (VEGF) receptors, and others (218). In most cases, the activation of RTKs occurs through the binding of the signal protein to the ligand-binding domain on the extracellular side of the receptor. This results in dimerization, bringing the two cytoplasmic kinase domains together and allowing trans-autophosphorylation and activation. However, there are some important exceptions, for example EGFR.

EGFR is a type 1 transmembrane glycoprotein that is a member of a family of 4 receptor tyrosine kinases (EGFR or ErbB1; Her2 or ErbB2; ErbB3; and ErbB4) ref. Several ligands can bind to EGFR with high affinity: epidermal growth factor (EGF), heparin-binding EGF-like growth factor (HB-EGF), transforming growth factor α (TGFα), and betacellulin (BTC). EGFR also has 3 low affinity ligands: epigen (EPGN), epiregulin (EREG), amphiregulin (AREG) (219–221). These ligands for EGFR are found as type 1 transmembrane pro-forms and are shed from cell surface (222–224). Together, EGFR can form either homo- or heterodimers with other ERBB receptors,

especially ERBB2 (225). ErbB2 and ErbB4 are capable of forming heterodimeric pairs with each other due their catalytic kinase domains. On the other hand, ErbB3 has an inactive kinase domain that can still pair with and activate the other ERBB receptors. Several studies have demonstrated that members of the ADAM (a disintegrin and metalloproteinase) family such as ADAM17 or 10 can induce EGFR transactivation through shedding of the ligands from the membrane (226). Under unstimulated conditions, EGFR is found at the plasma membrane in an auto-inhibited state, however, ligand binding leads to receptor dimerization and activation of RTK activity. Ligand-binding to the receptor causes a conformational change in its dimerization arm, which forms an asymmetric dimer. Thereby, this dimer phosphorylates multiple tyrosines in the C-terminal tails segments of both EGFR receptors (227). This triggers the assembly of an intracellular signaling complex that can activate many downstream pathways, including MAPK/ERK, PI3K/Akt, SRC, PLCγ/PKC, and JAK/STAT, as shown in **Figure 1.3.** The biology of ErbB receptors, including their structure, signaling, biochemistry, genetics, and their roles in development and disease have been studied extensively (228,229).

Figure 1. 3. Activation of Epidermal growth factor receptor and signaling pathways. Epidermal growth factor receptor (EGFR) is a receptor tyrosine kinase that signals via many downstream pathways. Activation of EGFR is triggered by several ligands. These ligands for EGFR family are found as type 1 transmembrane pro-forms and are shed from cell surface by members of the ADAM family such as ADAM17 or 10. Ligand binding results in either homo- or heterodimers of EGFR and activation of downstream pathways such as mitogen activated kinase (MAPK) cascades, JAK/STAT, Rho GTPases and various PKC family proteins, P13K (phosphoinositide 3-kinase). EGFR activation of these pathways is cell type specific. Mig-6 is a transcriptionally feedback inhibitor and has crucial activity in regulating EGFR signaling through two different mechanisms: inhibiting the catalytic activity of EGFR by docking the kinase domain and driving EGFR into endocytosis.
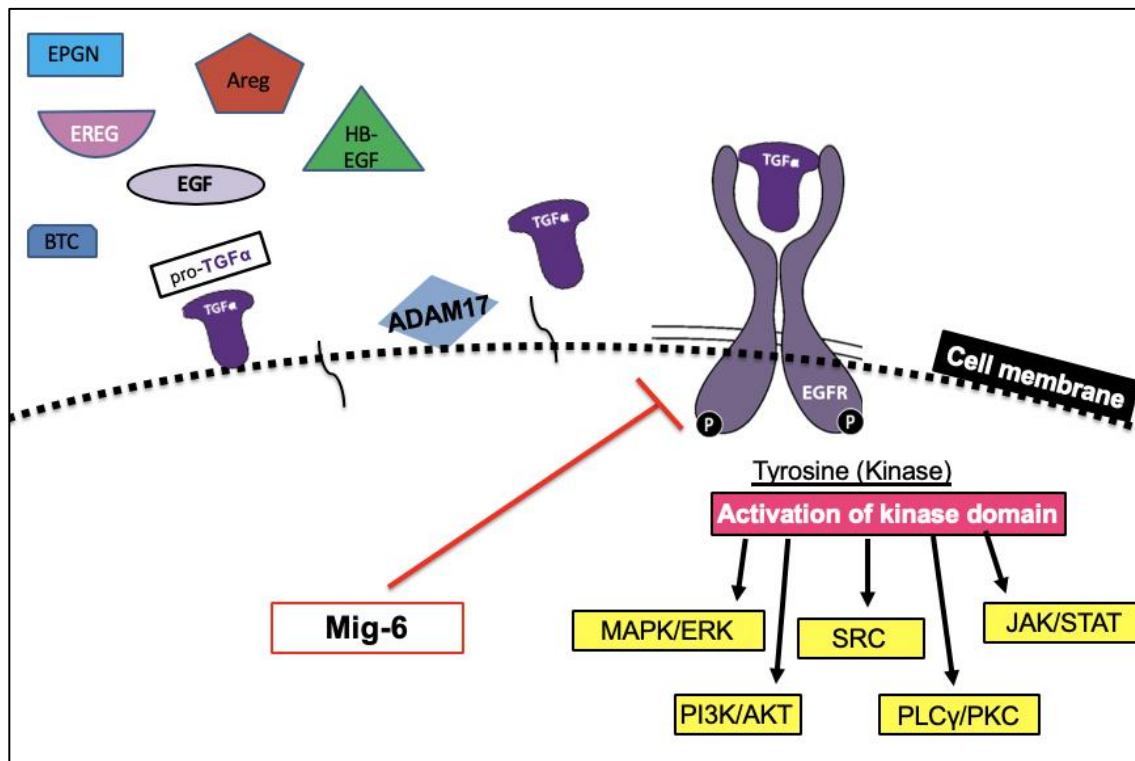
Figure 1.3 Epidermal growth factor receptor activation and signalling pathways

Deregulation of receptor tyrosine kinase signalling leads to the development of a variety of human diseases including non-small cell lung cancer (NSCLC), squamous cell carcinoma (SCC), large cell carcinoma (LCC) and osteosarcomas (230,231). Studies have shown a dual role for EGFR signaling in OA context related to the development, protection and destruction of articular cartilage (232–237). Some studies have found that EGFR is an anabolic regulator of bone formation as it maintains mesenchymal stem cells and osteoprogenitors in bone (238). A previous study has shown that EGFR can activate the MAPK/ERK pathway to induce osteoprogenitor proliferation and survival, and therefore can promote bone formation (239). Cartilage-specific *Egfr* knockout mice showed elongated growth plate due to down-regulation of MMPs (9, 13 and 14) and RANKL in the growth plate and subsequent delays in the conversion of cartilage to bone (238). Another study showed that MMP9 and RANKL are upregulated by EGFR via the canonical Wnt/β-catenin pathway (240).

Several studies have implicated EGFR and its ligands in OA. Previous studies have shown that EGF has been identified in rheumatoid arthritis (RA) and TGFα in the synovial fluid of OA patients (241,242). Interestingly, *in vitro* studies using chondrocytes treated with EGF showed chondrocyte phenotype alteration and up-regulation of inflammatory markers (242,243). In addition, heparin-binding epidermal growth factor-like growth factor (HB-EGF)is highly increased (494%) in joints of 12 month-old mice that underwent DMM (destabilization of medial meniscus) surgery to induce post-traumatic OA (244). Our lab has shown that TGFα mRNA and protein expression was increased in rats that underwent a surgical procedure to induce OA (transection of the anterior cruciate ligament with partial medial meniscectomy) (232). Moreover, TGFα supresses expression of anabolic genes such as Sox9, type II collagen and aggrecan, but induces MMP13 as well as TNFα in chondrocytes (233). Additional *in vitro* and *ex vivo* experiments using chondrocyte culture and osteochondral explants have demonstrated that activation of EGFR signalling in articular cartilage promotes cartilage degeneration and chondrocyte proliferation (245), and inhibits chondrogenesis (246). Evidence of the importance of TGFα/EGFR in OA stems from

analyses of young *Tgfa* KO mice that are protected from developing OA after DMM surgery, but there was no protection when surgery was performed in older mice or during normal aging (247).

Furthermore, pharmacologic inhibition of EGFR by AG1478 led to decreased progression of cartilage damage in a rat model of posttraumatic OA (248). Furthermore, the human *TGFA* gene is also reported amongst the genetic loci most strongly linked with OA and cartilage thickness in two genome-wide association studies (GWAS) (171,249). On the other hand, EGFR signaling plays a crucial role in articular cartilage development and for maintaining proliferation and survival of superficial chondrocytes as well as mechanical strength of cartilage (237,250). Mice heterozygote for a dominant negative EGFR ($Egfr^{Wa5/+}$) showed accelerated OA at 12 weeks after DMM surgery with accelerated loss of cartilage and subchondral bone plate thickening, compared to their WT siblings. Also, WT *129S2* mice that received DMM surgery followed by gefitinib treatment (anti-EGFR antibody) showed milder OA damage in comparison to $Egfr^{Wa5/+}$ mice (251). Furthermore, cartilage-specific (Col2-Cre) *Egfr KO* mice developed spontaneous OA initiation with subchondral bone sclerosis at 12 months of age, earlier than WT mice (252). Moreover, EGFR signaling enhances expression of Prg4 and hyaluronic acid (HA) at the cartilage surface (250). Since both catabolic and anabolic activity of EGFR signaling in the joint has been reported, it is strongly suggested that EGFR effects in articular cartilage are dose-and/or context-dependent, but the molecular mechanisms underlying these opposing roles are not understood.

1.4.2 Mitogen-Inducible Gene Mig-6 in development and joint pathology

First time described as a multi-hormonal inducible gene in 1985 by Kenney and colleagues, many different factors have been reported to be responsible for the induction of *Mig-6* (mitogen-inducible gene 6) gene expression including hormones (insulin, glucocorticoids), cyclic adenosine monophosphate (cAMP), phorbol esters and others (253). Moreover, growth factors (for example EGF, basic fibroblast growth factor (bFGF), hepatocyte growth factor/scatter factor (HGF/SF) and TGFα) and many stresses conditions such as joint mechanical impact, hypoxia, diabetic nephropathy, myocardial ischemic injury and infarction are also candidates to induce *Mig-6* gene expression (254). Mig-6 is a scaffolding adaptor protein involved in the regulation of the signaling by EGFR. Mig-6 is also known as Gene 33, ErbB receptor feedback inhibitor 1 (ERRFI1), or as receptor-associated late transducer (RALT) and is found in the cytosol of cells (255). *Mig-6* is

highly conserved in species such as *Xenopus,* rodent, and humans, but not in less in organisms like *S. cerevisae, C. elegans,* or *Drosophila* (256). Mig-6 is differentially expressed in different tissues and organs; for example, high levels of Mig-6 expression can be found in the liver and kidney, however expression is also found in the placenta, heart, brain, skeletal muscle, stomach and lung (257,258).*Mig-6* gene has been linked to human lung cancer, such as in squamous cell carcinoma patients, and late-stage patients with non-small cell lung cancer (NSCLC) (259). Disruption of the *MIG-6* gene can lead to bile duct, gastrointestinal (GI) tract, gallbladder, and skin cancer (231,260).

Structurally, Mig-6 contains important protein-protein interactions domains/motifs, including a Cdc42/Rac-interaction domain (responsible for regulators of actin cytoskeleton remodeling and signal transduction) (256,261). The CRIB domain interacts with Cdc42, and the Src-homology-3 (SH3) domain binding motif interacts with Grb2 and 14-3-3 protein binding motifs. The carboxyl terminus of Mig-6 has the ErbB-binding region (EBR) which connects to EGFR family receptors. The EBR domain shares a homology with a non-receptor protein tyrosine kinase Ack-1, another CRIB domain-containing protein that also interacts with EGFR (262–264). *Mig-6* transcription is induced by EGFR signaling at the transcriptional level (263,265). Mig-6 has been shown to block the activation of EGFR induced signaling modules, such as the RAS-ERK and PI3K/AKT pathways (265,266), as shown in **Figure 1.4.** Mig-6 can bind to and inhibit EGFR through a two-tiered mechanism: suppression of EGFR catalytic activity and receptor down-regulation (267).

Figure 1.4 Mitogen Inducible Gene 6 inhibits the activation of EGFR and RAS-ERK and PI3K/AKT pathways. Canonical signaling pathways including PI3K-AKT and Ras-Raf-MEK-ERK that are involved in cell proliferation, gene expression and cell survival might be suppressed in part by Mig-6.
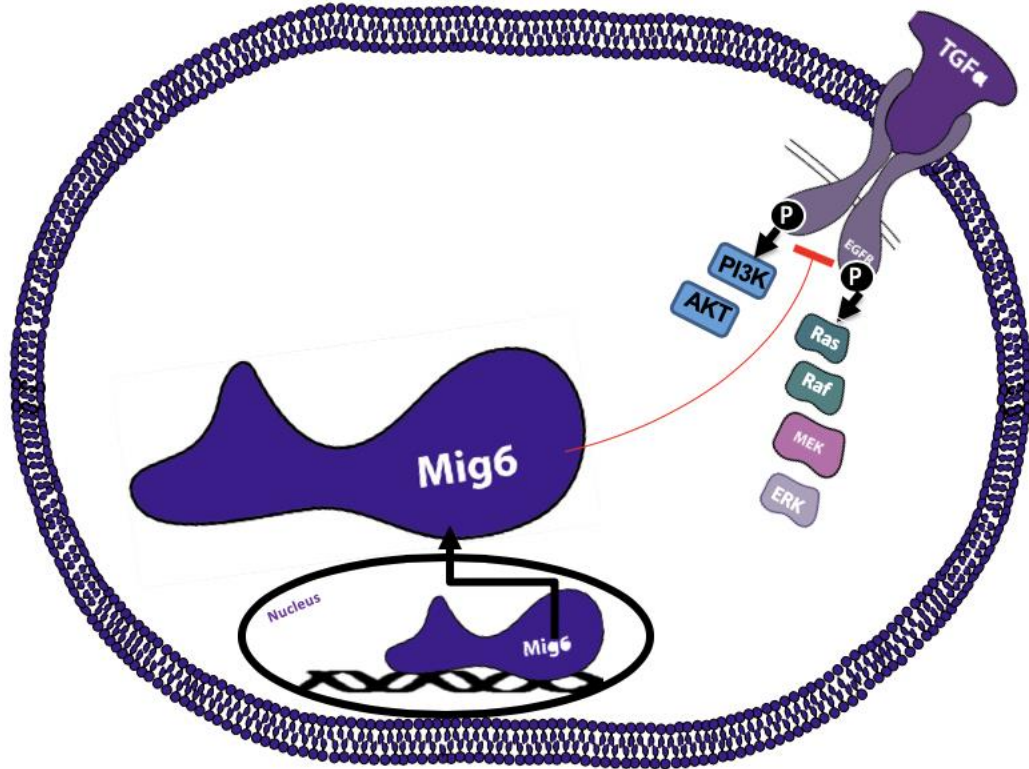
Figure 1.4 Mitogen Inducible Gene 6 inhibits the activation of EGFR and RAS-ERK and PI3K/AKT pathways.

The *Mig-6* protein includes two PEST sequences that can be targeted by ubiquitination and degradation by the proteasome. Receptor endocytosis is an important mechanism by which activated EGFR can be internalized, degraded or recycled, causing attenuation of EGFR activation. Mig-6 can mediate this process. Moreover, Mig-6 binds to different proteins such as the cell division control protein 42 homolog (Cdc42) (268) and c-Abl (269), in addition to all 4 EGFR family receptors (ErbB1-4). Also, it is frequently suggested that Mig-6 is a part of a negative feedback loop that diminishes HGF/Met (or c-Met) signalling, a ubiquitous pathway which profoundly influences cell differentiation (64).

Therefore, it is quite possible that Mig-6 might participate or fine tune signal transduction via different signaling pathways. Interestingly, various studies have reported that loss of Mig-6 induces the onset of OA-like symptoms (260,271–275). Global Mig-6-deficient mice showed degradation of the articular cartilage and the formation of bony outgrowths due to proliferation of mesenchymal-like progenitor cells followed by differentiation into chondrocytes. The most affected joints are the knee, ankle and temporal-mandibular joints in which it is suggested that mechanical stress could initiate this phenotype (271).

It has been shown that Mig-6 mRNA level were elevated in degenerating cartilage from a canine model of mechanical impact on cartilage explants, however, down regulation of Mig-6 were demonstrated followed induction of OA using a surgical rat model (272,276). The characterization of cartilage-specific (Col2-Cre) knockout of *Mig-6* mice showed formation of chondro-osseous nodules, but also increased thickness of articular cartilage in the knee, ankle and elbow. Moreover, the cartilage thickness was less pronounced at 36 weeks than in 12 week-old mice (277). Also, limb mesenchyme-specific (Prx1-cre) knockout of *Mig-6* resulted in a similar phenotype as that observed in cartilage-specific knockout mice (277). These phenotypes appeared to be caused by an increase in chondrocyte proliferation in articular cartilage, supported by increased expression of Sox9 and EGFR activation in cartilage (278).

Recent studies by Staal et al (279) show that the deletion of Mig-6 results in the hyperactivation of EGFR and histopathologically the mice showed formation of osteophyte-like nodules, formation of subchondral cysts and cartilage degeneration in their knees. The overall effect of Mig-6 signaling on OA development is determined by the balance of these two opposite actions

of anabolic and catabolic effects and most likely is age-, OA stage-, and context-dependent. Understanding how Mig-6 exerts its function under different physiological conditions will provide further insight into its potential roles in many cellular and biological processes, in particular in synovial joints and OA.

1.5   Overall Objectives and Hypotheses

Mitogen Inducible Gene 6 (Mig-6) and Epidermal growth factor receptor (EGFR) signaling have been implicated in many different diseases such as cancer as well as osteoarthritis pathology. *In vivo* and *in vitro* studies have shown that Mig-6/EGFR signaling and its ligands (EGF or TGFα) play a dual role in cartilage homeostasis and degeneration. My general hypothesis is that <u>regulation of Mig-6/ EGFR is crucial for articular cartilage health</u>.

1.5.1   Objective #1

To characterize the effects of cartilage-specific Mig-6 overexpression in mice using a cartilage specific *Mig-6* overexpressing mouse model.

1.5.1.1   Rationale #1

Previous research demonstrates that Mig-6 overexpression acts as a negative feedback regulator of EGFR signaling, but these studies did not yet analyze joint tissues. Since our previous studies suggest dosage- and/or context-specific roles of EGFR signalling in joint homeostasis and OA, we will now examine whether overexpression of Mig-6 alters these processes.

1.5.1.2   Hypothesis #1

Mig-6 overexpression will block EGFR signalling and thus lead to spontaneous cartilage breakdown and symptoms typical of OA.

1.5.2   Objective #2

To investigate the effects of skeletal-specific Mig-6 overexpression in the mouse limb mesenchyme on primary OA development.

1.5.2.1   Rationale #2

We propose to elucidate the role of EGFR in this model using the paired-related homeobox gene (Prx1) as Cre driver since it is more widely expressed in limb mesenchyme, including additional

joint structures other than cartilage. We will now address the function of Mig-6 overexpression mice in limb development and joint homeostasis *in vivo*.

1.5.2.2 Hypothesis #2

Mig-6 overexpression will decrease EGFR activity in the limb mesenchyme and will result in catabolic cartilage damage.

1.5.3 Objective #3

To determine the effects of Mig-6 overexpression on post-traumatic OA.

1.5.3.1 Rationale #3

Based on our *in vivo* data showing cartilage damage in aging Mig-6 overexpressing mice, we asked whether cartilage specific Mig-6 overexpression would protect or not from cartilage degeneration in osteoarthritis following surgical destabilization of medial meniscus (DMM), which is the most accepted surgical OA model in mice.

1.5.3.2 Hypothesis #3

Cartilage specific overexpression of Mig-6 will accelerate progression of post-traumatic OA.

1.6   References

1.   Jepsen, K. J. Systems analysis of bone. *Wiley Interdiscip. Rev. Syst. Biol. Med.* **1,** 73–88 (2009).

2.   Florencio-Silva, R., Sasso, G. R. da S., Sasso-Cerri, E., Simões, M. J. & Cerri, P. S. Biology of Bone Tissue: Structure, Function, and Factors That Influence Bone Cells. *Biomed Res. Int.* **2015,** 421746 (2015).

3.   Fulzele, K. *et al.* Insulin Receptor Signaling in Osteoblasts Regulates Postnatal Bone Acquisition and Body Composition. *Cell* **142,** 309–319 (2010).

4.   Wagner, D. O. & Aspenberg, P. Where did bone come from? *Acta Orthop.* **82,** 393–8 (2011).

5.   Butterfield, N. C., McGlinn, E. & Wicking, C. in *Curr. Top. Dev. Biol.* **90,** 319–341 (2010).

6.   Landis, W. J. The strength of a calcified tissue depends in part on the molecular structure and organization of its constituent mineral crystals in their organic matrix. *Bone* **16,** 533–44 (1995).

7.   Gilbert, S. F. Osteogenesis: The Development of Bones. (2000). at <https://www.ncbi.nlm.nih.gov/books/NBK10056/>

8.   Mirando, A. J., Dong, Y., Kim, J. & Hilton, M. J. Isolation and culture of murine primary chondrocytes. *Methods Mol. Biol.* **1130,** 267–77 (2014).

9.   Long, F. & Ornitz, D. M. Development of the endochondral skeleton. *Cold Spring Harb. Perspect. Biol.* **5,** a008334 (2013).

10.   Karsenty, G. Transcriptional Control of Skeletogenesis. doi:10.1146/annurev.genom.9.081307.164437

11.   Shapiro, F. Bone development and its relation to fracture repair. The role of mesenchymal osteoblasts and surface osteoblasts. *Eur. Cells Mater.* **15,** 53–76 (2008).

12.   Chen, G., Deng, C. & Li, Y. P. TGF-β and BMP signaling in osteoblast differentiation and bone formation. *Int. J. Biol. Sci.* **8,** 272–288 (2012).

13.   Kozhemyakina, E., Lassar, A. B. & Zelzer, E. A pathway to bone: Signaling molecules and transcription factors involved in chondrocyte development and maturation. *Dev.* **142,** 817–831 (2015).

14.   Kenkre, J. S. & Bassett, J. The bone remodelling cycle. doi:10.1177/0004563218759371

15.   Setiawati, R. & Rahardjo, P. in *Osteogenes. Bone Regen.* (IntechOpen, 2019). doi:10.5772/intechopen.82452

16. Akiyama, H., Chaboissier, M.-C., Martin, J. F., Schedl, A. & de Crombrugghe, B. The transcription factor Sox9 has essential roles in successive steps of the chondrocyte differentiation pathway and is required for expression of Sox5 and Sox6. *Genes Dev.* **16,** 2813–28 (2002).

17. Lefrebvre, V. & de Crombrugghe, B. Toward understanding S0X9 function in chondrocyte differentiation. *Matrix Biol.* **16,** 529–540 (1998).

18. Ikeda, T. *et al.* The combination of SOX5, SOX6, and SOX9 (the SOX trio) provides signals sufficient for induction of permanent cartilage. *Arthritis Rheum.* **50,** 3561–73 (2004).

19. Yang, C. *et al.* Apoptosis of chondrocytes in transgenic mice lacking collagen II. *Exp. Cell Res.* **235,** 370–3 (1997).

20. Lefebvre, V., Huang, W., Harley, V. R., Goodfellow, P. N. & de Crombrugghe, B. SOX9 is a potent activator of the chondrocyte-specific enhancer of the pro alpha1(II) collagen gene. *Mol. Cell. Biol.* **17,** 2336–2346 (1997).

21. Long, F. & Linsenmayer, T. F. Regulation of growth region cartilage proliferation and differentiation by perichondrium. *Development* **125,** 1067–73 (1998).

22. Di Nino, D. L., Long, F. & Linsenmayer, T. F. Regulation of endochondral cartilage growth in the developing avian limb: cooperative involvement of perichondrium and periosteum. *Dev. Biol.* **240,** 433–42 (2001).

23. Beier, F. Cell-cycle control and the cartilage growth plate. *J. Cell. Physiol.* **202,** 1–8 (2005).

24. Shum, L. & Nuckolls, G. The life cycle of chondrocytes in the developing skeleton. *Arthritis Res.* **4,** 94–106 (2002).

25. Tchetina, E. V *et al.* Chondrocyte hypertrophy can be induced by a cryptic sequence of type II collagen and is accompanied by the induction of MMP-13 and collagenase activity: implications for development and arthritis. *Matrix Biol.* **26,** 247–58 (2007).

26. Zelzer, E. *et al.* VEGFA is necessary for chondrocyte survival during bone development. *Development* **131,** 2161–2171 (2004).

27. Li, J. & Dong, S. The signaling pathways involved in chondrocyte differentiation and hypertrophic differentiation. *Stem Cells Int.* **2016,** (2016).

28. Aghajanian, P. & Mohan, S. The art of building bone: emerging role of chondrocyte-to-osteoblast transdifferentiation in endochondral ossification. *Bone Res.* **6,** 19 (2018).

29. Jonason, J. H., Xiao, G., Zhang, M., Xing, L. & Chen, D. Post-translational regulation of Runx2 in bone and cartilage. *J. Dent. Res.* **88,** 693–703 (2009).

30. Odgren, P. R., Witwicka, H. & Reyes-Gutierrez, P. The cast of clasts: catabolism and vascular invasion during bone growth, repair, and disease by osteoclasts, chondroclasts, and

septoclasts. doi:10.3109/03008207.2016.1140752

31.   Hayashi, S. *et al.* Interface between intramembranous and endochondral ossification in human foetuses. *Folia Morphol. (Warsz).* **73,** 199–205 (2014).

32.   Sivaraj, K. K. & Adams, R. H. Blood vessel formation and function in bone. *Dev.* **143,** 2706–2715 (2016).

33.   Roselló-Díez, A. & Joyner, A. L. Regulation of long bone growth in vertebrates; It is time to catch up. *Endocr. Rev.* **36,** 646–680 (2015).

34.   Xing, W., Cheng, S., Wergedal, J. & Mohan, S. Epiphyseal chondrocyte secondary ossification centers require thyroid hormone activation of Indian hedgehog and osterix signaling. *J. Bone Miner. Res.* **29,** 2262–2275 (2014).

35.   Provot, S. & Schipani, E. Molecular mechanisms of endochondral bone development. *Biochem. Biophys. Res. Commun.* **328,** 658–665 (2005).

36.   Shim, K. S. Pubertal growth and epiphyseal fusion. *Ann. Pediatr. Endocrinol. Metab.* **20,** 8 (2015).

37.   Karimian, E., Chagin, A. S. & Sävendahl, L. Genetic regulation of the growth plate. *Front. Endocrinol. (Lausanne).* **3,** (2012).

38.   Schipani, E., Kruse, K. & Jüppner, H. A constitutively active mutant PTH-PTHrP receptor in Jansen-type metaphyseal chondrodysplasia. *Science* **268,** 98–100 (1995).

39.   Ballock, R. T. & O'Keefe, R. J. Physiology and pathophysiology of the growth plate. *Birth Defects Res. Part C - Embryo Today Rev.* **69,** 123–143 (2003).

40.   Abad, V. *et al.* The Role of the Resting Zone in Growth Plate Chondrogenesis. *Endocrinology* **143,** 1851–1857 (2002).

41.   Mizuhashi, K. *et al.* Resting zone of the growth plate houses a unique class of skeletal stem cells. *Nature* **563,** 254–258 (2018).

42.   Schrier, L. *et al.* Depletion of resting zone chondrocytes during growth plate senescence. *J. Endocrinol.* **189,** 27–36 (2006).

43.   Wuelling, M. & Vortkamp, A. in *Endocr. Dev.* **21,** 1–11 (Karger Publishers, 2011).

44.   Yang, L., Tsang, K. Y., Tang, H. C., Chan, D. & Cheah, K. S. E. Hypertrophic chondrocytes can become osteoblasts and osteocytes in endochondral bone formation. *Proc. Natl. Acad. Sci. U. S. A.* **111,** 12097–102 (2014).

45.   Tsang, K. Y., Chan, D. & Cheah, K. S. E. Fate of growth plate hypertrophic chondrocytes: Death or lineage extension? *Dev. Growth Differ.* **57,** 179–192 (2015).

46. Wang, Y. *et al.* Insulin-Like Growth Factor-I Is Essential for Embryonic Bone Development. *Endocrinology* **147,** 4753–4761 (2006).

47. Lanske, B. *et al.* PTH/PTHrP Receptor in Early Development and Indian Hedgehog--Regulated Bone Growth. *Science (80-.).* **273,** 663–666 (1996).

48. Karaplis, A. C. *et al.* Lethal skeletal dysplasia from targeted disruption of the parathyroid hormone-related peptide gene. *Genes Dev.* **8,** 277–289 (1994).

49. Weir, E. C. *et al.* Targeted overexpression of parathyroid hormone-related peptide in chondrocytes causes chondrodysplasia and delayed endochondral bone formation. *Proc. Natl. Acad. Sci. U. S. A.* **93,** 10240–5 (1996).

50. O'Shea, P. & Williams, G. Insight into the physiological actions of thyroid hormone receptors from genetically modified mice. *J. Endocrinol.* **175,** 553–570 (2002).

51. Xing, W. *et al.* Genetic evidence that thyroid hormone is indispensable for prepubertal insulin-like growth factor-I expression and bone acquisition in mice. *J. Bone Miner. Res.* **27,** 1067–1079 (2012).

52. Garrison, P., Yue, S., Hanson, J., Baron, J. & Lui, J. C. Spatial regulation of bone morphogenetic proteins (BMPs) in postnatal articular and growth plate cartilage. *PLoS One* **12,** e0176752 (2017).

53. Dao, D. Y. *et al.* Cartilage-specific β-catenin signaling regulates chondrocyte maturation, generation of ossification centers, and perichondrial bone formation during skeletal development. *J. Bone Miner. Res.* **27,** 1680–1694 (2012).

54. Blumer, M. J. F., Longato, S. & Fritsch, H. Structure, formation and role of cartilage canals in the developing bone. *Ann. Anat. - Anat. Anzeiger* **190,** 305–315 (2008).

55. Álvarez, J., Costales, L., Serra, R., Balbín, M. & López, J. M. Expression Patterns of Matrix Metalloproteinases and Vascular Endothelial Growth Factor During Epiphyseal Ossification. *J. Bone Miner. Res.* **20,** 1011–1021 (2005).

56. Magne, D. *et al.* Cartilage formation in growth plate and arteries: from physiology to pathology. *BioEssays* **27,** 708–716 (2005).

57. Schatten, G. *Current topics in developmental biology. Volume 76*. (Academic Press, 2006).

58. Behonick, D. J. *et al.* Role of Matrix Metalloproteinase 13 in Both Endochondral and Intramembranous Ossification during Skeletal Regeneration. *PLoS One* **2,** e1150 (2007).

59. Mark, H., Penington, A., Nannmark, U., Morrison, W. & Messina, A. Microvascular invasion during endochondral ossification in experimental fractures in rats. *Bone* **35,** 535–42 (2004).

60. Chaudhary, L. ., Hofmeister, A. . & Hruska, K. . Differential growth factor control of bone

formation through osteoprogenitor differentiation. *Bone* **34,** 402–411 (2004).

61.   Day, T. F., Guo, X., Garrett-Beal, L. & Yang, Y. Wnt/β-Catenin Signaling in Mesenchymal Progenitors Controls Osteoblast and Chondrocyte Differentiation during Vertebrate Skeletogenesis. *Dev. Cell* **8,** 739–750 (2005).

62.   Samsa, W. E., Zhou, X. & Zhou, G. Signaling Pathways Regulating Cartilage Growth Plate Formation and Activity. doi:10.1016/j.semcdb.2016.07.008

63.   Knight, C. *et al.* Epidermal growth factor can signal via β-catenin to control proliferation of mesenchymal stem cells independently of canonical Wnt signalling. *Cell. Signal.* **53,** 256–268 (2019).

64.   Juneja, P. & Hubbard, J. B. *Anatomy, Joints*. *StatPearls* (2019). at <http://www.ncbi.nlm.nih.gov/pubmed/29939670>

65.   Salva, J. E. & Merrill, A. E. Signaling networks in joint development. *Dev. Dyn.* **246,** 262–274 (2017).

66.   Chijimatsu, R. & Saito, T. Mechanisms of synovial joint and articular cartilage development. *Cell. Mol. Life Sci.* **76,** 3939–3952 (2019).

67.   Hatakeyama, Y., Tuan, R. S. & Shum, L. Distinct functions of BMP4 and GDF5 in the regulation of chondrogenesis. *J. Cell. Biochem.* **91,** 1204–1217 (2004).

68.   Archer, C. W., Morrison, H. & Pitsillides, A. A. Cellular aspects of the development of diarthrodial joints and articular cartilage. *J. Anat.* **184 (Pt 3),** 447–56 (1994).

69.   Hyde, G., Dover, S., Aszodi, A., Wallis, G. A. & Boot-Handford, R. P. Lineage tracing using matrilin-1 gene expression reveals that articular chondrocytes exist as the joint interzone forms. *Dev. Biol.* **304,** 825–33 (2007).

70.   Singh, P. N. P., Ray, A., Azad, K. & Bandyopadhyay, A. A comprehensive mRNA expression analysis of developing chicken articular cartilage. *Gene Expr. Patterns* **20,** 22–31 (2016).

71.   Ray, A., Singh, P. N. P., Sohaskey, M. L., Harland, R. M. & Bandyopadhyay, A. Precise spatial restriction of BMP signaling is essential for articular cartilage differentiation. *Development* **142,** 1169–1179 (2015).

72.   Seemann, P. *et al.* Mutations in GDF5 Reveal a Key Residue Mediating BMP Inhibition by NOGGIN. *PLoS Genet.* **5,** e1000747 (2009).

73.   Koyama, E. *et al.* A distinct cohort of progenitor cells participates in synovial joint and articular cartilage formation during mouse limb skeletogenesis. *Dev. Biol.* **316,** 62–73 (2008).

74.   Heegaard, J. H., Beaupré, G. S. & Carter, D. R. Mechanically modulated cartilage growth

may regulate joint surface morphogenesis. *J. Orthop. Res.* **17,** 509–517 (1999).

75. Stevens, S. S., Beaupré, G. S. & Carter, D. R. Computer model of endochondral growth and ossification in long bones: Biological and mechanobiological influences. *J. Orthop. Res.* **17,** 646–653 (1999).

76. Pacifici, M., Koyama, E. & Iwamoto, M. Mechanisms of synovial joint and articular cartilage formation: Recent advances, but many lingering mysteries. *Birth Defects Res. Part C Embryo Today Rev.* **75,** 237–248 (2005).

77. Longobardi, L. *et al.* Synovial joints: from development to homeostasis. *Curr. Osteoporos. Rep.* **13,** 41–51 (2015).

78. Kurowska-Stolarska, M. & Alivernini, S. Synovial tissue macrophages: friend or foe? *RMD Open* **3,** e000527 (2017).

79. BANK, R. A., BAYLISS, M. T., LAFEBER, F. P. J. G., MAROUDAS, A. & TEKOPPELE, J. M. Ageing and zonal variation in post-translational modification of collagen in normal human articular cartilage: The age-related increase in non-enzymatic glycation affects biomechanical properties of cartilage. *Biochem. J.* **330,** 345–351 (1998).

80. Rhee, D. K. *et al.* The secreted glycoprotein lubricin protects cartilage surfaces and inhibits synovial cell overgrowth. *J. Clin. Invest.* **115,** 622–631 (2005).

81. Bennike, T. *et al.* A normative study of the synovial fluid proteome from healthy porcine knee joints. *J. Proteome Res.* **13,** 4377–87 (2014).

82. Tamer, T. M. Hyaluronan and synovial joint: function, distribution and healing. *Interdiscip. Toxicol.* **6,** 111–25 (2013).

83. Bartok, B. & Firestein, G. S. Fibroblast-like synoviocytes: key effector cells in rheumatoid arthritis. *Immunol. Rev.* **233,** 233–55 (2010).

84. Suri, S. & Walsh, D. A. Osteochondral alterations in osteoarthritis. *Bone* **51,** 204–211 (2012).

85. Sharma, A. R., Jagga, S., Lee, S.-S. & Nam, J.-S. Interplay between cartilage and subchondral bone contributing to pathogenesis of osteoarthritis. *Int. J. Mol. Sci.* **14,** 19805–30 (2013).

86. Birchard, Z. & Tuck, J. A. *Discoid Meniscus*. *StatPearls* (StatPearls Publishing, 2019). at <http://www.ncbi.nlm.nih.gov/pubmed/29261944>

87. Makris, E. A., Hadidi, P. & Athanasiou, K. A. The knee meniscus: structure-function, pathophysiology, current repair techniques, and prospects for regeneration. *Biomaterials* **32,** 7411–31 (2011).

88. Goldring, M. B. & Goldring, S. R. Articular cartilage and subchondral bone in the

pathogenesis of osteoarthritis. *Ann. N. Y. Acad. Sci.* **1192,** 230–237 (2010).

89.   Stewart, H. L. & Kawcak, C. E. The Importance of Subchondral Bone in the Pathophysiology of Osteoarthritis. *Front. Vet. Sci.* **5,** 178 (2018).

90.   Kaspiris, A. *et al.* Subchondral cyst development and MMP-1 expression during progression of osteoarthritis: An immunohistochemical study. *Orthop. Traumatol. Surg. Res.* **99,** 523–529 (2013).

91.   Adebayo, O. O. *et al.* Role of subchondral bone properties and changes in development of load-induced osteoarthritis in mice. *Osteoarthr. Cartil.* **25,** 2108–2118 (2017).

92.   Zhou, S., Cui, Z. & Urban, J. P. G. Factors influencing the oxygen concentration gradient from the synovial surface of articular cartilage to the cartilage-bone interface: A modeling study. *Arthritis Rheum.* **50,** 3915–3924 (2004).

93.   Gupte, C. & Mart, J.-P. S. The acute swollen knee: diagnosis and management. *J. R. Soc. Med.* **106,** 259 (2013).

94.   Hukkanen, M. *et al.* Distribution of nerve endings and sensory neuropeptides in rat synovium, meniscus and bone. *Int. J. Tissue React.* **14,** 1–10 (1992).

95.   Grässel, S. & Muschter, D. Peripheral Nerve Fibers and Their Neurotransmitters in Osteoarthritis Pathology. *Int. J. Mol. Sci.* **18,** (2017).

96.   Budd, E., Nalesso, G. & Mobasheri, A. Extracellular genomic biomarkers of osteoarthritis. *Expert Rev. Mol. Diagn.* **18,** 55–74 (2018).

97.   Sandell, L. & Aigner, T. Articular cartilage and changes in artritis An introduction: Cell biology of osteoarthritis. *Arthritis Res* **3,** 107–113 (2001).

98.   Green, E. M., Mansfield, J. C., Bell, J. S. & Winlove, C. P. The structure and micromechanics of elastic tissue. *Interface Focus* **4,** 20130058 (2014).

99.   Mansfield, J. *et al.* The elastin network: its relationship with collagen and cells in articular cartilage as visualized by multiphoton microscopy. *J. Anat.* **215,** 682–691 (2009).

100.   Becker, I., Woodley, S. J. & Stringer, M. D. The adult human pubic symphysis: a systematic review. *J. Anat.* **217,** 475–87 (2010).

101.   Gharpuray, V. M. in *Handb. Biomater. Prop.* 48–58 (Springer US, 1998). doi:10.1007/978-1-4615-5801-9_5

102.   Delgado-Martos, M. J. *et al.* Does the epiphyseal cartilage of the long bones have one or two ossification fronts? *Med. Hypotheses* **81,** 695–700 (2013).

103.   Goldring, M. B. Chondrogenesis, chondrocyte differentiation, and articular cartilage metabolism in health and osteoarthritis. *Ther. Adv. Musculoskelet. Dis.* **4,** 269–285 (2012).

104. Pomin, V. H. & Mulloy, B. Glycosaminoglycans and Proteoglycans. *Pharmaceuticals (Basel).* **11,** (2018).

105. Chubinskaya, S. *et al.* Response of Human Chondrocytes Prepared for Autologous Implantation to Growth Factors. *J Knee Surg* **2121,** 192–199 (2008).

106. Ling, W., Regatte, R. R., Navon, G. & Jerschow, A. Assessment of glycosaminoglycan concentration in vivo by chemical exchange-dependent saturation transfer (gagCEST). *Proc. Natl. Acad. Sci.* **105,** 2266–2270 (2008).

107. Waller, K. A. *et al.* Role of lubricin and boundary lubrication in the prevention of chondrocyte apoptosis. *Proc. Natl. Acad. Sci. U. S. A.* **110,** 5852–7 (2013).

108. Loeser, R. F., Collins, J. A. & Diekman, B. O. Ageing and the pathogenesis of osteoarthritis. *Nat. Publ. Gr.* **12,** (2016).

109. Goldring, M. B. & Goldring, S. R. Osteoarthritis. *J. Cell. Physiol.* **213,** 626–634 (2007).

110. Eyre, D. R., Weis, M. A. & Wu, J.-J. Articular cartilage collagen: an irreplaceable framework? *Eur. Cell. Mater.* **12,** 57–63 (2006).

111. Mobasheri, A. The future of osteoarthritis therapeutics: emerging biological therapy. *Curr. Rheumatol. Rep.* **15,** 385 (2013).

112. Fox, A. J. S., Bedi, A. & Rodeo, S. A. The Basic Science of Articular Cartilage: Structure, Composition, and Function. (2009). doi:10.1177/1941738109350438

113. Poole, A. R. *et al.* Composition and Structure of Articular Cartilage. *Clin. Orthop. Relat. Res.* **391,** S26–S33 (2003).

114. Wong, B. L., Bae, W. C., Gratz, K. R. & Sah, R. L. Shear deformation kinematics during cartilage articulation: effect of lubrication, degeneration, and stress relaxation. *Mol. Cell. Biomech.* **5,** 197–206 (2008).

115. Jessop, Z. M. *et al.* Tissue specific stem/progenitor cells for cartilage tissue engineering: A systematic review of the literature. *Appl. Phys. Rev.* **6,** 031301 (2019).

116. Kong, L., Zheng, L.-Z., Qin, L. & Ho, K. K. W. Role of mesenchymal stem cells in osteoarthritis treatment. *J. Orthop. Transl.* **9,** 89–103 (2017).

117. Jay, G. D., Harris, D. A. & Cha, C. J. Boundary lubrication by lubricin is mediated by O-linked beta(1-3)Gal-GalNAc oligosaccharides. *Glycoconj. J.* **18,** 807–15 (2001).

118. Karamchedu, N. P. *et al.* Superficial zone cellularity is deficient in mice lacking lubricin: a stereoscopic analysis. *Arthritis Res. Ther.* **18,** 64 (2016).

119. Thompson, A. M. & Stockwell, R. A. An ultrastructural study of the marginal transitional zone in the rabbit knee joint. *J. Anat.* **136,** 701–13 (1983).

120. Decker, R. S., Koyama, E. & Pacifici, M. Articular Cartilage: Structural and Developmental Intricacies and Questions. *Curr. Osteoporos. Rep.* **13,** 407–14 (2015).

121. Amanatullah, D. F., Yamane, S. & Reddi, A. H. Distinct patterns of gene expression in the superficial, middle and deep zones of bovine articular cartilage. *J. Tissue Eng. Regen. Med.* **8,** n/a-n/a (2012).

122. Lotz, M. K. *et al.* Cartilage cell clusters. *Arthritis Rheum.* **62,** 2206–18 (2010).

123. Schultz, M., Molligan, J., Schon, L. & Zhang, Z. Pathology of the calcified zone of articular cartilage in post-traumatic osteoarthritis in rat knees. *PLoS One* **10,** e0120949 (2015).

124. Lammi, P. E. *et al.* Site-specific immunostaining for type X collagen in noncalcified articular cartilage of canine stifle knee joint. *Bone* **31,** 690–6 (2002).

125. Li, G. *et al.* Subchondral bone in osteoarthritis: insight into risk factors and microstructural changes. *Arthritis Res. Ther.* **15,** 223 (2013).

126. Luo, Y. *et al.* The minor collagens in articular cartilage. *Protein Cell* **8,** 560–572 (2017).

127. Wilusz, R. E., Sanchez-Adams, J. & Guilak, F. The structure and function of the pericellular matrix of articular cartilage. *Matrix Biol.* **39,** 25–32 (2014).

128. Guilak, F. & Mow, V. C. The mechanical environment of the chondrocyte: a biphasic finite element model of cell-matrix interactions in articular cartilage. *J. Biomech.* **33,** 1663–73 (2000).

129. Muir, H. The chondrocyte, architect of cartilage. Biomechanics, structure, function and molecular biology of cartilage matrix macromolecules. *BioEssays* **17,** 1039–1048 (1995).

130. Nugent-Derfus, G. E. *et al.* Continuous passive motion applied to whole joints stimulates chondrocyte biosynthesis of PRG4. *Osteoarthr. Cartil.* **15,** 566–574 (2007).

131. Shioji, S., Imai, S., Ando, K., Kumagai, K. & Matsusue, Y. Extracellular and Intracellular Mechanisms of Mechanotransduction in Three-Dimensionally Embedded Rat Chondrocytes. *PLoS One* **9,** e114327 (2014).

132. Mueller, M. B. & Tuan, R. S. Anabolic/Catabolic Balance in Pathogenesis of Osteoarthritis: Identifying Molecular Targets. *PM&R* **3,** S3–S11 (2011).

133. Sachs, F. Stretch-activated ion channels: what are they? *Physiology (Bethesda).* **25,** 50–6 (2010).

134. Felsenthal, N. & Zelzer, E. Mechanical regulation of musculoskeletal system development. *Development* **144,** 4271–4283 (2017).

135. Goldring, M. B. & Berenbaum, F. The Regulation of Chondrocyte Function by Proinflammatory Mediators. *Clin. Orthop. Relat. Res.* **427,** S37–S46 (2004).

136. Longobardi, L. *et al.* Effect of IGF-I in the Chondrogenesis of Bone Marrow Mesenchymal Stem Cells in the Presence or Absence of TGF-β Signaling. *J. Bone Miner. Res.* **21,** 626–636 (2005).

137. Poniatowski, Ł. A., Wojdasiewicz, P., Gasik, R. & Szukiewicz, D. Transforming growth factor Beta family: insight into the role of growth factors in regulation of fracture healing biology and potential clinical applications. *Mediators Inflamm.* **2015,** 137823 (2015).

138. Beenken, A. & Mohammadi, M. The FGF family: biology, pathophysiology and therapy. *Nat. Rev. Drug Discov.* **8,** 235–253 (2009).

139. Davidson, D. *et al.* Fibroblast Growth Factor (FGF) 18 Signals through FGF Receptor 3 to Promote Chondrogenesis. *J. Biol. Chem.* **280,** 20509–20515 (2005).

140. Cawston, T. E. & Young, D. A. Proteinases involved in matrix turnover during cartilage and bone breakdown. *Cell Tissue Res.* **339,** 221–35 (2010).

141. Kobayashi, M. *et al.* Role of interleukin-1 and tumor necrosis factor ? in matrix degradation of human osteoarthritic cartilage. *Arthritis Rheum.* **52,** 128–135 (2005).

142. López-Armada, M. J. *et al.* Cytokines, tumor necrosis factor-α and interleukin-1β, differentially regulate apoptosis in osteoarthritis cultured human chondrocytes. *Osteoarthr. Cartil.* **14,** 660–669 (2006).

143. Vincenti, M. P. & Brinckerhoff, C. E. Transcriptional regulation of collagenase (MMP-1, MMP-13) genes in arthritis: integration of complex signaling pathways for the recruitment of gene-specific transcription factors. *Arthritis Res.* **4,** 157 (2002).

144. Millward-Sadler, S. J. *et al.* Integrin-regulated Secretion of Interleukin 4: A Novel Pathway of Mechanotransduction in Human Articular Chondrocytes. *J. Cell Biol.* **145,** 183–189 (1999).

145. Meszaros, E. & Malemud, C. J. Prospects for treating osteoarthritis: enzyme-protein interactions regulating matrix metalloproteinase activity. *Ther. Adv. Chronic Dis.* **3,** 219–29 (2012).

146. Ge, H., Zou, F., Li, Y., Liu, A. & Tu, M. JNK pathway in osteoarthritis: pathological and therapeutic aspects. *J. Recept. Signal Transduct.* **37,** 431–436 (2017).

147. Pereira, D. *et al.* The effect of osteoarthritis definition on prevalence and incidence estimates: a systematic review. *Osteoarthr. Cartil.* **19,** 1270–1285 (2011).

148. Sandell, L. J. Etiology of osteoarthritis: genetics and synovial joint development. *Nat. Rev. Rheumatol.* **8,** 77–89 (2012).

149. Chen, D. *et al.* Osteoarthritis: toward a comprehensive understanding of pathological mechanism. *Nat. Publ. Gr.* **5,** (2016).

150. Øiestad, B. E., Engebretsen, L., Storheim, K. & Risberg, M. A. Winner of the 2008 Systematic Review Competition: Knee Osteoarthritis after Anterior Cruciate Ligament Injury. *Am. J. Sports Med.* **37,** 1434–1443 (2009).

151. Sharma, L. *et al.* Varus and valgus alignment and incident and progressive knee osteoarthritis. *Ann. Rheum. Dis.* **69,** 1940–1945 (2010).

152. ARDEN, N. & NEVITT, M. Osteoarthritis: Epidemiology. *Best Pract. Res. Clin. Rheumatol.* **20,** 3–25 (2006).

153. Martin, J. A. & Buckwalter, J. A. Aging, articular cartilage chondrocyte senescence and osteoarthritis. *Biogerontology* **3,** 257–64 (2002).

154. Aigner, T., Zien, A., Gehrsitz, A., Gebhard, P. M. & McKenna, L. Anabolic and catabolic gene expression pattern analysis in normal versus osteoarthritic cartilage using complementary DNA-array technology. *Arthritis Rheum.* **44,** 2777–89 (2001).

155. Yu, S.-M. & Kim, S.-J. The thymoquinone-induced production of reactive oxygen species promotes dedifferentiation through the ERK pathway and inflammation through the p38 and PI3K pathways in rabbit articular chondrocytes. *Int. J. Mol. Med.* **35,** 325–32 (2015).

156. Vaamonde-García, C. *et al.* Mitochondrial dysfunction increases inflammatory responsiveness to cytokines in normal human chondrocytes. *Arthritis Rheum.* **64,** 2927–2936 (2012).

157. Jeon, O. H. *et al.* Local clearance of senescent cells attenuates the development of post-traumatic osteoarthritis and creates a pro-regenerative environment. *Nat. Med.* **23,** 775–781 (2017).

158. Yamada, K., Healey, R., Amiel, D., Lotz, M. & Coutts, R. Subchondral bone of the human knee joint in aging and osteoarthritis. *Osteoarthr. Cartil.* **10,** 360–369 (2002).

159. Goodpaster, B. H. *et al.* The Loss of Skeletal Muscle Strength, Mass, and Quality in Older Adults: The Health, Aging and Body Composition Study. *Journals Gerontol. Ser. A Biol. Sci. Med. Sci.* **61,** 1059–1064 (2006).

160. Hasegawa, A. *et al.* Anterior cruciate ligament changes in the human knee joint in aging and osteoarthritis. *Arthritis Rheum.* **64,** 696–704 (2012).

161. Hame, S. L. & Alexander, R. A. Knee osteoarthritis in women. doi:10.1007/s12178-013-9164-0

162. Hanna, F. S. *et al.* Women have increased rates of cartilage loss and progression of cartilage defects at the knee than men. *Menopause* **16,** 666–670 (2009).

163. Chappell, J. D., Yu, B., Kirkendall, D. T. & Garrett, W. E. A Comparison of Knee Kinetics between Male and Female Recreational Athletes in Stop-Jump Tasks. *Am. J. Sports Med.* **30,** 261–267 (2002).

164. Xiao, Y.-P. *et al.* Are estrogen-related drugs new alternatives for the management of osteoarthritis? *Arthritis Res. Ther.* **18,** 151 (2016).

165. Ma, H.-L. *et al.* Osteoarthritis severity is sex dependent in a surgical mouse model. *Osteoarthr. Cartil.* **15,** 695–700 (2007).

166. Fernández-Moreno, M., Rego, I., Carreira-Garcia, V. & Blanco, F. J. Genetics in osteoarthritis. *Curr. Genomics* **9,** 542–7 (2008).

167. MacGregor, A. & Spector, T. D. Twins and the genetic architecture of osteoarthritis. *Rheumatology* **38,** 583–588 (1999).

168. Loughlin, J. Genetic contribution to osteoarthritis development: current state of evidence. doi:10.1097/BOR.0000000000000171

169. Stefánsson, S. E. *et al.* Genomewide scan for hand osteoarthritis: a novel mutation in matrilin-3. *Am. J. Hum. Genet.* **72,** 1448–59 (2003).

170. Loughlin, J., Dowling, B., Mustafa, Z. & Chapman, K. Association of the interleukin-1 gene cluster on chromosome 2q13 with knee osteoarthritis. *Arthritis Rheum.* **46,** 1519–1527 (2002).

171. Castaño-Betancourt, M. C. *et al.* Novel Genetic Variants for Cartilage Thickness and Hip Osteoarthritis. *PLoS Genet.* **12,** e1006260 (2016).

172. Cui, G. *et al.* Association of Common Variants in TGFA with Increased Risk of Knee Osteoarthritis Susceptibility. *Genet. Test. Mol. Biomarkers* gtmb.2017.0045 (2017). doi:10.1089/gtmb.2017.0045

173. Coggon, D. *et al.* Knee osteoarthritis and obesity. *Int. J. Obes.* **25,** 622–627 (2001).

174. Kalichman, L. & Hernández-Molina, G. Hand Osteoarthritis: An Epidemiological Perspective. *Semin. Arthritis Rheum.* **39,** 465–476 (2010).

175. Gualillo, O. Further evidence for leptin involvement in cartilage homeostases. *Osteoarthr. Cartil.* **15,** 857–860 (2007).

176. Sommer, C. & Kress, M. Recent findings on how proinflammatory cytokines cause pain: peripheral mechanisms in inflammatory and neuropathic hyperalgesia. *Neurosci. Lett.* **361,** 184–187 (2004).

177. Liu, Q. *et al.* Effects of mechanical stress on chondrocyte phenotype and chondrocyte extracellular matrix expression. *Sci. Reports 2016 6* **6,** 37268 (2016).

178. Sandmark, H. & Vingård, E. Sports and risk for severe osteoarthrosis of the knee. *Scand. J. Med. Sci. Sports* **9,** 279–284 (2007).

179. Punzi, L. *et al.* Post-traumatic arthritis: overview on pathogenic mechanisms and role of

inflammation. *RMD open* **2,** e000279 (2016).

180. Englund, M., Roos, E. M. & Lohmander, L. S. Impact of type of meniscal tear on radiographic and symptomatic knee osteoarthritis: A sixteen-year followup of meniscectomy with matched controls. *Arthritis Rheum.* **48,** 2178–2187 (2003).

181. Mansfield, J. C., Bell, J. S. & Winlove, C. P. The micromechanics of the superficial zone of articular cartilage. *Osteoarthr. Cartil.* **23,** 1806–1816 (2015).

182. Glasson, S. S., Chambers, M. G., Van Den Berg, W. B. & Little, C. B. The OARSI histopathology initiative – recommendations for histological assessments of osteoarthritis in the mouse. *Osteoarthr. Cartil.* **18,** S17–S23 (2010).

183. Hunter, D. J., Guermazi, A., Roemer, F., Zhang, Y. & Neogi, T. Structural correlates of pain in joints with osteoarthritis. *Osteoarthr. Cartil.* **21,** 1170–1178 (2013).

184. Loeser, R. F., Goldring, S. R., Scanzello, C. R. & Goldring, M. B. Osteoarthritis: A disease of the joint as an organ. *Arthritis Rheum.* **64,** 1697–1707 (2012).

185. Wen, C., Lu, W. W. & Chiu, K. Y. Importance of subchondral bone in the pathogenesis and management of osteoarthritis from bench to bed. *J. Orthop. Transl.* **2,** 16–25 (2014).

186. Netzer, C. *et al.* Comparative Analysis of Bone Structural Parameters Reveals Subchondral Cortical Plate Resorption and Increased Trabecular Bone Remodeling in Human Facet Joint Osteoarthritis. *Int. J. Mol. Sci.* **19,** 845 (2018).

187. Lyons, T. J., McClure, S. F., Stoddart, R. W. & McClure, J. The normal human chondro-osseous junctional region: evidence for contact of uncalcified cartilage with subchondral bone and marrow spaces. *BMC Musculoskelet. Disord.* **7,** 52 (2006).

188. Link, T. M. *et al.* Osteoarthritis: MR Imaging Findings in Different Stages of Disease and Correlation with Clinical Findings. *Radiology* **226,** 373–381 (2003).

189. van der Kraan, P. M. & van den Berg, W. B. Osteophytes: relevance and biology. *Osteoarthr. Cartil.* **15,** 237–244 (2007).

190. Blaney Davidson, E. N., Vitters, E. L., van der Kraan, P. M. & van den Berg, W. B. Expression of transforming growth factor- (TGF) and the TGF signalling molecule SMAD-2P in spontaneous and instability-induced osteoarthritis: role in cartilage degradation, chondrogenesis and osteophyte formation. *Ann. Rheum. Dis.* **65,** 1414–1421 (2006).

191. Geurts, J. *et al.* Elevated marrow inflammatory cells and osteoclasts in subchondral osteosclerosis in human knee osteoarthritis. *J. Orthop. Res.* **34,** 262–269 (2016).

192. AIGNER, T., SACHSE, A., GEBHARD, P. & ROACH, H. Osteoarthritis: Pathobiology—targets and ways for therapeutic intervention☆. *Adv. Drug Deliv. Rev.* **58,** 128–149 (2006).

193. de Lange-Brokaar, B. J. E. *et al.* Synovial inflammation, immune cells and their cytokines in osteoarthritis: a review. *Osteoarthr. Cartil.* **20,** 1484–1499 (2012).

194. TAMAKI, Y. *et al.* Expression of Toll-like Receptors and Their Signaling Pathways in Rheumatoid Synovitis. *J. Rheumatol.* **38,** 810–820 (2011).

195. Kawai, T. & Akira, S. Signaling to NF-κB by Toll-like receptors. *Trends Mol. Med.* **13,** 460–469 (2007).

196. Loeuille, D. *et al.* Macroscopic and microscopic features of synovial membrane inflammation in the osteoarthritic knee: Correlating magnetic resonance imaging findings with disease severity. *Arthritis Rheum.* **52,** 3492–3501 (2005).

197. Bartley, E. J., Assistant Professor, R., Palit, S., Graduate Student, M. & Staud, R. Predictors of Osteoarthritis Pain: The Importance of Resilience. doi:10.1007/s11926-017-0683-3

198. Lee, A. *et al.* A Current Review of Molecular Mechanisms Regarding Osteoarthritis and Pain. *Gene* **527,** 440–447 (2013).

199. Miller, R. E. *et al.* The Role of Peripheral Nociceptive Neurons in the Pathophysiology of Osteoarthritis Pain. *Curr. Osteoporos. Rep.* **13,** 318 (2015).

200. Barr, A. J. *et al.* A systematic review of the relationship between subchondral bone features, pain and structural pathology in peripheral joint osteoarthritis. *Arthritis Res. Ther.* **17,** 228 (2015).

201. Hunter, D. J., McDougall, J. J. & Keefe, F. J. The Symptoms of Osteoarthritis and the Genesis of Pain. *Med. Clin. North Am.* **93,** 83–100 (2009).

202. Man, G. S. & Mologhianu, G. Osteoarthritis pathogenesis - a complex process that involves the entire joint. *J. Med. Life* **7,** 37–41 (2014).

203. Zarebska, J. M. *et al.* CCL2 and CCR2 regulate pain-related behaviour and early gene expression in post-traumatic murine osteoarthritis but contribute little to chondropathy. *Osteoarthr. Cartil.* **25,** 406 (2017).

204. Brown, M. T. *et al.* Tanezumab Reduces Osteoarthritic Hip Pain: Results of a Randomized, Double-Blind, Placebo-Controlled Phase III Trial. *Arthritis Rheum.* **65,** 1795–1803 (2013).

205. Li, Q., Amano, K., Link, T. M. & Ma, C. B. Advanced Imaging in Osteoarthritis. *Sports Health* **8,** 418 (2016).

206. Siebelt, M., Agricola, R., Weinans, H. & Kim, Y. J. The role of imaging in early hip OA. *Osteoarthr. Cartil.* **22,** 1470–1480 (2014).

207. Mcalindon, T. E. E. *et al.* OARSI guidelines for the non-surgical management of knee osteoarthritis. *Osteoarthr. Cartil.* **22,** 363–388 (2014).

208. Demehri, S., Hafezi-Nejad, N. & Carrino, J. A. Conventional and novel imaging modalities in osteoarthritis. *Curr. Opin. Rheumatol.* **27,** 295–303 (2015).

209. Cho, H., Walker, A., Williams, J. & Hasty, K. A. Study of Osteoarthritis Treatment with Anti-Inflammatory Drugs: Cyclooxygenase-2 Inhibitor and Steroids. *Biomed Res. Int.* **2015,** (2015).

210. Bisicchia, S. & Tudisco, C. Hyaluronic acid vs corticosteroids in symptomatic knee osteoarthritis: a mini-review of the literature. *Clin. Cases Miner. Bone Metab.* **14,** 182 (2017).

211. Bannuru, R. R. *et al.* Therapeutic trajectory of hyaluronic acid versus corticosteroids in the treatment of knee osteoarthritis: A systematic review and meta-analysis. *Arthritis Rheum.* **61,** 1704–1711 (2009).

212. Roddy, E., Zhang, W. & Doherty, M. Aerobic walking or strengthening exercise for osteoarthritis of the knee? A systematic review. *Ann. Rheum. Dis.* **64,** 544 (2005).

213. Van Baar, M. E., Assendelft, W. J. J., Dekker, J., Oostendorp, R. A. B. & Bijlsma, J. W. J. Effectiveness of exercise therapy in patients with osteoarthritis of the hip or knee: A systematic review of randomized clinical trials. *Arthritis Rheum.* **42,** 1361–1369 (1999).

214. St. Clair, S. F. *et al.* Hip and Knee Arthroplasty in the Geriatric Population. *Clin. Geriatr. Med.* **22,** 515–533 (2006).

215. Knowles, L., Luth, W. & Bubela, T. Paving the road to personalized medicine: recommendations on regulatory, intellectual property and reimbursement challenges. *J. Law Biosci.* **4,** 453 (2017).

216. Kang, E. H. *et al.* Adiponectin is a potential catabolic mediator in osteoarthritis cartilage. *Arthritis Res. Ther.* **12,** R231 (2010).

217. Stannus, O. *et al.* Circulating levels of IL-6 and TNF-α are associated with knee radiographic osteoarthritis and knee cartilage loss in older adults. *Osteoarthr. Cartil.* **18,** 1441–1447 (2010).

218. Schlessinger, J. Receptor Tyrosine Kinases: Legacy of the First Two Decades. *Cold Spring Harb. Perspect. Biol.* **6,** a008912 (2014).

219. Schneider, M. R. The EGFR network in bone biology and pathology. *Trends Endocrinol. Metab.* **20,** (2009).

220. Schneider, M. R. & Wolf, E. The epidermal growth factor receptor ligands at a glance. *J. Cell. Physiol.* **218,** 460–6 (2009).

221. Olayioye, M. A., Neve, R. M., Lane, H. A. & Hynes, N. E. The ErbB signaling network: receptor heterodimerization in development and cancer. *EMBO J.* **19,** 3159–67 (2000).

222. Dawson, J. P. *et al.* Epidermal Growth Factor Receptor Dimerization and Activation Require Ligand-Induced Conformational Changes in the Dimer Interface. *Mol. Cell. Biol.* **25,** 7734 (2005).

223. Cross, D. A. E., Alessi, D. R., Cohen, P., Andjelkovich, M. & Hemmings, B. A. Inhibition of glycogen synthase kinase-3 by insulin mediated by protein kinase B. *Nature* **378,** 785–789 (1995).

224. Fan, H. Ectodomain shedding of TGF-alpha and other transmembrane proteins is induced by receptor tyrosine kinase activation and MAP kinase signaling cascades. *EMBO J.* **18,** 6962–6972 (1999).

225. Wilson, K. J., Gilmore, J. L., Foley, J., Lemmon, M. A. & Riese, D. J. Functional selectivity of EGF family peptide growth factors: Implications for cancer. *Pharmacol. Ther.* **122,** 1–8 (2009).

226. Blobel, C. P. ADAMs: key components in EGFR signalling and development. *Nat. Rev. Mol. Cell Biol.* **6,** 32–43 (2005).

227. Burgess, A. W. *et al.* An Open-and-Shut Case? Recent Insights into the Activation of EGF/ErbB Receptors. *Mol. Cell* **12,** 541–552 (2003).

228. Zhang, X., Gureasko, J., Shen, K., Cole, P. A. & Kuriyan, J. An Allosteric Mechanism for Activation of the Kinase Domain of Epidermal Growth Factor Receptor. *Cell* **125,** 1137–1149 (2006).

229. Anastasi, S., Castellani, L., Alemà, S. & Segatto, O. A pervasive role for MIG6 in restraining cell proliferation. *Cell Death Differ.* **21,** 345–347 (2013).

230. Selvarajah, G. T. *et al.* Expression of epidermal growth factor receptor in canine osteosarcoma: association with clinicopathological parameters and prognosis. *Vet. J.* **193,** 412–9 (2012).

231. Zhang, Y.-W. *et al.* Evidence that MIG-6 is a tumor-suppressor gene. *Oncogene* **26,** 269–276 (2007).

232. Appleton, C. T. G., Usmani, S. E., Bernier, S. M., Aigner, T. & Beier, F. Transforming growth factor alpha suppression of articular chondrocyte phenotype and Sox9 expression in a rat model of osteoarthritis. *Arthritis Rheum.* **56,** 3693–705 (2007).

233. Appleton, C. T. G., Pitelka, V., Henry, J. & Beier, F. Global analyses of gene expression in early experimental osteoarthritis. *Arthritis Rheum.* **56,** 1854–1868 (2007).

234. Usmani, S. E. *et al.* Transforming growth factor alpha controls the transition from hypertrophic cartilage to bone during endochondral bone growth. *Bone* **51,** 131–141 (2012).

235. Appleton, C. T. G., Usmani, S. E., Mort, J. S. & Beier, F. Rho/ROCK and MEK/ERK activation by transforming growth factor-α induces articular cartilage degradation. *Lab.*

Investig. **90,** 20 (2009).

236. Appleton, C. T. G., McErlain, D. D., Henry, J. L., Holdsworth, D. W. & Beier, F. Molecular and histological analysis of a new rat model of experimental knee osteoarthritis. *Ann. N. Y. Acad. Sci.* **1117,** 165–174 (2007).

237. Qin, L. & Beier, F. EGFR Signaling: Friend or Foe for Cartilage? *JBMR Plus* **3,** e10177 (2019).

238. Zhang, X. *et al.* The critical role of the epidermal growth factor receptor in endochondral ossification. *J. Bone Miner. Res.* **26,** 2622–33 (2011).

239. Chandra, A., Lan, S., Zhu, J., Siclari, V. A. & Qin, L. Epidermal Growth Factor Receptor (EGFR) Signaling Promotes Proliferation and Survival in Osteoprogenitors by Increasing Early Growth Response 2 (EGR2) Expression. *J. Biol. Chem.* **288,** 20488–20498 (2013).

240. Zhang, X. *et al.* Epidermal Growth Factor Receptor (EGFR) Signaling Regulates Epiphyseal Cartilage Development through β-Catenin-dependent and -independent Pathways. *J. Biol. Chem.* **288,** 32229–32240 (2013).

241. Hallbeck, A. L., Walz, T. M., Briheim, K. & Wasteson, A. TGF-alpha and ErbB2 production in synovial joint tissue: increased expression in arthritic joints. *Scand. J. Rheumatol.* **34,** 204–11

242. Klooster, A. R. *et al.* Tumor necrosis factor alpha and epidermal growth factor act additively to inhibit matrix gene expression by chondrocyte. *Arthritis Res. Ther.* **7,** R127 (2005).

243. Tajima, Y., Kato, K., Kashimata, M., Hiramatsu, M. & Utsumi, N. Immunohistochemical analysis of EGF in epiphyseal growth plate from normal, hypophysectomized, and growth hormone-treated hypophysectomized rats. *Cell Tissue Res.* **278,** 279–282 (1994).

244. Long, D. L., Ulici, V., Chubinskaya, S. & Loeser, R. F. Heparin-binding epidermal growth factor-like growth factor (HB-EGF) is increased in osteoarthritis and regulates chondrocyte catabolic and anabolic activities. *Osteoarthritis Cartilage* **23,** 1523–31 (2015).

245. Halevy, O., Schindler, D., Hurwitz, S. & Pines, M. Epidermal growth factor receptor gene expression in avian epiphyseal growth-plate cartilage cells: effect of serum, parathyroid hormone and atrial natriuretic peptide. *Mol. Cell. Endocrinol.* **75,** 229–35 (1991).

246. Yoon, Y. M. *et al.* Epidermal growth factor negatively regulates chondrogenesis of mesenchymal cells by modulating the protein kinase C-alpha, Erk-1, and p38 MAPK signaling pathways. *J. Biol. Chem.* **275,** 12353–9 (2000).

247. Usmani, S. E. *et al.* Context-specific protection of TGFα null mice from osteoarthritis. *Sci. Rep.* **6,** 30434 (2016).

248. Appleton, C. T. G. *et al.* Reduction in disease progression by inhibition of transforming growth factor α-CCL2 signaling in experimental posttraumatic osteoarthritis. *Arthritis*

Rheumatol. (Hoboken, N.J.) **67,** 2691–701 (2015).

249. Zengini, E. *et al.* Genome-wide analyses using UK Biobank data provide insights into the genetic architecture of osteoarthritis. *Nat. Genet. 2018* 1 (2018). doi:10.1038/s41588-018-0079-y

250. Jia, H. *et al.* EGFR signaling is critical for maintaining the superficial layer of articular cartilage and preventing osteoarthritis initiation. *Proc. Natl. Acad. Sci. U. S. A.* 201608938 (2016). doi:10.1073/pnas.1608938113

251. Zhang, X. *et al.* Reduced EGFR signaling enhances cartilage destruction in a mouse osteoarthritis model. *Bone Res.* **2,** 14015 (2014).

252. Jia, H. *et al.* Subchondral bone plate sclerosis during late osteoarthritis is causedby loading-induced reduction in Sclerostin. *Arthritis Rheumatol. (Hoboken, N.J.)* **70,** 230 (2018).

253. Lee, K. L., Isham, K. R., Stringfellow, L., Rothrock, R. & Kenney, F. T. Molecular cloning of cDNAs cognate to genes sensitive to hormonal control in rat liver. *J. Biol. Chem.* **260,** 16433–8 (1985).

254. Zhang, Y.-W. & Vande Woude, G. F. Mig-6, Signal Transduction, Stress Response and Cancer. *Cell Cycle* **6,** 507–513 (2007).

255. Ferby, I. *et al.* Mig6 is a negative regulator of EGF receptor–mediated skin morphogenesis and tumor formation. *Nat. Med.* **12,** 568–573 (2006).

256. Pirone, D. M., Carter, D. E. & Burbelo, P. D. Evolutionary expansion of CRIB-containing Cdc42 effector proteins. *Trends Genet.* **17,** 370–3 (2001).

257. van Laar, T., Schouten, T., van der Eb, A. J. & Terleth, C. Induction of the SAPK activatorMIG-6 by the alkylating agent methyl methanesulfonate. *Mol. Carcinog.* **31,** 63–67 (2001).

258. Saarikoski, S. T., Rivera, S. P. & Hankinson, O. Mitogen-inducible gene 6 (MIG-6), adipophilin and tuftelin are inducible by hypoxia. *FEBS Lett.* **530,** 186–90 (2002).

259. Tseng, R.-C. *et al.* Genomewide loss of heterozygosity and its clinical associations in non small cell lung cancer. *Int. J. Cancer* **117,** 241–247 (2005).

260. Ferby, I. *et al.* Mig6 is a negative regulator of EGF receptor–mediated skin morphogenesis and tumor formation. *Nat. Med.* **12,** 568–573 (2006).

261. Burbelo, P. D., Drechsel, D. & Hall, A. A Conserved Binding Motif Defines Numerous Candidate Target Proteins for Both Cdc42 and Rac GTPases. *J. Biol. Chem.* **270,** 29071–29074 (1995).

262. Makkinje, A. *et al.* Gene 33/Mig-6, a Transcriptionally Inducible Adapter Protein That Binds GTP-Cdc42 and Activates SAPK/JNK. *J. Biol. Chem.* **275,** 17838–17847 (2000).

263. Hackel, P. O., Gishizky, M. & Ullrich, A. Mig-6 Is a Negative Regulator of the Epidermal Growth Factor Receptor Signal. *Biol. Chem.* **382,** (2001).

264. Shen, F., Lin, Q., Gu, Y., Childress, C. & Yang, W. Activated Cdc42-associated Kinase 1 Is a Component of EGF Receptor Signaling Complex and Regulates EGF Receptor Degradation. *Mol. Biol. Cell* **18,** 732–742 (2007).

265. Fiorini, M. *et al.* Expression of RALT, a feedback inhibitor of ErbB receptors, is subjected to an integrated transcriptional and post-translational control. *Oncogene* **21,** 6530–6539 (2002).

266. Anastasi, S., Baietti, M. F., Frosi, Y., Alemà, S. & Segatto, O. The evolutionarily conserved EBR module of RALT/MIG6 mediates suppression of the EGFR catalytic activity. *Oncogene* **26,** 7833–7846 (2007).

267. Frosi, Y. *et al.* A two-tiered mechanism of EGFR inhibition by RALT/MIG6 via kinase suppression and receptor degradation. *J. Cell Biol.* **189,** 557–71 (2010).

268. Jiang, X. *et al.* Inhibition of Cdc42 is essential for Mig-6 suppression of cell migration induced by EGF. *Oncotarget* (2016). doi:10.18632/oncotarget.10205

269. Hopkins, S. *et al.* Mig6 is a sensor of EGF receptor inactivation that directly activates c-Abl to induce apoptosis during epithelial homeostasis. *Dev. Cell* **23,** 547–59 (2012).

270. Pante, G. *et al.* Mitogen-inducible gene 6 is an endogenous inhibitor of HGF/Met-induced cell migration and neurite growth. *J. Cell Biol.* **171,** 337–48 (2005).

271. Zhang, Y.-W. *et al.* Targeted disruption of Mig-6 in the mouse genome leads to early onset degenerative joint disease. *Proc. Natl. Acad. Sci. U. S. A.* **102,** 11740–5 (2005).

272. Mateescu, R. G., Todhunter, R. J., Lust, G. & Burton-Wurster, N. Increased MIG-6 mRNA transcripts in osteoarthritic cartilage. *Biochem. Biophys. Res. Commun.* **332,** 482–6 (2005).

273. Jin, N., Gilbert, J. L., Broaddus, R. R., Demayo, F. J. & Jeong, J.-W. Generation of a Mig-6 conditional null allele. *Genesis* **45,** 716–21 (2007).

274. Velasquillo, C. *et al.* Expression of MIG-6, WNT-9A, and WNT-7B during osteoarthritis. *Ann. N. Y. Acad. Sci.* **1117,** 175–80 (2007).

275. Joiner, D. M. *et al.* Accelerated and increased joint damage in young mice with global inactivation of mitogen-inducible gene 6 after ligament and meniscus injury. *Arthritis Res. Ther.* **16,** R81 (2014).

276. Burton-Wurster, N. *et al.* Genes in Canine Articular Cartilage That Respond to Mechanical Injury: Gene Expression Studies With Affymetrix Canine GeneChip. doi:10.1093/jhered/esi105

277. Pest, M. A., Russell, B. A., Zhang, Y.-W., Jeong, J.-W. & Beier, F. Disturbed cartilage and

joint homeostasis resulting from a loss of mitogen-inducible gene 6 in a mouse model of joint dysfunction. *Arthritis Rheumatol. (Hoboken, N.J.)* **66,** 2816–27 (2014).

278. Shepard, J. B., Jeong, J.-W., Maihle, N. J., O'Brien, S. & Dealy, C. N. Transient anabolic effects accompany epidermal growth factor receptor signal activation in articular cartilage in vivo. *Arthritis Res. Ther.* **15,** R60 (2013).

279. Staal, B., Williams, B. O., Beier, F., Vande Woude, G. F. & Zhang, Y.-W. Cartilage-specific deletion of Mig-6 results in osteoarthritis-like disorder with excessive articular chondrocyte proliferation. doi:10.1073/pnas.1400744111

Chapter 2

2   Overexpression of Mig-6 In Cartilage Induces an Osteoarthritis-Like Phenotype in Mice

Bellini, Melina[1,2], Pest, Michael A.[1,2]; Miranda-Rodrigues, M.[1,2,3], Qin, Ling[4], Jeong JW[5], Beier, Frank[1,2,3]

[1] Department of Physiology and Pharmacology, Western University, London, ON, Canada

[2] Western University Bone and Joint Institute, London, ON, Canada

[3] Children's Health Research Institute, London, ON, Canada

[4] Department of Orthopaedic Surgery, Perelman School of Medicine, University of Pennsylvania, Philadelphia, PA, USA

[5] Department of Obstetrics, Gynecology and Reproductive Biology, Michigan State University College of Human Medicine, Grand Rapids, Michigan.

Corresponding author: Dr. Frank Beier, Department of Physiology and Pharmacology, Western University, London, ON, Canada; Phone 519-661-02111 ext 85344; email: fbeier@uwo.ca

2.1 Abstract

Background: Osteoarthritis (OA) is the most common form of arthritis and characterised by degeneration of articular cartilage. Mitogen-inducible gene 6 (Mig-6) has been identified as a negative regulator of the Epidermal Growth Factor Receptor (EGFR). Cartilage-specific *Mig-6* knockout (KO) mice display increased EGFR signaling, an anabolic buildup of articular cartilage and formation of chondro-osseous nodules. Since our understanding of the EGFR/Mig-6 network in cartilage remains incomplete, we characterised mice with cartilage-specific overexpression of Mig-6 in this study.

Methods: Utilizing knee joints from cartilage-specific *Mig-6* overexpressing (*Mig-6$^{over/over}$*) mice (at multiple time points), we evaluated the articular cartilage using histology, immunohistochemical staining and semi-quantitative OARSI scoring at multiple ages. MicroCT analysis was employed to examine skeletal morphometry, body composition, and bone mineral density.

Results: Our data show that cartilage-specific *Mig-6* overexpression did not cause any major developmental abnormalities in articular cartilage, although *Mig-6$^{over/over}$* mice have slightly shorter long bones compared to the control group. Moreover, there was no significant difference in bone mineral density and body composition in any of the groups. However, our results indicate that *Mig-6$^{over/over}$* male mice show accelerated cartilage degeneration at 12 and 18 months of age. Immunohistochemistry for SOX9 demonstrated that the number of positively stained cells in *Mig-6$^{over/over}$* mice decreased relative to controls. Immunostaining for MMP13 staining is increased in areas of cartilage degeneration in *Mig-6$^{over/over}$* mice. Moreover, staining for phospho-EGFR (Tyr-1173) and lubricin (PRG4) was decreased in the articular cartilage of *Mig-6$^{over/over}$* mice.

Conclusion: Overexpression of *Mig-6* in articular cartilage causes no major developmental phenotype; however, these mice develop earlier OA during aging than control mice. These data demonstrate that Mig-6/EGFR pathways is critical for joint homeostasis and might present a promising therapeutic target for OA.

2.2   Introduction

Osteoarthritis (OA), a chronic degenerative joint disease, is the most common form of arthritis. OA affects nearly five million Canadians currently (1), but that number will grow to more than 10 million by 2040 (2). This statistic is alarming, considering the disability, the loss of quality of life, and the costs to the health system generated by OA. Currently, there are pharmacological treatments available to manage OA symptoms such as pain (3–5) as well as surgical joint replacement at the end stage of disease (6,7). Unfortunately, however, there is no known cure for OA. Progressive understanding of the pathophysiology of OA suggests that the disease is a heterogeneous condition, so further research is needed to direct the clinical approaches to disease management (8).

Recent studies have shown that OA is a multifactorial disease of the whole joint, however its pathogenesis remains still poorly understood (9). Genetic, environmental, and biomechanical factors can accelerate the onset of OA (10). Articular cartilage is a highly specialized tissue that forms the smooth gliding surface of synovial joints, with chondrocytes as the only cellular component of cartilage (11). The homeostasis of the cartilage extracellular matrix (ECM) involves a dynamic equilibrium between anabolic and catabolic pathways controlled by chondrocytes (12). The progression of OA is associated with dramatic alteration in the integrity of the cartilage ECM network formed by a large number of proteoglycans (mostly aggrecan), collagen II, and other non-collagenous matrix proteins (13). In addition, ECM synthesis is regulated by a number of transcriptional regulators involved in chondrogenesis, specifically Sex- determining- region-Y Box 9 (SOX9), L-SOX 5 and SOX6 that regulate type II collagen (*Col2a1*) and Aggrecan (*Acan*) gene expression (14). On the other hand, catabolic events are dominant in OA and cells are exposed to degenerative enzymes such as aggrecanases (e.g. ADAMTS-4, -5) (13,15), collagenases (e.g. MMP-1,-3, -8, -13) (16), and gelatinases (e.g.MMP-2, and MMP-9), all of which have implications in articular cartilage degeneration (17). A number of growth factors (18) play a role in OA pathology, such as transforming growth factor-β (19), BMP-2 (20), Insulin growth factor 1 (IGF-1) (21) fibroblast growth factor (FGF) and others, but the exact regulation of chondrocyte physiology is still not completely understood.

Recent studies in our laboratory (22,23) have identified the epidermal growth factor receptor (EGFR) and its ligand transforming growth factor alpha (TGFα) as possible mediators of cartilage degeneration (24–26). The human *TGFA* gene locus was also strongly linked to hip OA and cartilage thickness in genome-wide association studies (27,28). TGFα stimulates EGFR signaling and activates various cell-signaling pathways in chondrocytes, including extracellular signal-regulated kinase 1 and 2 (ERK1/2) and P13K (phosphoinositide 3-kinase) (29). EGFR signaling plays important roles in endochondral ossification (30,31), growth plate development (30) and cartilage maintenance and homeostasis (32–34), but many aspects of its action in cartilage are still not well understood. However, both protective and catabolic effects of EGFR signaling in OA have been reported, suggesting context-specific roles of this pathway (35).

Mitogen-inducible gene 6 (Mig-6) is also known as Gene 33, ErbB receptor feedback inhibitor 1 (ERRFI1), or RALT, and is found in the cytosol (36). *Mig-6* protein binds to and inhibits EGFR signaling through a two-tiered mechanism: suppression of EGFR catalytic activity and receptor down-regulation (37). Interestingly, various studies have reported that loss of Mig-6 induces the onset of OA-like symptoms in mice (36,38–40). Cartilage-specific (Col2-Cre) knockout of *Mig-6* mice results in formation of chondro-osseous nodules in the knee, but also increased thickness of articular cartilage in the knee, ankle, and elbow (41). Prx1-cre-mediated knockout of *Mig-6* results in a similar phenotype as that observed in cartilage-specific knockout mice(42). These phenotypes appeared to be caused by an increase in chondrocyte proliferation in articular cartilage, supported by increased expression of Sox9 and EGFR activation in cartilage (42). Since our studies suggest dosage- and/or context-specific roles of EGFR signaling in the process of cartilage degeneration in OA, in this study we used a Col2a1 promoter–driven Cre/lox system to examine effects of Mig-6 overexpression specifically in articular cartilage.

2.3   Materials and Methods

2.3.1   Generation of Mig-6 overexpression mice

Mig-6 overexpression animals on a mixed C57Bl/6 and agouti mouse background, with the overexpression cassette in the Rosa26 locus (43) and bred for 10 generations into a C57Bl/6 background. Transcription of *Mig-6* is under the control of a ubiquitously expressed chicken beta actin-cytomegalovirus hybrid (CAGGS) promoter, but blocked by a "Stop Cassette" flanked by

LoxP sites (LSL) (43). *Mig-6* overexpression mice were bred to mice carrying the Cre recombinase gene under the control of the Collagen 2 promoter (44), to induce recombination and removal of the STOP Cassette specifically in cartilage. Throughout the manuscript, animals for homozygote overexpression of Mig-6 from both alleles are termed *Mig-6 over/over (Mig-6 over/over Col2a1-Cre+/-)*, while control mice are identical but without the Cre gene (noted as "control" in this manuscript for simplicity). Mice were group housed (at least 1 pair of littermate-matched control and overexpression animals), on a standard 12-hour light/dark cycle, without access to running wheels, and with free access to mouse chow and water. Animals were weighed prior to euthanization by asphyxiation with CO_2. All animal experiments were done in accordance with the Animal Use Subcommittee at the University of Western Ontario and conducted in accordance with guidelines from the Canadian Council on Animal Care.

2.3.2   Genotyping

Genotype was determined by polymerase chain reaction (PCR) analysis using DNA processed from biopsy samples of ear tissue from mice surviving to at least 21 days of age. PCR strategy: Primer set P1 and P2 can amplify a 300 bp fragment from the wild-type allele, whereas P1 and P3 can amplify a 450 bp fragment from the targeted ROSA26 locus allele (43) (Supp. Figure/Table 1).

2.3.3   RNA isolation and Quantitative real-time PCR

Total RNA was isolated from post-natal day 0 (P0) mouse cartilage of *Mig-6 over/over* and control littermates using TRIzol® (Invitrogen) as per manufacturer's instructions and as previously described (45). Complementary DNA (cDNA) was synthesized using the iScript cDNA Synthesis kit (Bio-Rad) with 1µg of RNA (Bio-Rad Laboratories), and combined with 300nM of forward and reverse primers (for primer sequences, please see Supplementary Table 1) as well as iQ™ SYBR® Green Supermix (Bio-Rad Laboratories) for PCR on a Bio-Rad CFX384 RT-PCR system. (Supp. Figure/Table 1).   Relative gene expression was normalized to the internal control Glyceraldehyde 3-phosphate dehydrogenase (*Gapdh)*, calculated using the ΔΔCT method.

2.3.4   Histopathology of the knee

Limbs from *Mig-6 over/over* and control mice were harvested and fixed in 4% paraformaldehyde

(Sigma) for 24 hours and decalcified in ethylenediaminetetraacetic acid (5% EDTA in phosphate buffered saline (PBS), pH 7.0. Joints were processed and embedded in paraffin in sagittal or frontal orientation, with serial sections taken at a thickness of 5 μm. Sections were stained with Toluidine Blue (0.04% toluidine blue in 0.2M acetate buffer, pH 4.0, for 10 minutes) for glycosaminoglycan content and general evaluation of articular cartilage. All images were taken with a Leica DFC295 digital camera and a Leica DM1000 microscope.

2.3.5 Thickness of proximal tibia growth plate

For early developmental time points such as newborn (P0), sagittal knee sections stained with toluidine blue were used to measure the width of the zones of the epiphyseal growth plate in the proximal tibia. The average thickness of the resting and proliferative zones combined was evaluated by taking three separate measurements at approximately equal intervals across the width of the growth plate. The average hypertrophic zone thickness was also measured using 3 different measurements across the width of the growth plate, starting each measurement at the border of the proliferative and hypertrophic zones and ending at the subchondral bone interface. A third average measurement was then taken of the thickness of the entire growth plate. ImageJ Software (v.1.51) (46) was used for all measures, with the observer blinded to the genotype.

2.3.6 Articular cartilage evaluation

Articular cartilage thickness was measured from toluidine blue-stained frontal sections by a blinded observer. Articular cartilage thickness was measured separately for the non-calcified articular cartilage (measured from the superficial tangential zone to the tidemark) and the calcified articular cartilage (measured from the subchondral bone to the tidemark) across three evenly spaced points from all four quadrant of the joint (medial/lateral tibia and femur) in 4 sections spanning at least 500 μm. ImageJ Software (v.1.51) (46) was used to measure the thickness of articular cartilage.

2.3.7 Micro-Computerized Tomography (μCT)

Whole body scans were collected in 6 week-, 11 week-, 12 month-, and 18-month-old control and *Mig-6* $^{over/over}$ male and female mice. Mice were euthanized and imaged using General Electric (GE) SpeCZT microCT machine (47) at a resolution of 50μm/voxel or 100μm/voxel. GE

Healthcare MicroView software (v2.2) was used to generate 2D maximum intensity projection and 3D isosurface images to evaluate skeletal morphology. MicroView was used to create a line measurement tool in order to calculate the bone lengths, femurs lengths were calculated from the proximal point of the greater trochanter to the base of the lateral femoral condyle. Tibiae lengths were measured from the midpoint medial plateau to the medial malleolus. Humerus lengths were measured from the midpoint of the greater tubercle to the center of the olecranon fossa.

2.3.8   Body Composition Analysis

MicroView software (GE Healthcare Biosciences) was used to analyse the microCT scans at the resolution of 100um/voxel. Briefly, the region of interest (ROI) was used to calculate the mean of air, water and an epoxy-based, cortical bone-mimicking calibrator (SB3; Gammex, Middleton, WI, USA) (1100mg/cm^3) (48). A different set of global thresholds was applied to measure adipose, lean and skeletal mass (-275, -40 and 280 Hounsfield Units (HU), respectively). Moreover, bone mineral density (BMD) was acquired as the ratio of the average HU (from the value of skeletal region of interest) in order to calculate HU value of the SB3 calibrator, multiplied by the known density of the SB3 as described (47).

2.3.9   OARSI histopathology scoring

Serial sections through the entire knee joint were scored according to the OARSI histopathology scoring system (49) by two blinded observers on the four quadrants of the knee: lateral femoral condyle (LFC), lateral tibial plateau (LTP), medial femoral condyle (MFC), and medial tibial plateau (MTP). Histologic scoring from 0-6 represent the OA severity, from 0 (healthy cartilage) to 6 (erosion of more than 75% of articular cartilage). Individual scores are averaged across observers and OA severity is shown as described for each graph. Scores were compared between male and female *Mig-6 $^{over/over}$* and control mice at both 12 and 18 months of age. All images were taken with a Leica DFC295 digital camera and a Leica DM1000 microscope.

2.3.10 Immunohistochemistry

Frontal paraffin sections of knees were used to for immunohistochemical analysis, with slides with 'no primary antibody' as control. All sections were deparaffinized and rehydrated as previously described (41,50). Subsequently, the sections were incubated in 3% H2O2 in methanol for 15

minutes to inhibit endogenous peroxidase activity. After rising with water, 5% goat or donkey serum in PBS was applied to reduce nonspecific background staining. Sections were incubated overnight at 4°C with primary antibodies against SOX9 (R&D Systems, AF3075), MMP13 (Protein Tech, Chicago, IL, USA, 18165-1-AP), lubricin (Abcam, ab28484) and phospho-EGFR (phosphoTyr-1173; Cell Signaling Technology). After washing, sections were incubated with horseradish peroxidase (HRP)-conjugated donkey anti-goat or goat anti-rabbit secondary antibody (R&D system and Santa Cruz), before incubation with diaminobenzidine substrate as a chromogen (Dako, Canada). Finally, sections were counterstained with 0.5% methyl green (Sigma) and mounted. Cell density of articular cartilage chondrocytes from 6 and 11 weeks-old male mice was determined by counting all lacunae with evidence of nuclear staining in the lateral and medial femur/tibia using a centered region of interest measuring 200 μm wide and 70 μm deep from the articular surface by a blinded observer. For newborn (P0) animals the region of interest measured 200 μm wide and 100 μm deep from the proliferative zone.

2.3.11 Statistical Analysis

All statistical analyses were performed using GraphPad Prism (v6.0). Differences between two groups were evaluated using Student's *t*-test, and Two-Way ANOVA was used to compare 4 groups followed by a Bonferroni multiple comparisons test. All *n* values represent the number of mice used in each group/genotyping.

2.4   Results

2.4.1   Overexpression of Mig-6 has minor effects on skeletal phenotypes during development

We bred mice for conditional overexpression of Mig-6 (43) to mice expressing Cre recombinase under control of the collagen II promoter. Homozygote mice overexpressed Mig-6 in all collagen II-producing cells (and their progeny) from both Rosa26 alleles and are referred to as *Mig-6* $^{over/over}$ from here on. Control mice do not express Cre. Genomic DNA was extracted from ear notches to identify homozygous mice *Mig-6* $^{over/over}$ using standard PCR analysis. Overexpressing mice were obtained at the expected Mendelian ratios (data not shown). Male mutant gained weight at the same rate as controls over the examined at 10-week period, while female *Mig-6* $^{over/over}$ mice were slightly lighter than controls starting at 8 weeks of age **(Fig. 2.1A, B)**. These differences persisted

at 12 months of age for female mice, while at 18 months both male and female mutant mice were lighter than their controls **(Fig. 2.1C, D)**. Growth plates of post-natal day 0 (P0) *Mig-6 over/over* and control mice were analyzed by histology. No major differences in tibia growth plate architecture were seen between genotypes **(Fig. 2.2A)**. While the length of the total growth plate was slightly reduced in *Mig-6 over/over* mice, differences in lengths of either the combined resting/proliferative or hypertrophic zones were not statistically significant **(Fig. 2.2B-D).**

Figure 2.1 Body weight of control and *Mig-6*^{over/over} male and female mice during growth.Body weight of male Mig-6 overexpression mice did not show any significant differences compared to control **(A)** Female Mig-6 overexpression mice showed statistically significant differences compared to control at 8w, 9w and 10w **(B).** Two-Way ANOVA was used with Bonferroni post hoc analysis (n=5/genotyping). Data are presented with mean and error ± SEM (P<0.05). Weights of 12 months old **(C)** and 18 months old **(D)** male and female cartilage specific *Mig-6*^{over/over} mice and controls taken immediately prior to sacrifice. Individual data points presented with mean ± SEM (P<0.05). Data analyzed by two tailed student t-tests from 6-12 mice per group (age/genotyping).
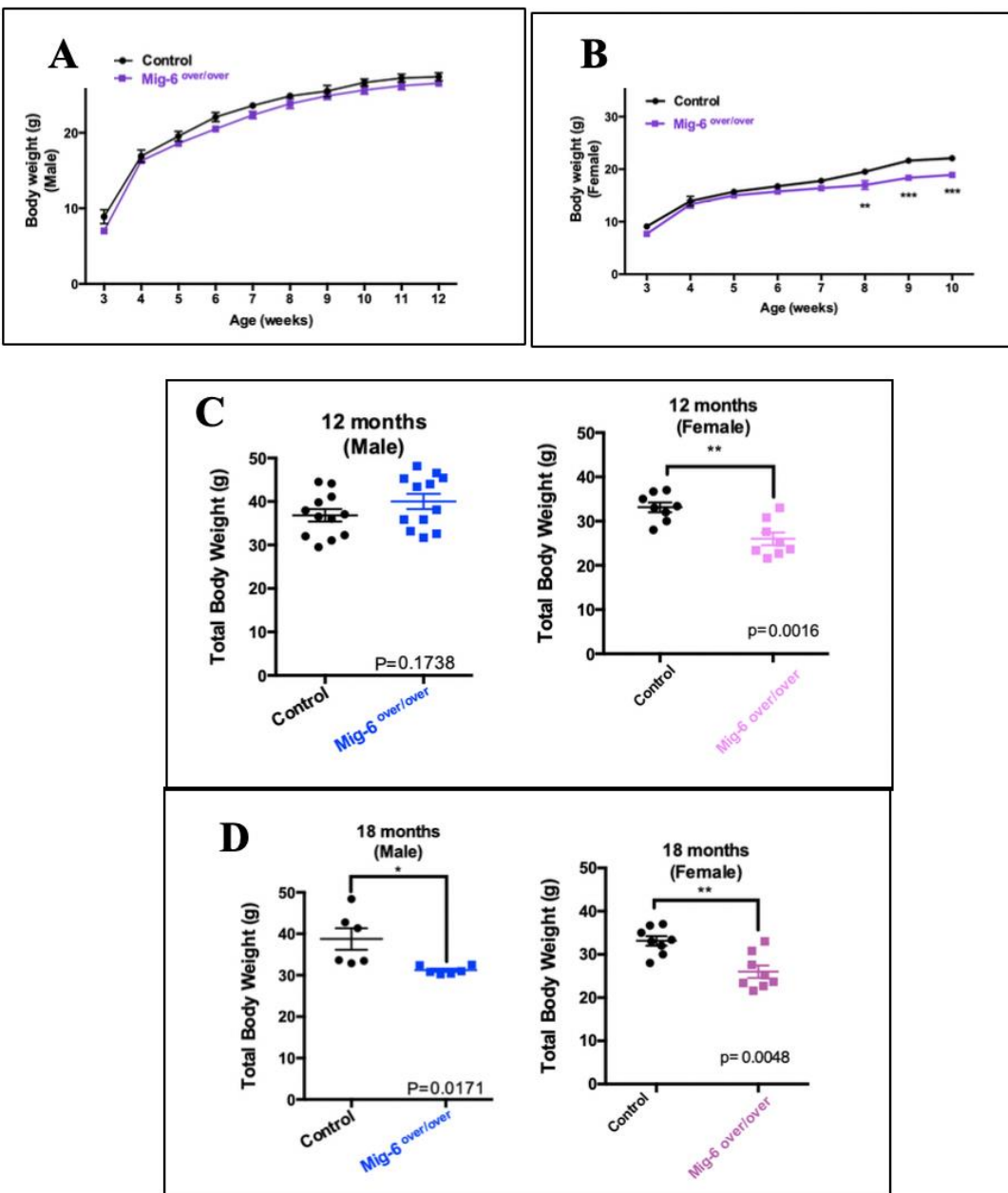
Figure 2.1. Body weight of control and *Mig-6^{over/over}* male and female mice during growth

Figure 2.2 Cartilage-specific Mig6-overexpressing mice display no major developmental phenotype. Representative toluidine Blue staining on postnatal day 0 (P0) of *Mig-6^{over/over}* **(A)** and control animals. Thickness of total proximal tibia growth plates in the mice containing articular cartilage specific mitogen inducible gene 6 overexpression (n=6), when compared to age matched controls (n=6) was significantly decreased when analyzed by two tailed student t-tests **(B)**; The average of hypertrophic zone thickness from postnatal day 0 in the mice containing articular cartilage specific mitogen inducible gene 6 overexpression had mean of 188.9 µm and control mice had mean of 184.4 µm **(C).** The thickness of the combined resting and proliferative zones from the control had mean of 728 µm and *Mig-6^{over/over}* 706.5 µm *Mig-6^{over/over}***(D).** Therefore, there was no significant differences within the groups. Individual data points presented with mean ± SEM analyzed by two tailed student t-tests; (P<0.05).
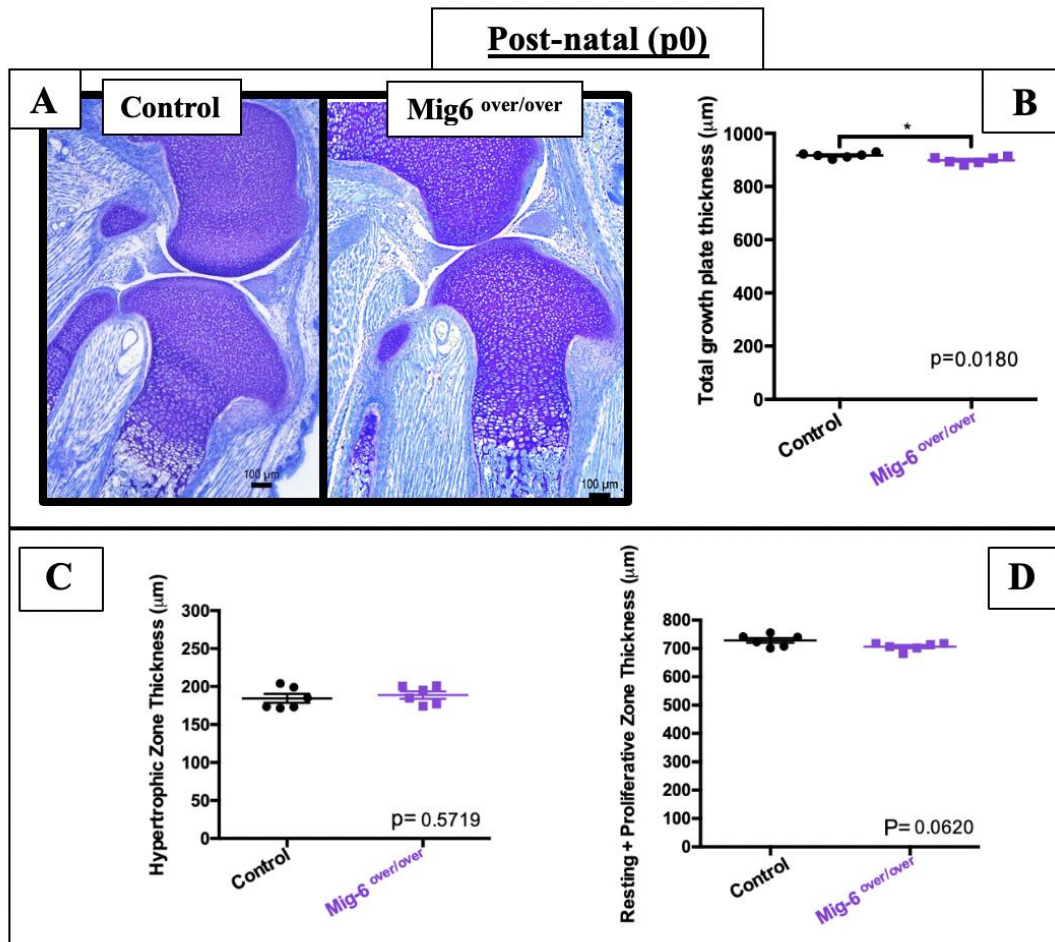
Figure 2.2 Cartilage-specific Mig6-overexpressing mice display no major developmental phenotype

2.4.2 Mice overexpressing Mig-6 have shorter long bones than control mice

Skeletal morphology and bone length were examined by microCT mice at the ages of 6 and weeks, and 12 and 18 months. Scans of *Mig-6* $^{over/over}$ male and female mice and their controls were used to generate 3D isosurface reconstructions of 100μm/voxel uCT scans, in order to measure long bones lengths (femurs, humeri, and tibiae) in GE MicroView v2.2 software. Mutant bones were slightly shorter throughout life, with the exception of the male humeri at 12 months that did not show any statistically significant difference **(Fig. 2.3)**. In contrast, male mice did not show any differences in bone mineral density at 11 weeks, 12 months, or 18 months, compared to controls **(Suppl. Fig. 2)**. In addition, no differences in body mass composition were seen in male mutant and control mice at 11 weeks, 12 months, and 18 months of age **(Suppl. Fig. 3)**.

Figure 2.3 Long bone lengths of Mig-6 overexpression are significantly shorter than control long bone lengths during growth and aging. The lengths of right humeri, tibiae and femora were measured on microCT scan of mice in each different time-points of age using GE MicroView software. **(A)** 6 weeks-old male and female control and Mig-6 overexpressors. **(B)** 11 weeks-old male and female control and Mig-6 overexpressors. **(C)** 12 months-old male and female control and Mig-6 overexpressors. **(D)** 18 months-old male and female control and Mig-6 overexpressors. **(A1)** Representative 3D isosurface reconstructions of 100μm/voxel μCT scans. There were statistically significant differences among control and *Mig-6$^{over/over}$* male and female groups. Individual data points presented with mean ± SEM (P<0.05). Data analyzed by two tailed student t-tests from 6-12 mice per group (age/gender).
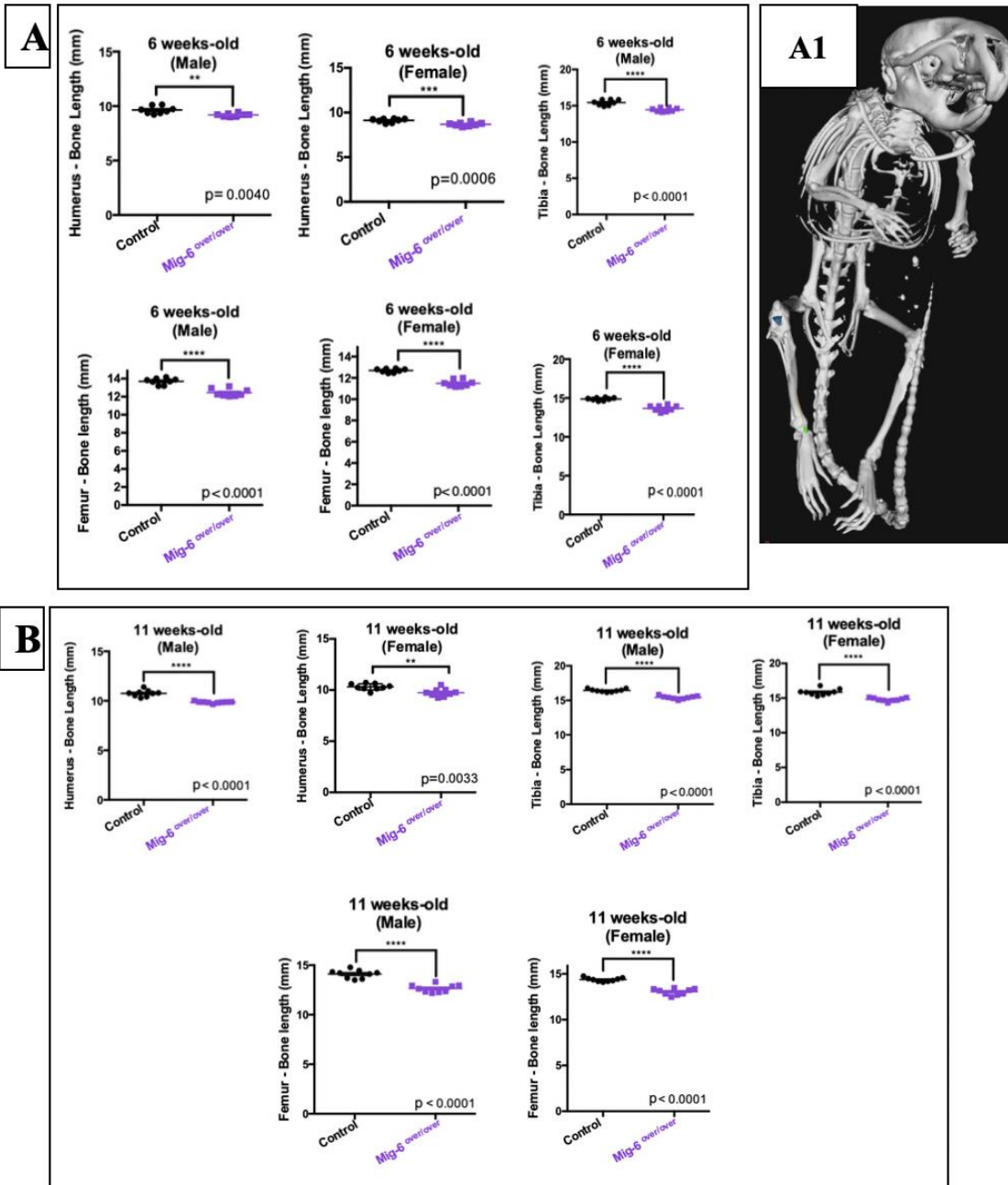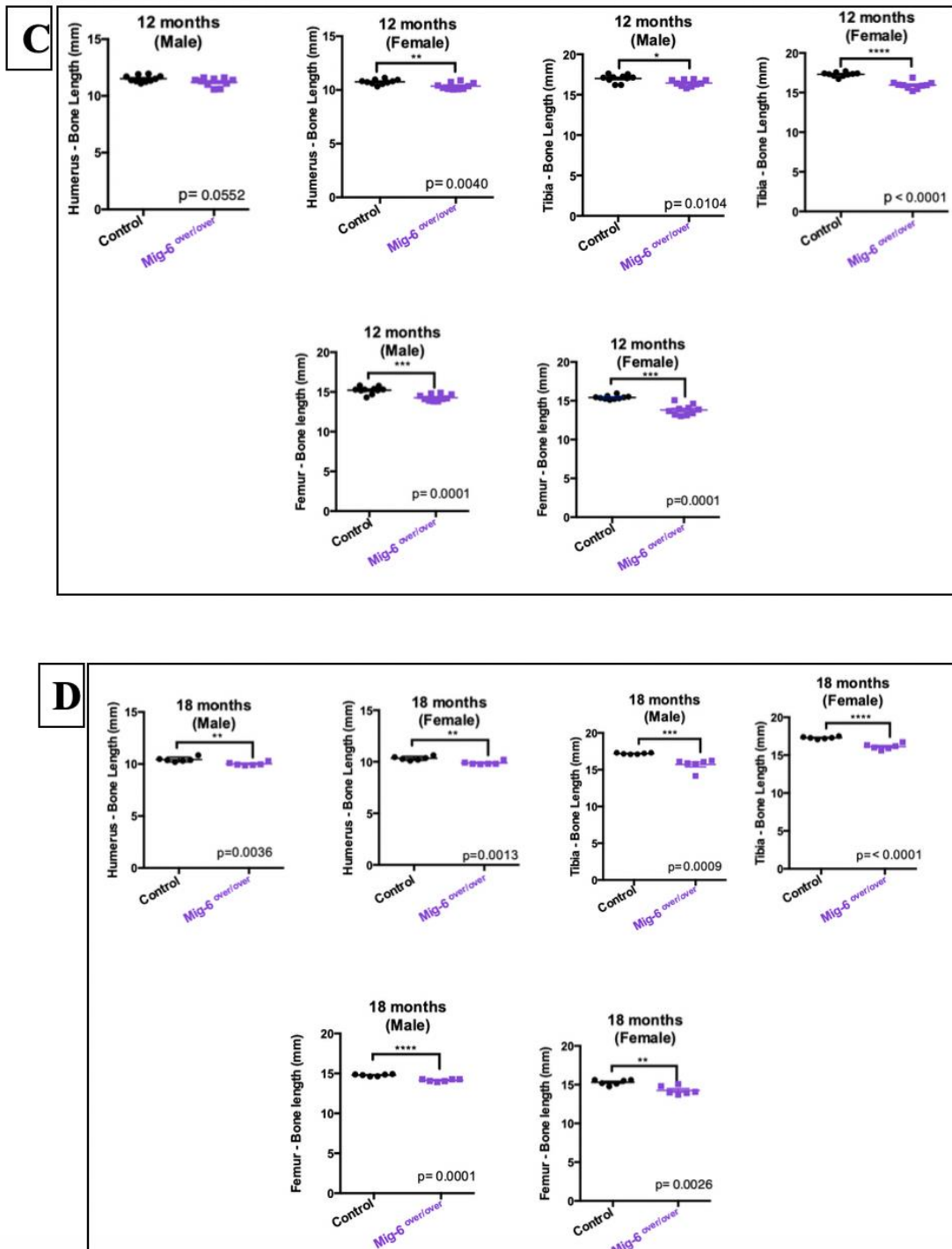
Figure 2.3 Long bone lengths of Mig-6 overexpression are significantly shorter than control long bone lengths during growth and aging

2.4.3 Mig-6 overexpressing mice have healthy articular cartilage during skeletal maturity

We next examined articular cartilage morphology in 11-week-old mutant and control mice using toluidine blue stained paraffin frontal knee sections **(Fig. 2.4A-B)**. The average thickness of the calcified articular cartilage and non-calcified articular cartilage in the lateral femoral condyle (LFC), lateral tibial plateau (LTP), medial femoral condyle (MFC), and medial tibial plateau (MTP) from control and *Mig-6* $^{over/over}$ male **(Fig. 2.4C-D)** and female **(Suppl. Fig. 4A-D)** mice did not show statistically significant differences. Histological analyses of knee sections from male and female mice did not show any loss of proteoglycan, fibrillation or erosion in the articular cartilage of mutant mice.

Figure 2.4 Articular cartilage from 11 weeks-old *Mig-6^over/over* male mice appeared healthy during skeletal maturity. Representative (n=5/group, toluidine blue) stained frontal sections of knee joints from 11-week-old control **(A)** and Mig-6over **(B).** Mig-6 overexpressors mice show similar articular cartilage thickness when compared to controls at 11 weeks-old male mice. The average thickness of the calcified articular cartilage **(C)** and non-calcified articular cartilage **(D)** in the lateral femoral condyle (LFC), lateral tibial plateau (LTP), medial femoral condyle (MFC), medial tibial plateau (MTP) was measured. Individual data points presented with mean ± SEM. Data analyzed by two-way ANOVA (95% CI) with Bonferroni post-hoc test. Scale bar = 100µm.
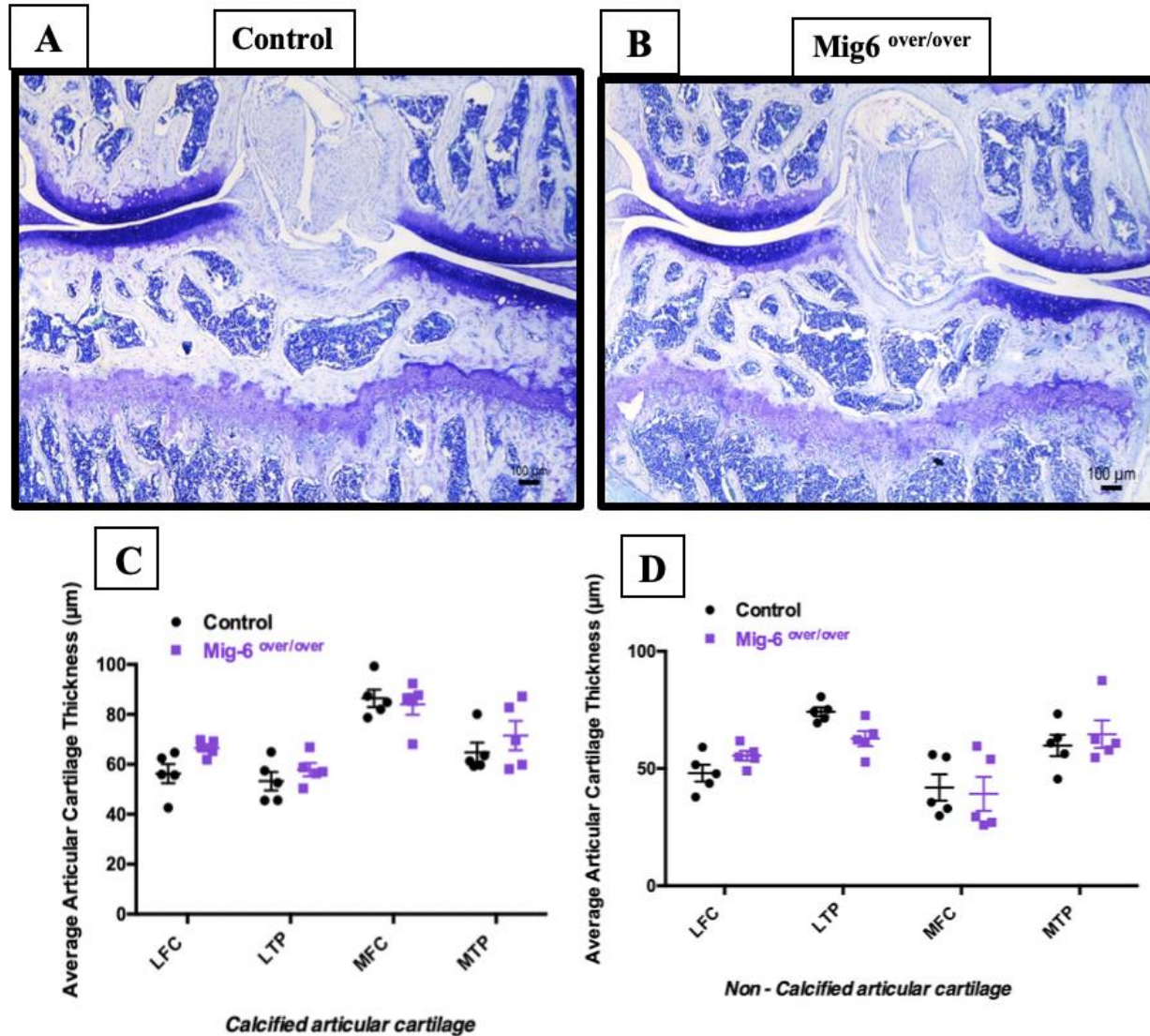
Figure 2.4 Articular cartilage from 11 weeks-old *Mig-6^{over/over}* male mice appeared healthy during skeletal maturity

2.4.4 Overexpression of Mig-6 in cartilage induces an osteoarthritis-like phenotype in mice during aging

Since aging is a primary risk factor in OA (51), we next examined knee joints in 12 and 18 month-old control and *Mig-6 over/over* mice. Toluidine blue stained sections were evaluated by two blinded observers, using OARSI recommendations (49). At 12 month of age, male control mice showed minor signs of cartilage damage, such as loss of proteoglycan staining, but no significant structural degeneration **(Fig. 2.5A).** However, seven of nine *Mig-6 over/over* male mice showed more extensive cartilage damage in their medial side (erosion to the calcified layer lesion for 25% to 50% of the medial quadrant). OARSI scoring confirmed increased OA-like damage in mutant mice **(Fig. 2.5C).** Similarly, at 18 months of age the male control group showed minimal cartilage degeneration in 3 of 6 mice **(Fig. 2.6A).** *Mig-6 over/over* male mice showed more severe cartilage erosion in the medial tibial plateau in 4/6 animals. This result was again supported by significantly increased OARSI cartilage damage scores **(Fig. 2.6C).** Moreover, for the female group at 12 months, control mice did not show cartilage damage in any quadrant of the knee. *Mig-6 over/over* female mice showed sign of OA-like cartilage damage in 3/8 animals **(Supplementary Fig. 5).** In addition, at 18 months of age, female control mice showed healthy cartilage, and 4/8 *Mig-6 over/over* female mice showed some proteoglycan loss and cartilage degeneration on the medial side **(Suppl. Fig. 6).**

Figure 2.5 12 months old _Mig-6$^{over/over}$_ male mice develop OA-like cartilage degeneration. Representative images of Toluidine Blue stained sections of knee joints from 12-month male control **(A)** and male Mig-6 over **(B)** mice were evaluated for cartilage damage following OARSI histopathological scale on the two quadrants of the knee: MFC = medial femoral condyle, MTP = medial tibial plateau. OARSI based cartilage degeneration scores are significantly higher in the MFC and MTP of Mig-6 overexpressing mice, corresponding to the increased damage observed histologically **(C)**. Data analyzed by two-way ANOVA with Bonferroni's multiple comparisons test. Individual data points presented with mean ± SEM. All scale bars =100 μm. N = 9 mice/group.
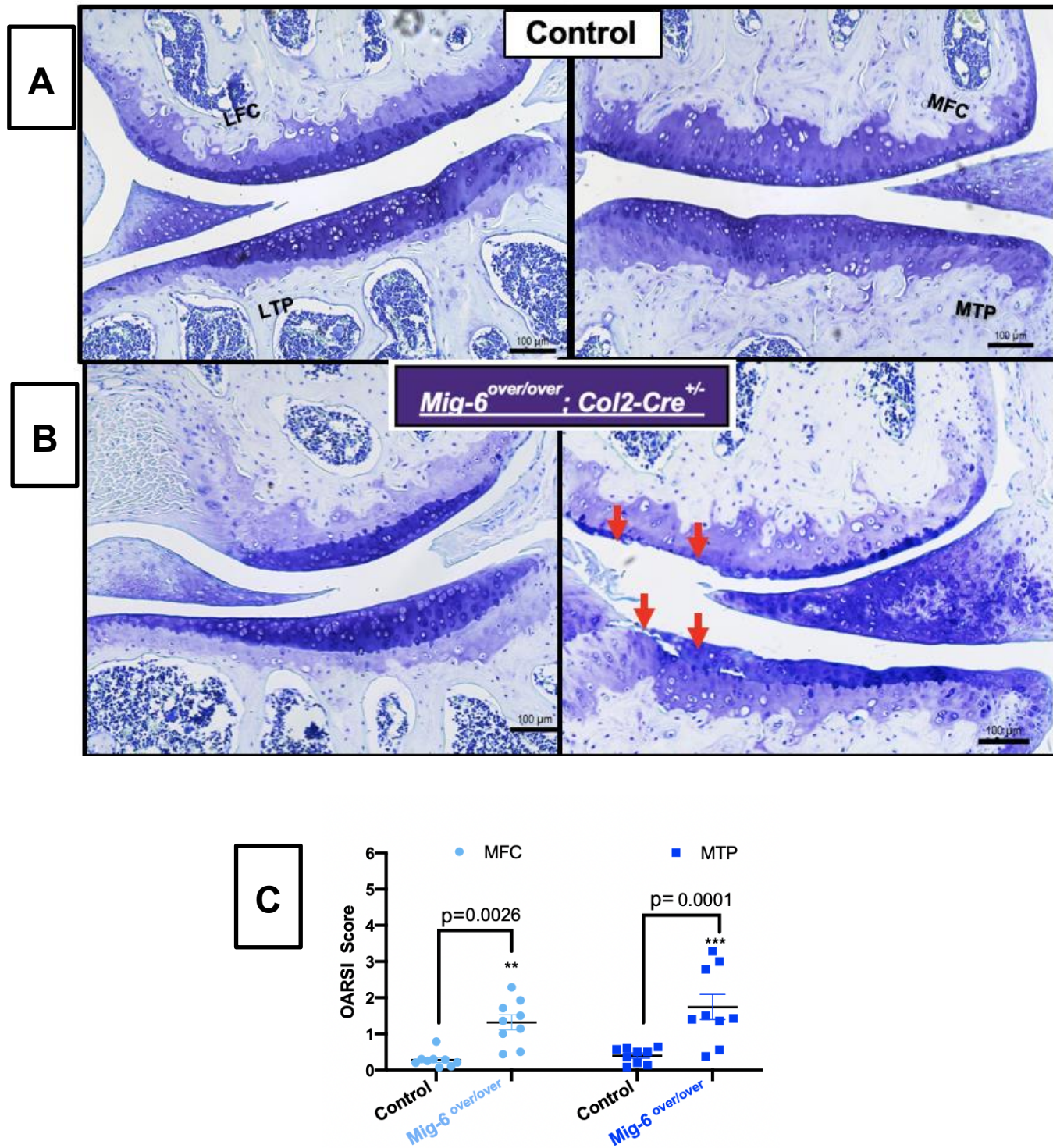
Figure 2.5 12 months old *Mig-6^{over/over}* male mice develop OA-like cartilage degeneration

Figure 2.6 18 months old *Mig-6^{over/over}* **mice leads to advanced OA-like cartilage.** Representative images of Toluidine Blue stained sections of knee joints from 18-month male control **(A)** and male Mig-6 over **(B)** mice were evaluated for cartilage damage following OARSI histopathological scale on the two quadrants of the knee: MFC = medial femoral condyle, MTP = medial tibial plateau. OARSI based cartilage degeneration scores are higher both in the MFC and MTP of Mig-6 overexpressing mice, corresponding to the increased damage observed histologically. **(C)** Data analyzed by two-way ANOVA with Bonferroni's multiple comparisons test. Individual data points presented with mean $\pm$ SEM. All scale bars =100 μm. N = 6 mice/group.
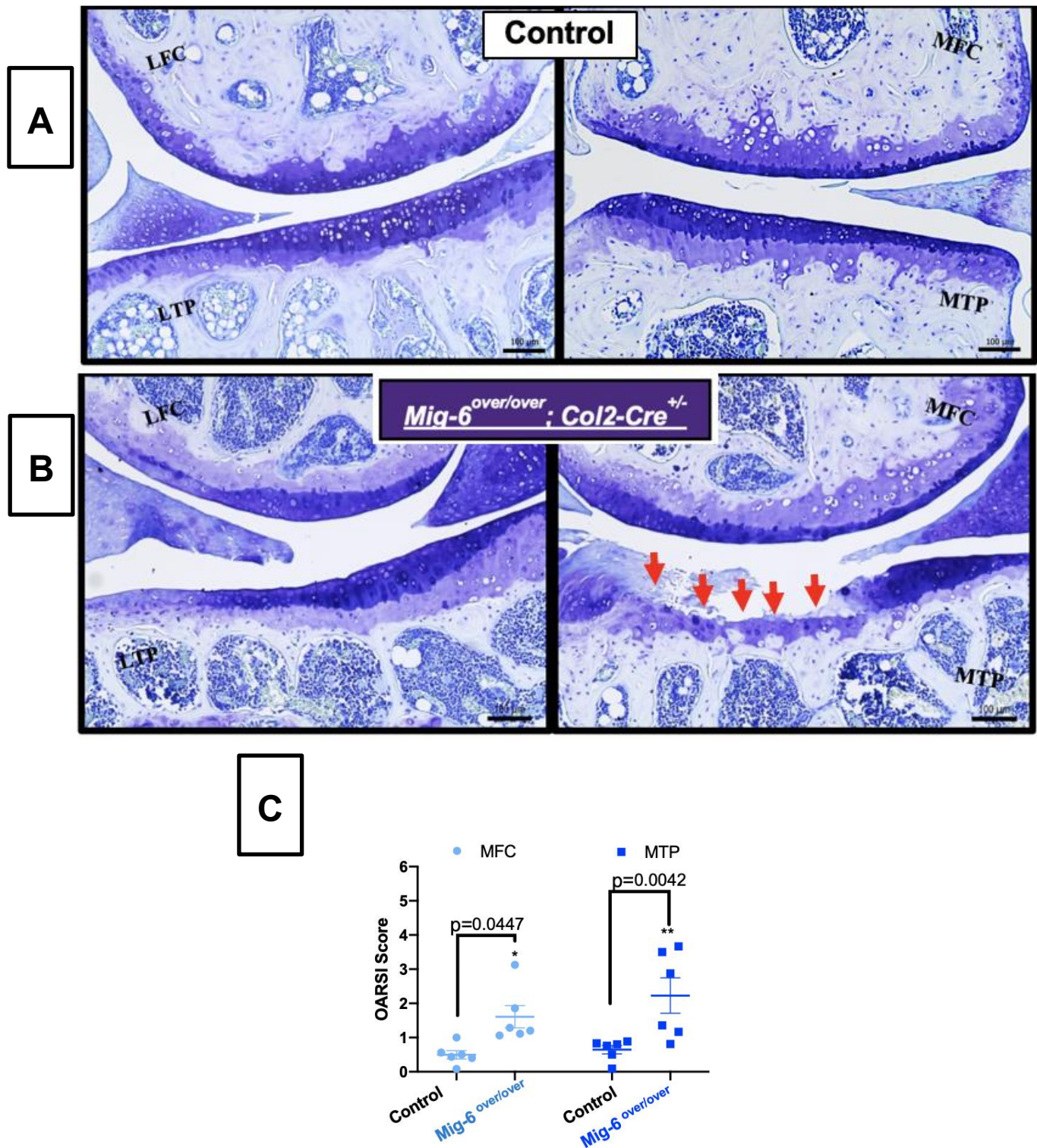
Figure 2.6 18 months old *Mig-6^(over/over)* mice leads to advanced OA-like cartilage

2.4.5 Overexpression of *Mig-6* decreases EGFR phosphorylation and Sox9 expression

Since Mig-6 *negatively regulates EGFR* signaling (32,33,41), immunohistochemistry was performed for phospho-EGFR (Tyr-1173) (pEGFR), with no primary antibody controls. Frontal knee sections from 11 weeks-old male *Mig-6 over/over* mice showed decreased pEGFR staining in the medial compartment in the knee joint (Fig.7), as expected upon Mig-6 overexpression. During chondrogenesis, the transcription factor SOX9 is required for cartilage formation and normal expression of collagen and aggrecan (52). Sagittal and frontal sections of paraffin embedded knees from post-natal day 0 (P0), 6 weeks-old, 11 weeks-old, 12 months and 18 months male mice were used for SOX9 immunostaining. At P0, nuclear SOX9 expression was observed in the resting and proliferative zone of the growth plate in both genotypes **(Fig. 2.8A, B).** Cell density was not different between genotypes (Fig. 8C). In control mice, 78 % of chondrocytes were positive for SOX 9 immunostaining, while the proportion of positive cells was only 53 % in *Mig-6 over/over* mice **(Fig 2.8D).** In 6 and 11-weeks-old mice, SOX9 was present in the articular cartilage in all four quadrants **(Fig. 2.9A, B).** At 6 weeks-old the total cell number in control male and *Mig-6over/over* mice is similar **(Fig. 2.9C),** but the percentage of SOX9 positive cells was decreased in mutant mice **(Fig 2.9D).** A similar phenotype was present at 11 weeks **(Supplementary Fig 7).** At 12 months of age, SOX9 is present more in the lateral side (LTP and LFC) than the medial side (MTP and MFC) in both strains, with a few positive cells present in the medial side of the control strain. On the other hand, *Mig-6 over/over* mice showed fewer SOX9-positive cells on the medial side due the articular cartilage damage **(Fig 2.10).** Similar results were found at 18 months of age in *Mig-6 over/over* with decreased SOX9 immunostaining in their medial side compared to the control (data not shown). For all ages, negative controls did not show staining in chondrocytes.

Figure 2.7 Phospho-EGFR staining is decreased in the articular cartilage of cartilage specific Mig-6 overexpressing mice at 11 weeks of age. Immunostaining of phosphorylated epidermal growth factor receptor (pEGFR; Tyr-1173) in the knee joints of 11-week-old *Mig-6 $^{over/over}$Col2a1-Cre$^{+/-}$* **(B)** is decreased in response to increased Mig-6 levels. Frontal sections of mice articular cartilage, as negative control, exhibited no staining **(C)**. Also, cartilage-specific deletion of *Mig-6*, serving as positive control **(D)**. N=5 mice/genotyping. MFC = medial femoral condyle and MTP = medial tibial plateau. Scale bar = 100µm.

Figure 2.7 Phospho-EGFR staining is decreased in the articular cartilage of cartilage specific Mig-6 overexpressing mice at 11 weeks of age

Figure 2.8 SOX9 immunostaining shows a decrease in Mig-6 overexpressors mice at post-natal day 0 (p0). Ratio between the total cell number from control and Mig-6$^{over/over}$ **(B).** Ratio between the percentage of Sox9 positive cells from control and Mig-6$^{over/over}$ at p0 mice **(C).** Data analyzed by two tailed student t-tests from 5 mice per group. Individual data points presented with mean ± SEM (P<0.05). Scale bar = 100μm.
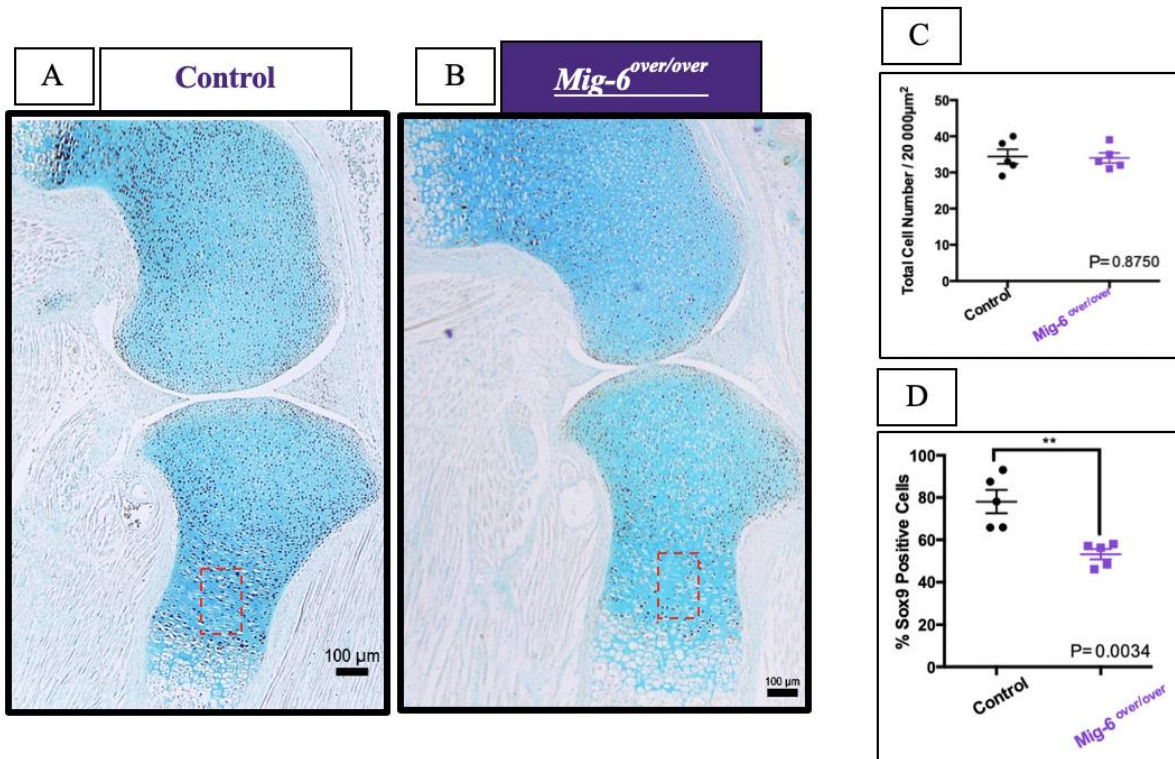
Figure 2.8 SOX9 immunostaining shows a decrease in Mig-6 overexpressors mice at post-natal day 0 (p0)

Figure 2.9 SOX9 immunostaining shows a decrease in Mig-6 overexpressors mice at 6 weeks-old male mice control and Mig-6$^{over/over}$. No primary antibody for SOX9 display no staining with methyl green counterstain in mice. Ratio between the total cell number from control and Mig-6$^{over/over}$ at 6 weeks-old male mice **(C).** Ratio between the percentage of Sox9 positive cells from control and Mig-6over at 6 weeks-old male mice **(D).** Data analyzed by two-way ANOVA (95% CI) with Bonferroni post-hoc test. Individual data points presented with mean ± SEM; N= 5 mice/genotyping. LFC = lateral femoral condyle, LTP = lateral tibial plateau, MFC = medial femoral condyle and MTP = medial tibial plateau. Scale bar = 100µm.

Figure 2.9 SOX9 immunostaining shows a decrease in Mig-6 overexpressors mice at 6 weeks-old male mice control and Mig-6$^{over/over}$

Figure 2.10 12-month-old cartilage specific Mig-6 overexpressing mice show decreased SOX9 immunostaining. Representative SOX9 immunostained in male mice (n=5) in MFC and MTP show decreased staining intensity in Mig-6 over mice **(B)** when compared to control **(A).** No primary control for articular cartilage **(C).** LFC = lateral femoral condyle, LTP = lateral tibial plateau, MFC = medial femoral condyle and MTP = medial tibial plateau. Scale bar = 100µm.

Figure 2.10 12-month-old cartilage specific Mig-6 overexpressing mice show decreased SOX9 immunostaining

2.4.6   Overexpression of Mig-6 decreases expression of lubricin

Lubricin (aka PRG4/superficial zone protein) is a proteoglycan that plays an important role as lubricant in the joint (53). EGFR signaling is crucial for the cartilage lubrication function and regulates the induction of *Prg4* expression which is necessary for smooth movement (33,54). Immunohistochemistry for Lubricin in 11-week-old and 12 months-old animals demonstrated less staining in the superficial zone of the medial side of *Mig-6* $^{over/over}$ mice than in the control group **(Fig. 2.11 and Fig. 2.12).**

Figure 2.11 Lubricin immunostaining is slightly decreased in the articular cartilage of cartilage specific Mig-6 overexpressing mice at 11 weeks of age. Immunostaining of sections of the knee joint indicate the presence of Lubricin (*PRG4*) in the superficial zone chondrocytes. IHC reveals no staining for the negative control **(C)** and *Mig-6* KO, serving as positive control **(D)**. N=4-5 mice/genotyping. MFC = medial femoral condyle and MTP = medial tibial plateau. Scale bar = 100µm.
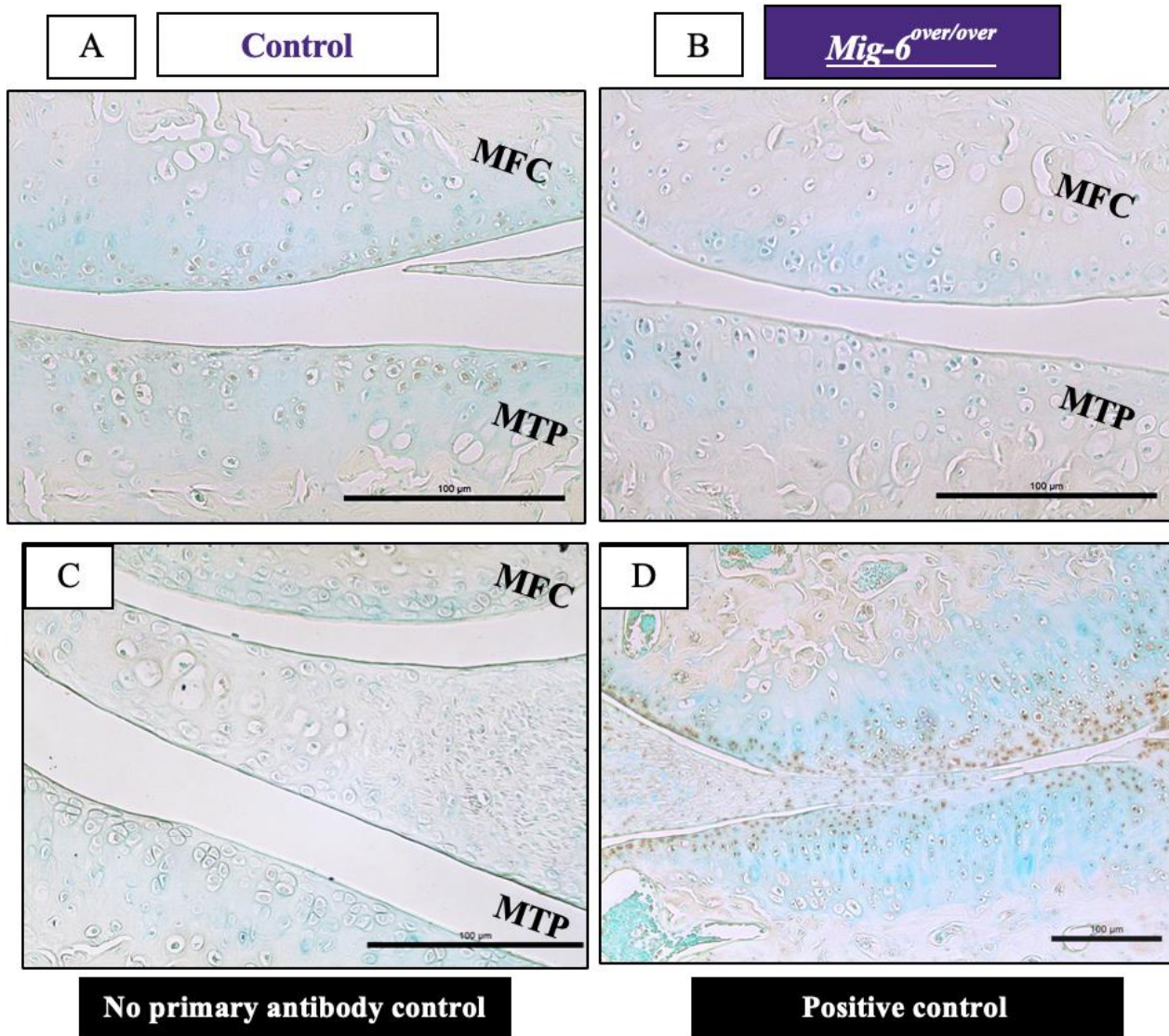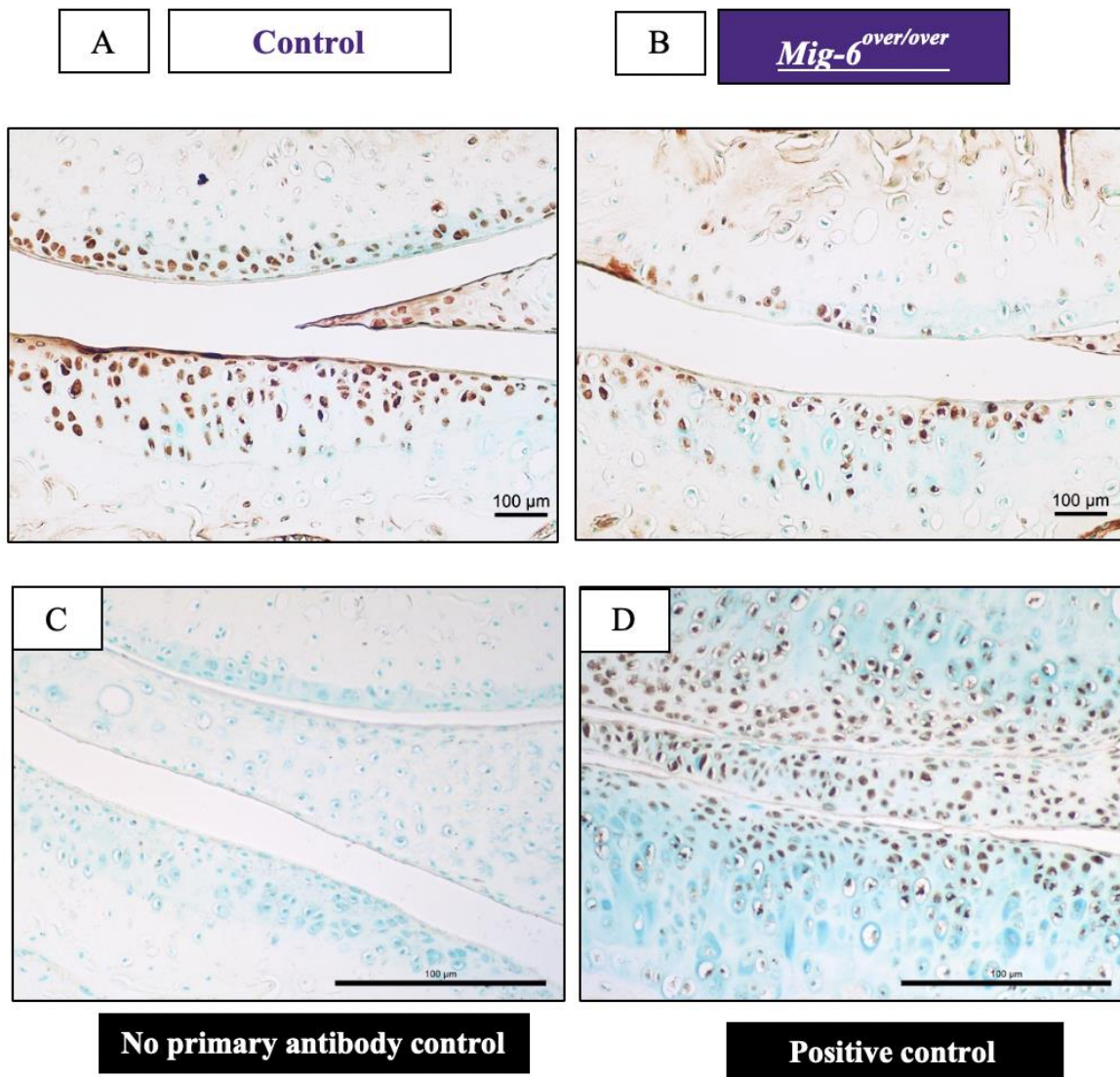
Figure 2.11 Lubricin immunostaining is slightly decreased in the articular cartilage of cartilage specific Mig-6 overexpressing mice at 11 weeks of age

Figure 2.12 Lubricin immunostaining is decreased in the articular cartilage of cartilage specific Mig-6 overexpressing mice at 12 months of age. Immunostaining of sections of the knee joint indicate the presence of Lubricin (*PRG4*) in the superficial zone chondrocytes. N=4-5 mice/genotyping. MFC = medial femoral condyle and MTP = medial tibial plateau. Scale bar = 100µm.

A **Control**

MFC

MTP

100 µm

B ***Mig-6^{over/over}***

MFC

MTP

100 µm
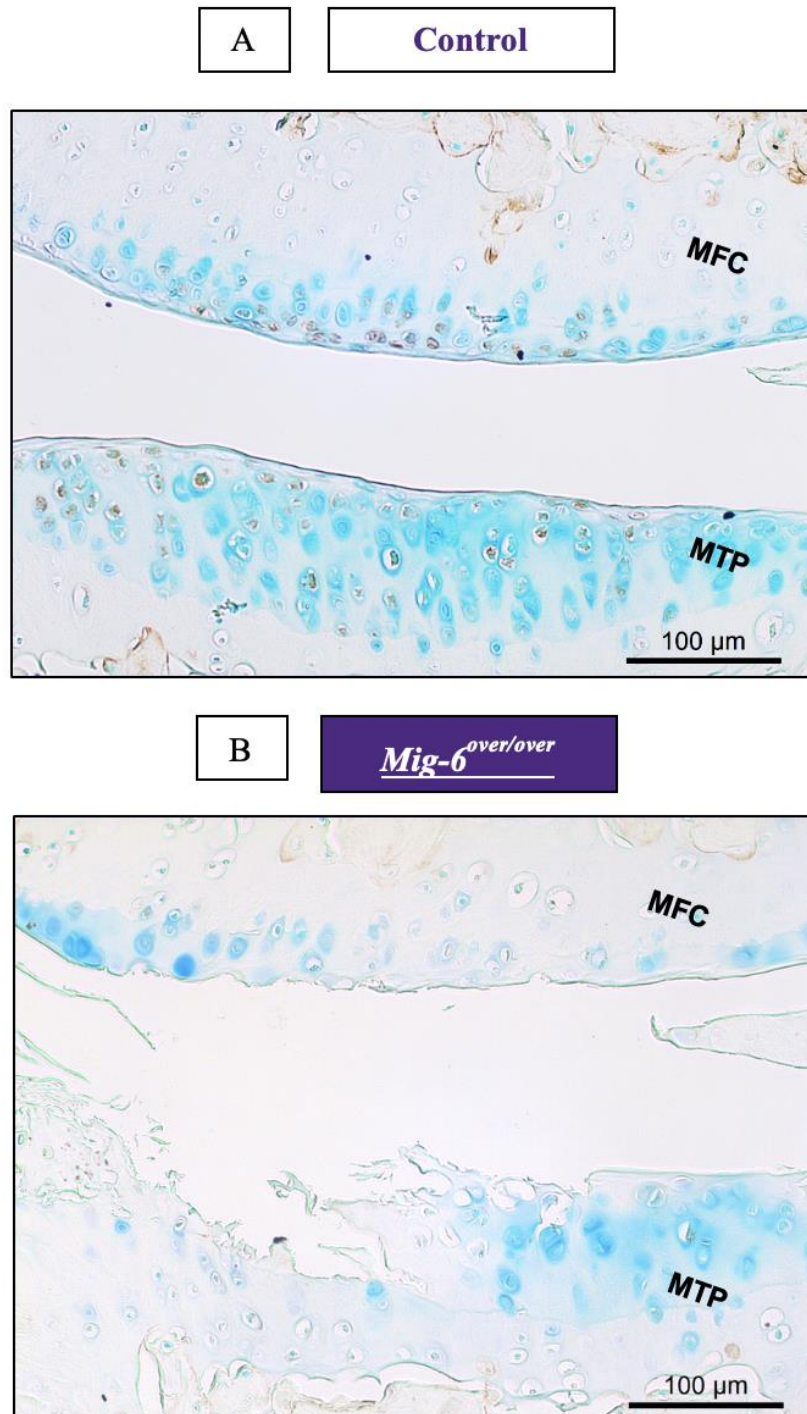
Figure 2.12 Lubricin immunostaining is decreased in the articular cartilage of cartilage specific Mig-6 overexpressing mice at 12 months of age

2.4.7 MMP13 immunostaining is increased in Mig-6-overexpressing and control mice

Matrix metalloproteinase (MMP) 13 is highly expressed in OA (55,56). Frontal sections of knees from 12- and 18-month-old control and *Mig-6* $^{over/over}$ male mice were used for MMP13 immunohistochemistry. At 12 months, pericellular staining was observed in the lateral articular cartilage of male mice from both genotypes, along with the expected subchondral bone staining **(Fig. 2.13).** Immunostaining for MMP13 on serial sections of lesions revealed strong staining in the same areas of cartilage degeneration in mutant mice than control mice. Negative controls did not show staining in cartilage or subchondral bone. Articular cartilage from 18 months-old mice showed similar staining patterns and intensity of MMP13 immunostaining in the lateral side of both genotypes, however in the medial side of *Mig-6* $^{over/over}$ mice, MMP13 staining is seen on the cartilage surface (lesion sites) and also observed in the subchondral bone (data not shown).

Figure 2.13 12-month-old cartilage specific Mig-6 overexpressing mice show similar pattern of MMP13 as the control mice. Representative immunohistochemistry of matrix metalloproteinase 13 (MMP13) for Mig-6 overexpression mice at 12 months control **(A)** and cartilage specific Mig-6 overexpression **(B).** No primary control for articular cartilage **(C).** N=5 mice/genotyping. LFC = lateral femoral condyle, LTP = lateral tibial plateau, MFC = medial femoral condyle and MTP = medial tibial plateau. Scale bar = 100µm.
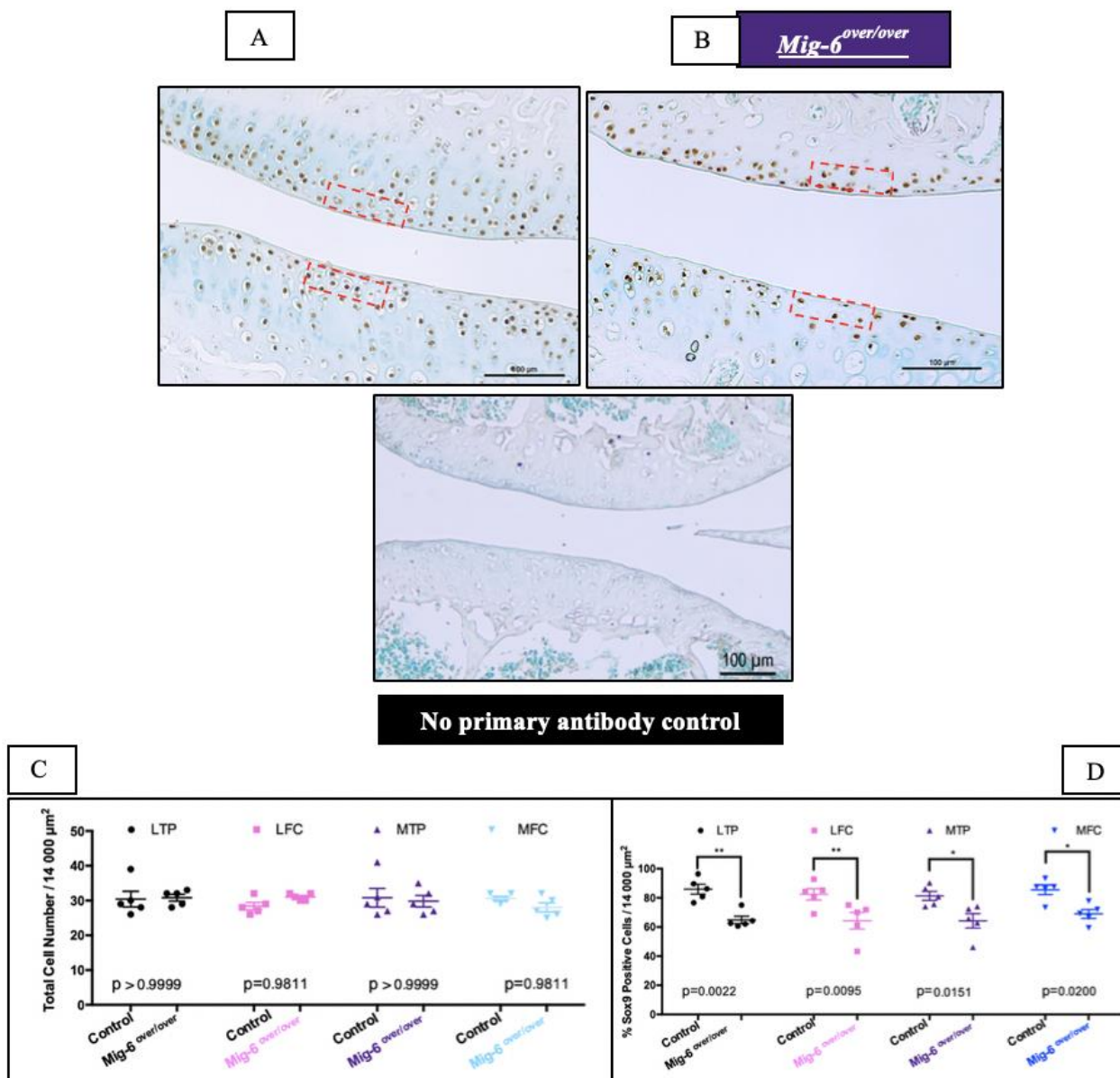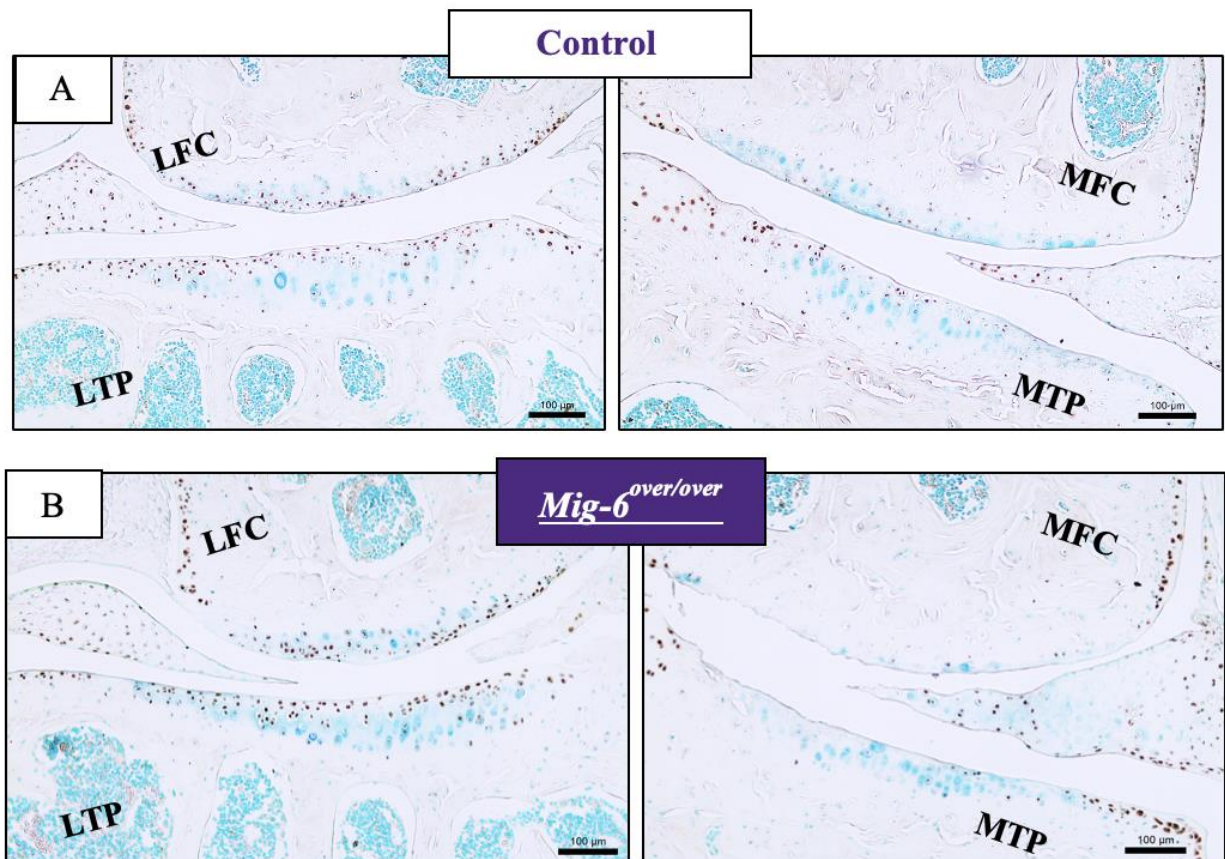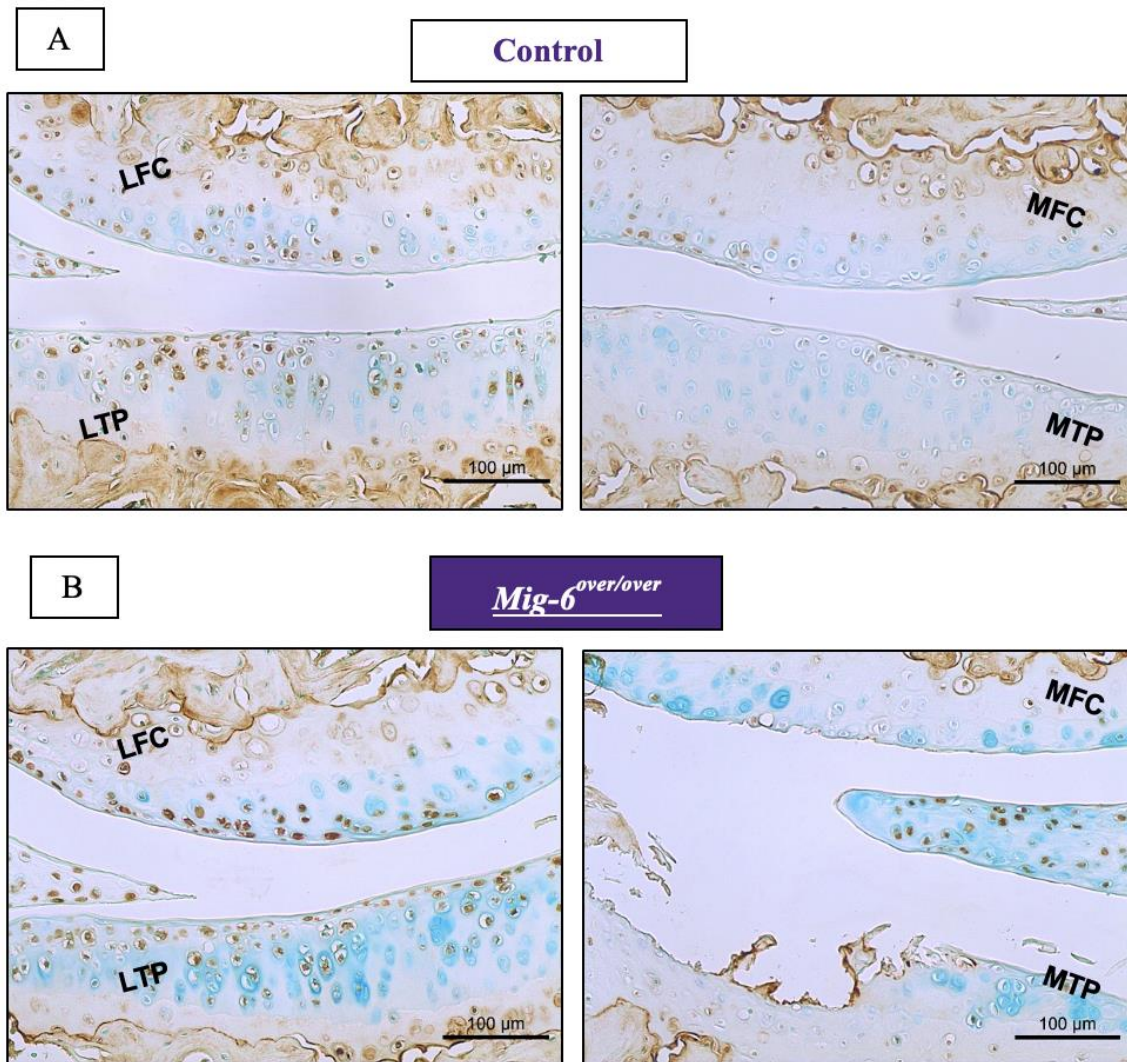
Figure 2.13 12 month-old cartilage specific Mig-6 overexpressing mice show similar pattern of MMP13 as the control mice

2.5   Discussion

The maintenance of articular cartilage homeostasis relies on a dynamic equilibrium involving growth factors (57), genetics (58), mechanical forces (59), obesity and injury, that all play a role in the onset of osteoarthritis (60). Better understanding of the underlying molecular mechanism is required to design therapies for preventing progression of OA. Recent studies from our laboratory and others have identified the epidermal growth factor receptor (EGFR) and Mig-6 as possible mediators of articular cartilage homeostasis (35,41,54,61). *Mig-6* is a cytosolic protein and negative feedback regulator of EGFR signalling (62); thus, *Mig-6* can be a potential tumor suppressor (43,63–66). In addition, whole body knockout of the *Mig-6* gene in mice results in degenerative joint disease (38). We also have shown previously that constitutive cartilage-specific deletion of *Mig-6* (Mig-6 KO) results in increased articular cartilage thickness and cell density in the joints of 12 week-old mice (41). Cartilage-specific Mig-6 KO mice show the same anabolic effect in joint cartilage at 21 months of age (unpublished).

Previous research demonstrates that Mig-6 overexpression acts as a negative feedback regulator of EGFR-ERK signalling (43), however these studies did not yet analyze joint tissues. Since our studies suggest dosage- and/or context-specific roles of EGFR signaling in joint homeostasis and OA (35), we now examined whether overexpression of Mig-6 alters these processes. Here, we report that cartilage-specific constitutive overexpression of *Mig-6* did not cause cartilage degeneration in young mice, but early onset OA in middle aged mice. While we observed some effects of Mig-6 overexpression on bone length and weight, these effects were subtle and not accompanied by major morphological or histological changes in growth plate cartilage, overall skeletal morphology, or body composition. A previous study showed that deletion of EGFR in bone tissue (*Col1-Cre Egfr^{Wa5/f}*) resulted in shorter femurs compared to wild-type mice (67), consistent with our findings. The EGFR network is essential during long bone development, since previous studies have shown that EGFR- or TGFα-deficient mice exhibit a widened zone of hypertrophic chondrocytes (24,68). Moreover, Qin and colleagues have shown that administration of the EGFR inhibitor, gefitinib, into 1-monht-old rats results in an enlarged hypertrophic zone due down-regulation of MMP-9,-13 and -14 (31). Together these data suggest a critical role of EGFR during endochondral ossification and elucidate downstream mechanism of EGFR (69). Further research is required to provide more evidence of EGFR/*Mig-6^{over/over}* signalling during

bone formation, but many of these effects are relatively subtle and transient, and likely unrelated to much more severe phenotypes observed later.

Histologically, our findings showed that mice with cartilage-specific *Mig-6* overexpressing showed healthy articular cartilage with no significant difference in articular cartilage thickness from control group at the ages of 6 weeks and 11 weeks. However, *Mig-6 [over/over]* mice developed severe degeneration of articular cartilage with aging. More prevalent, the knee joints of *Mig-6 [over/over]* male mice showed significantly advanced cartilage degeneration. The same pattern but with more severe damage, was seen in 18-month-old mice. As previously described, sex hormones play a role in OA disease where male mice develop more severe OA (70).

SOX9 is crucial in chondrogenesis during endochondral bone formation, articular cartilage development and cartilage homeostasis (52). Previous *in vivo* models using cartilage *(Col2)-Cre* or limb *(Prx1)-Cre* specific ablation of *Mig-6* showed increased expression of SOX9 in the articular cartilage. Also, TGFα supresses expression of anabolic genes such as Sox9, type II collagen and aggrecan in primary chondrocytes (71). Interestingly, in the medial and lateral compartment of the knee joints of 6 and 11-week-old male *Mig-6 [over/over]* mice, the percentage of SOX9- positive chondrocytes was decreased compared to controls, despite the absence of histological defects in articular cartilage. These data suggest that reduced number of Sox9-expressing cells precede the degeneration of articular chondrocytes in our mutant mice. The number of SOX9-expressing cells was also reduced in *Mig-6 [over/over]* mice at later ages. These data suggest that reduced numbers of Sox9-expressing cells could be one cause of the advanced OA in our mutant mice. In addition, we observed decreased expression of lubricin/PRG4 in these joints, which might also contribute to the observed joint pathologies. PRG4 has been shown to be regulated by EGFR signaling before (42,54), in support of our findings.

While the EGFR is the best characterised substrate of Mig-6, other substrates have been described. Mig-6 binds to different proteins such as the cell division control protein 42 homolog (Cdc42) (72), c-Abl (73), and the hepatocyte growth factor receptor c-Met (74). While we cannot exclude that deregulation of these other substrates contributes to the observed phenotypes, the similarities of defects in our mice with those seen upon cartilage-specific deletion of EGFR suggest that decreased EGFR signaling is the main cause for the advanced OA observed in our mutant mice.

Nevertheless, it will be important to determine whether signaling through cMet and other pathways is altered as well.

In conclusion, we show for the first time that cartilage-specific Mig-6 overexpression in mice results in reduced EGFR activity in chondrocytes, reduced SOX9 and PRG4 expression, and accelerated development of OA. These data highlight the important and context-specific role of the EGFR-Mig-6 signaling pathway in joint homeostasis and point towards potential targeting of this pathway for OA therapy.

2.6   Acknowledgements

2.7   Supplemental Figures

Supplementary Figure 1) Construction of the targeting vectors and generation of *Mig-6^{over/over}* mice. Adapted from Kim, T. H. *et al.* Mig-6 suppresses endometrial cancer associated with pten deficiency and ERK activation. *Cancer Res.* **74,** 7371–7382 (2014). **(A)** The overexpression of *Mig-6* is accomplished by placing the transcription of *Mig-6* under the control of a ubiquitously expressed promoter, the chicken b actin-cytomegalovirus hybrid (CAGGS) promoter. The construction also contained the "Stop Cassette" flanked by LoxP sites (LSL). **(B)** PCR strategy. P1 and P2 can amplify a 300 bp fragment from the wild-type allele, whereas P1 and P3 can amplify a 450 bp fragment from the targeted ROSA26 locus allele. **(C)** A representative agarose gel image of PCR genotyping, heterozygous (Het), wild-type (WT) and homozygous (Homo). **(D)** PCR primer sequence for wild type and *Mig-6^{LSL}* allele. **(E)** RT- PCR primer sequence for *Mig-6^{over/over}*. **(F)** Individual data points presented with mean ± SEM (P<0.05). Data analyzed by two tailed student t-tests from 11 mice per group.
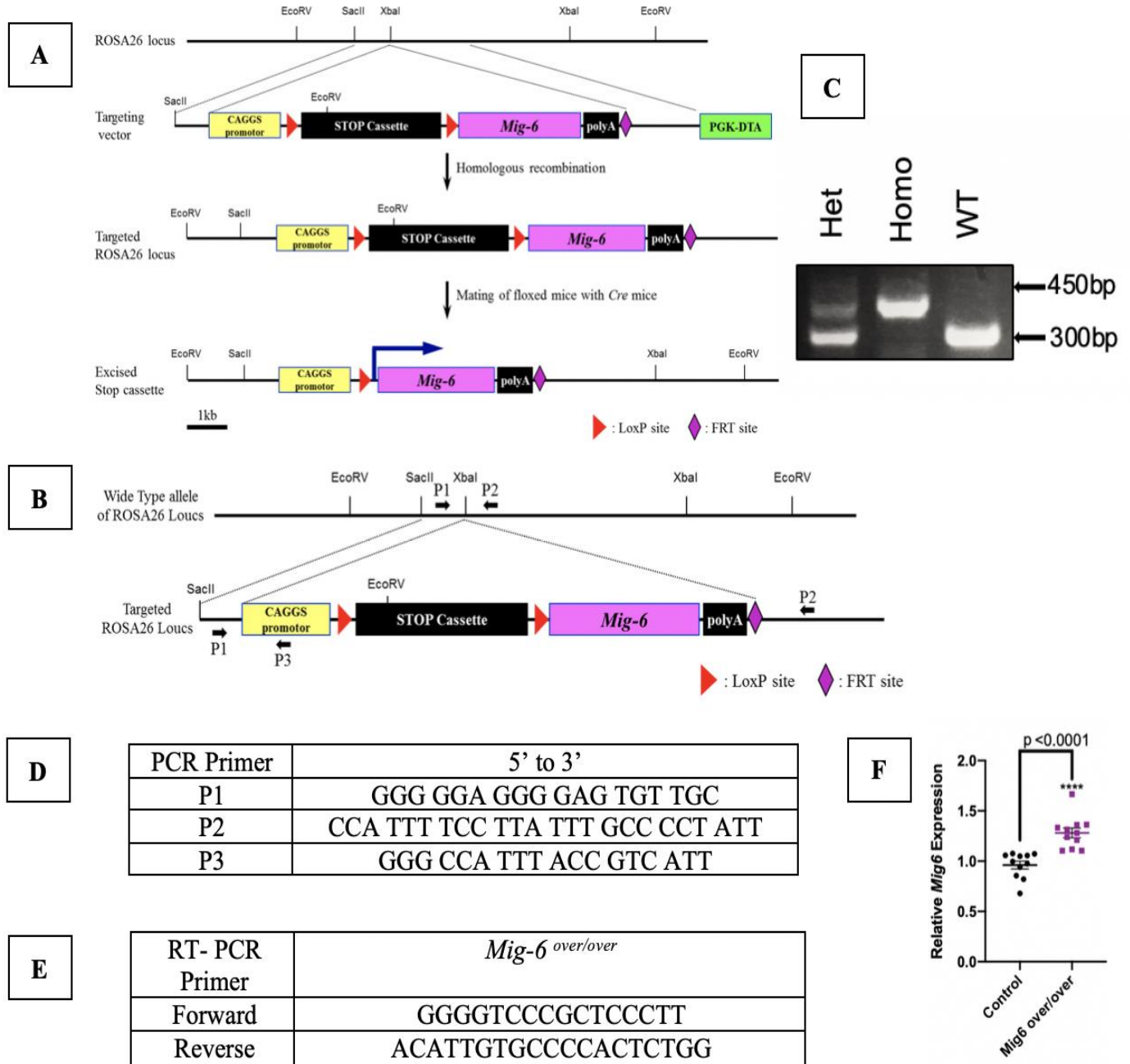
Supplementary Figure 1) Construction of the targeting vectors and generation of *Mig-6$^{over/over}$* mice

Supplementary Figure 2) Bone mineral densities were measured from µCT scan volumes from control and *Mig-6^{over/over}* male mice. (A) Mean bone mineral densities were 323.7 mg/cc (control) and 318.5 mg/cc (*Mig-6^{over/over}*) at 11 weeks-old. Moreover, **(B)** At 12 months of age male *Mig-6^{over/over}* mice had mean bone mineral density (342.9 mg/cc) and controls male mice (341.0 mg/cc). **(C)** At 18 months of age, there were no significance difference between the mean bone mineral density from control male mice (342.1 mg/cc) and male *Mig-6^{over/over}* (333.2 mg/cc). There were not significantly different among 11 weeks-old, 12 and 18 months for bone mineral density for male control and Mig-6 overexpression mice. Individual data points presented with mean ± SEM (P<0.05). Data analyzed by two tailed student t-tests from 6-12 mice per group (age/gender).
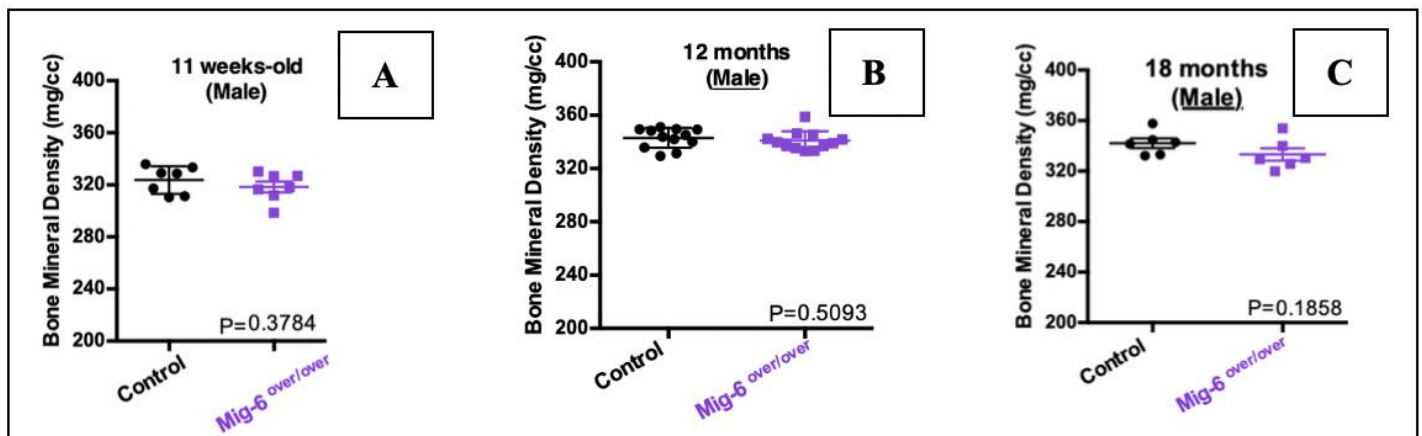
Supplementary Figure 2) Bone mineral densities were measured from µCT scan volumes from control and *Mig-6^{over/over}* male mice

Supplementary Figure 3) Body composition and body mass from growth and aging male control and *Mig-6$^{over/over}$*. Body composition was calculated from control and *Mig-6$^{over/over}$* male mice. At 11 weeks-old **(A1/A2)**, 12 months **(B1/B2)** and 18 months **(C1/C2)** neither the average lean mass percent nor mean body fat were statistically significant between genotypes. Individual data points presented with mean ± SEM (P<0.05). Data analyzed by two tailed student t-tests from 6-12 mice per group (age/genotyping).
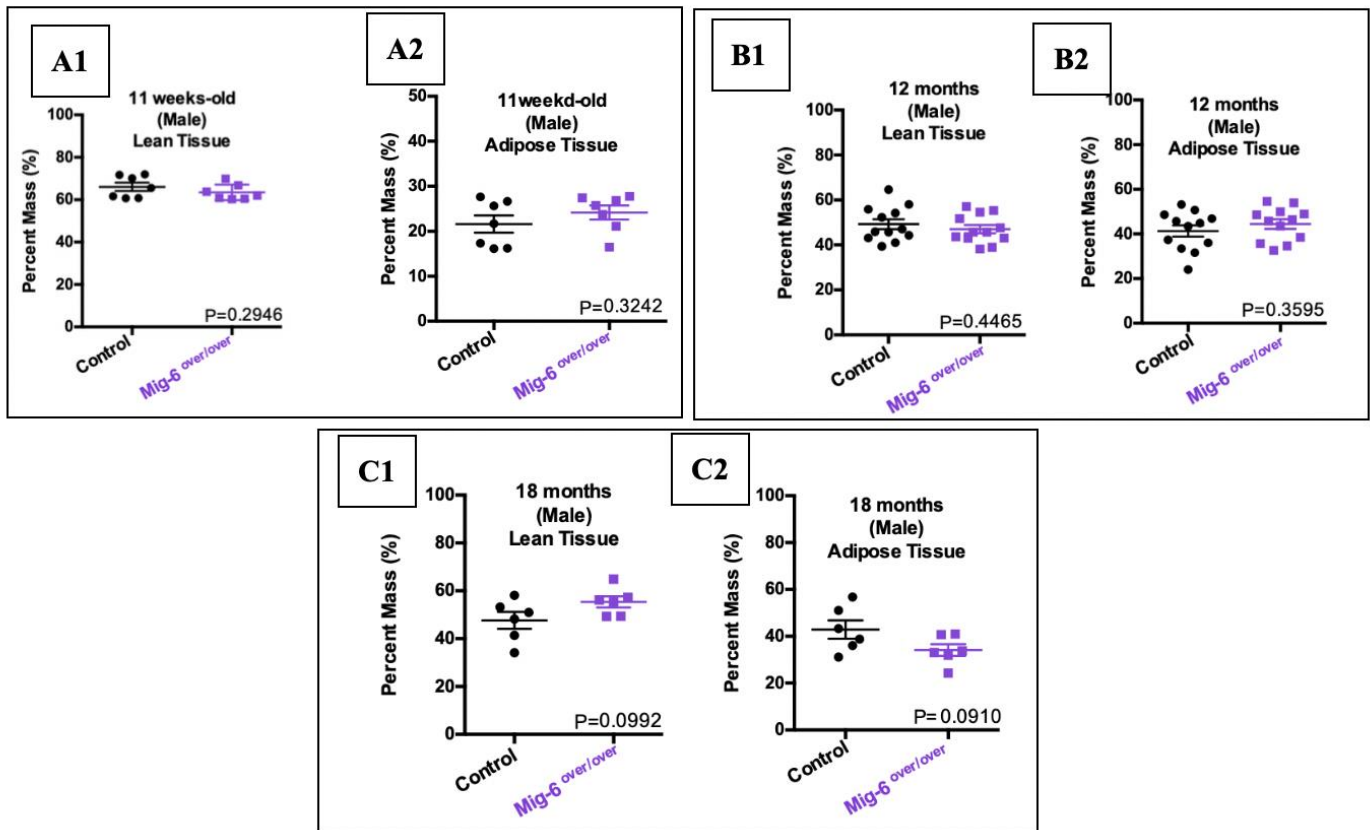
Supplementary Figure 3) Body composition and body mass from growth and aging male control and *Mig-6over/over*

Supplementary Figure 4) Articular cartilage from 11 weeks-old *Mig-6^{over/over}* female mice appeared healthy during skeletal maturity. Representative (n=5/group, toluidine blue) stained frontal sections of knee joints from 11-week-old control **(A)** and *Mig-6^{over/over}* **(B).** Mig-6 overexpressors mice show similar articular cartilage thickness when compared to controls at 11 weeks-old female mice. The average thickness of the calcified articular cartilage **(C)** and non-calcified articular cartilage **(D)** in the lateral femoral condyle (LFC), lateral tibial plateau (LTP), medial femoral condyle (MFC), medial tibial plateau (MTP) was measured. Individual data points presented with mean ± SEM. Data analyzed by two-way ANOVA (95% CI) with Bonferroni post-hoc test. Scale bar = 100µm.
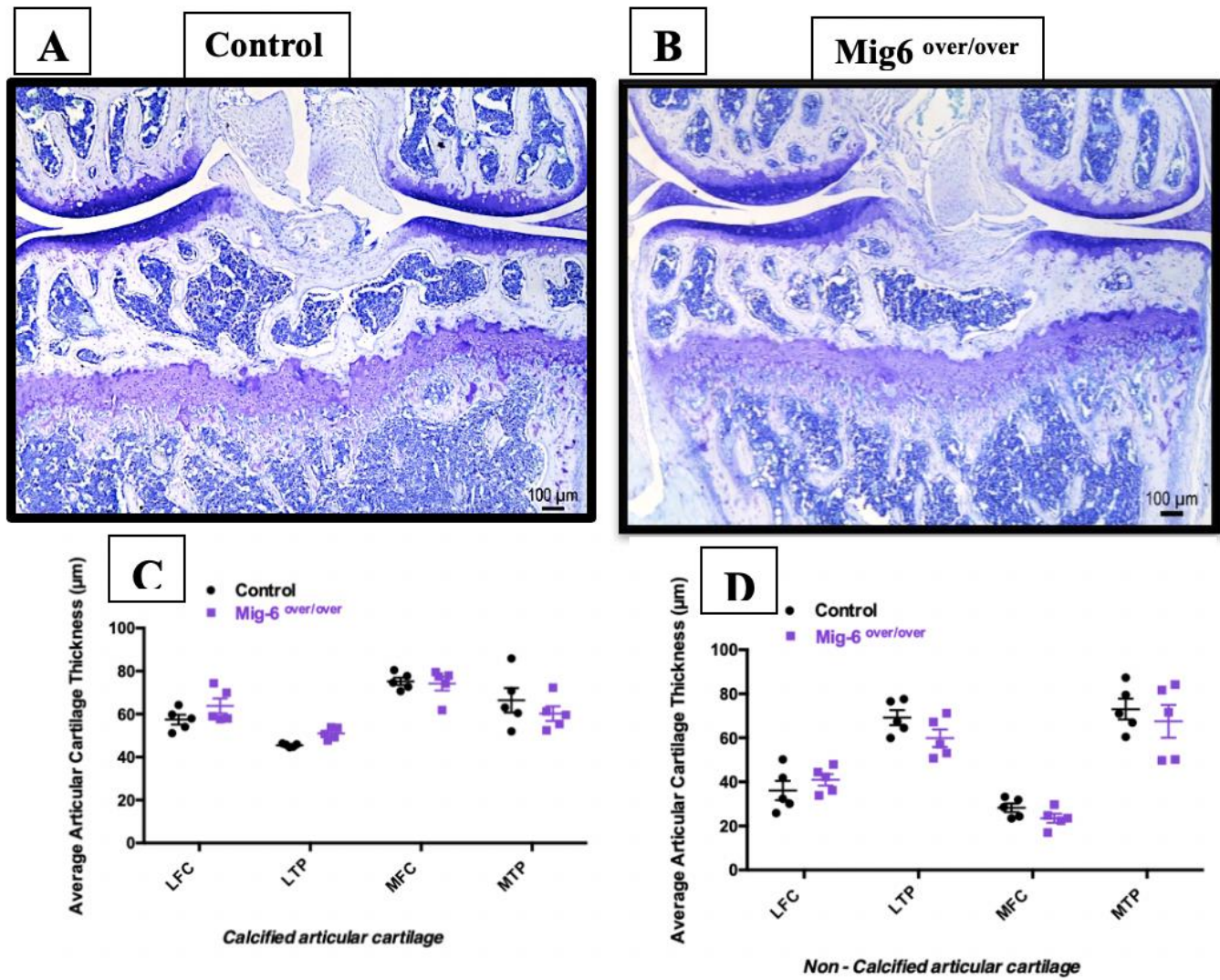
Supplementary Figure 4) Articular cartilage from 11 weeks-old *Mig-6^{over/over}* female mice appeared healthy during skeletal maturity

Supplementary Figure 5) 12-month-old *Mig-6^{over/over}* female mice showed joint damage.
Representative images of Toluidine Blue stained sections of knee joints from 12 month-old female
control **(A)** and *Mig-6^{over/over}* **(B)** mice were evaluated for cartilage damage following the OARSI
histopathological scale on the four quadrants of the knee: LFC = lateral femoral condyle, LTP =
lateral tibial plateau, MFC = medial femoral condyle and MTP = medial tibial plateau. OARSI
based cartilage degeneration scores are higher both in the MFC and MTP of Mig-6 overexpressing
mice, corresponding to the increased damage observed histologically **(C)**. Data analyzed by two-
way ANOVA with Bonferroni's multiple comparisons test. Individual data points presented with
mean ± SEM. All scale bars =100 µm. N = 8 mice/group. Scale bar = 100µm.

Supplementary Figure 5) 12-month-old *Mig-6*^{*over/over*} female mice showed joint damage

Supplementary Figure 6) 18 months-old *Mig-6^{over/over}* female mice showed increased damage in the medial tibial plateau. Representative images of Toluidine Blue stained sections of knee joints from 18 month-old female control **(A)** and female Mig-6 over **(B)** mice were evaluated for cartilage damage following OARSI histopathological scale on the four quadrants of the knee: LFC = lateral femoral condyle, LTP = lateral tibial plateau, MFC = medial femoral condyle and MTP = medial tibial plateau. OARSI based cartilage degeneration scores are higher both in the MFC and MTP of Mig-6 overexpressing mice, corresponding to the increased damage observed histologically. **(C)**. Data analyzed by two-way ANOVA with Bonferroni's multiple comparisons test. Individual data points presented with mean ± SEM. All scale bars =100 μm. N = 8 mice/group. Scale bar = 100μm.

Supplementary Figure 6) 18 months old *Mig-6^over/over* female mice showed joint damage

Supplementary Figure 7) SOX9 immunostaining shows a decrease in Mig-6 overexpressors mice at 11 weeks-old male mice control and *Mig-6$^{over/over}$*. No primary antibody staining. Ratio between the total cell number from control and Mig-6over at 11 weeks-old male mice **(A).** Ratio between the percentage of Sox9 positive cells from control and Mig-6over at 11 weeks-old male mice **(B).** Data analyzed by two-way ANOVA (95% CI) with Bonferroni post-hoc test. Individual data points presented with mean ± SEM; N= 5 mice/genotyping. LFC = lateral femoral condyle, LTP = lateral tibial plateau, MFC = medial femoral condyle and MTP = medial tibial plateau. Scale bar = 100µm.
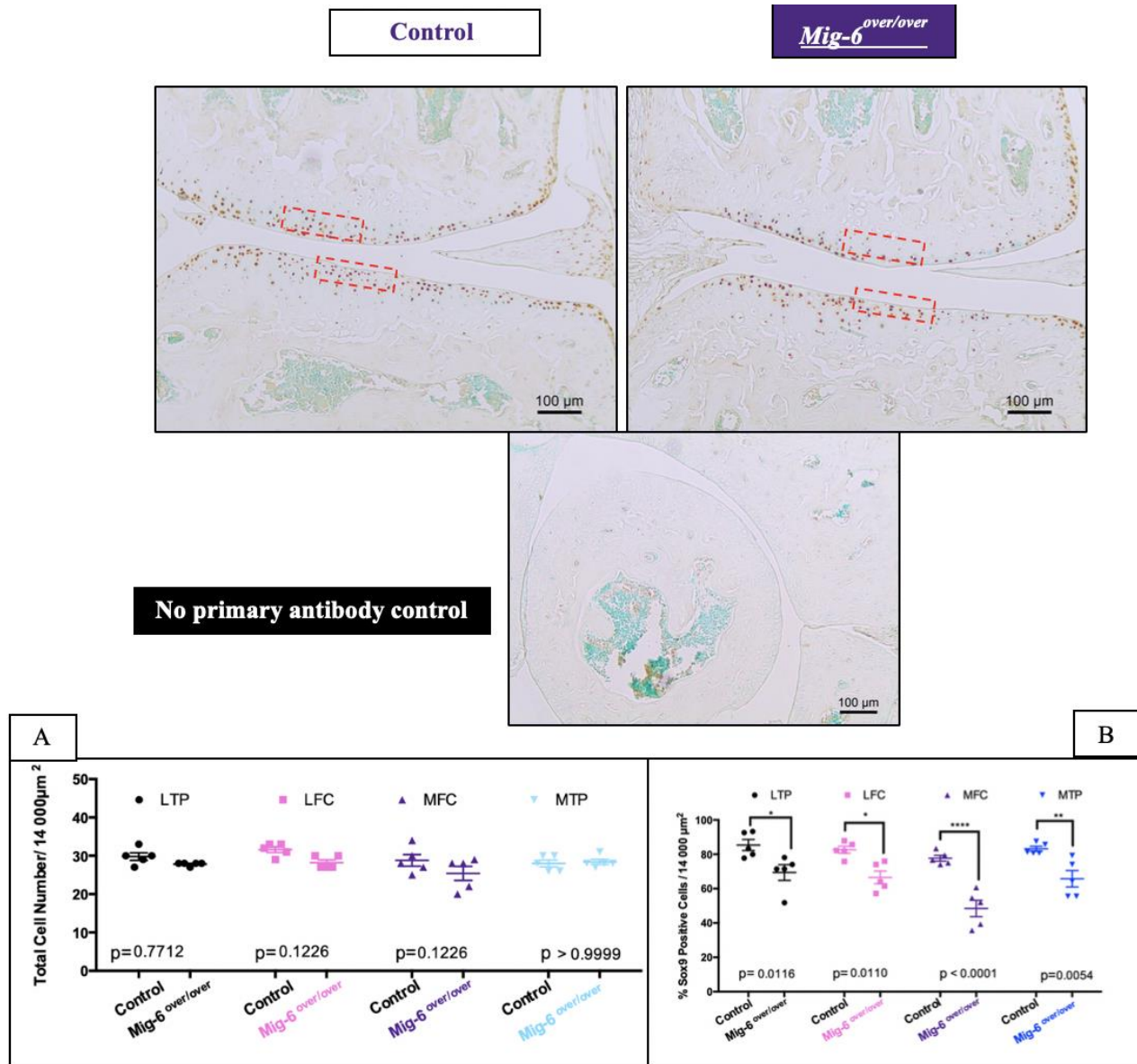
Supplementary Figure 7) SOX9 immunostaining shows a decrease in Mig-6 overexpressors mice at 11 weeks-old male mice control and *Mig-6$^{over/over}$*.

2.8 References

1.   Hunter, D. J., Schofield, D. & Callander, E. The individual and socioeconomic impact of osteoarthritis. *Nat. Rev. Rheumatol.* **10,** 437–441 (2014).

2.   Bombardier C, Hawker G, M. D. *The Impact Of Arthritis In Canada: Today And Over The Next 30 Years*. (2011).

3.   Kramer, W. C., Hendricks, K. J. & Wang, J. Pathogenetic mechanisms of posttraumatic osteoarthritis: Opportunities for early intervention. *Int. J. Clin. Exp. Med.* (2011).

4.   Ruan, M. Z. *et al.* Treatment of osteoarthritis using a helper-dependent adenoviral vector retargeted to chondrocytes. *Mol. Ther. — Methods Clin. Dev.* **3,** 16008 (2016).

5.   Sokolove, Jeremy and Lepus, C. M. Role of inflammation in the pathogenesis of osteoarthritis: latest findings and interpretations. *Ther Adv Musculoskel Dis* **5,** 77–94 (2013).

6.   Mcalindon, T. E. *et al.* OARSI guidelines for the non-surgical management of knee osteoarthritis. *Osteoarthr. Cartil.* **22,** 363–388 (2014).

7.   Hunter, D. J. Osteoarthritis. *Best Pract. Res. Clin. Rheumatol.* **25,** 801–814 (2011).

8.   Driban, J. B., Sitler, M. R., Barbe, M. F. & Balasubramanian, E. Is osteoarthritis a heterogeneous disease that can be stratified into subsets? doi:10.1007/s10067-009-1301-1

9.   Gs, M. & Mologhianu G. *Osteoarthritis pathogenesis-a complex process that involves the entire joint*. *J. Med. Life* **7,** 37-41 (2014).

10.   Felson, D. T. Osteoarthritis as a disease of mechanics. (2012). doi:10.1016/j.joca.2012.09.012

11.   Poole, A. R. *et al.* Composition and Structure of Articular Cartilage. *Clin. Orthop. Relat. Res.* **391,** S26–S33 (2003).

12.   Saha, A. K. & Kohles, S. S. A cell-matrix model of anabolic and catabolic dynamics during cartilage biomolecule regulation. (2012). doi:10.1504/IJCIH.2012.046995

13.   Goldring, M. B. *et al.* Cartilage homeostasis in health and rheumatic diseases. *Arthritis Res. Ther.* **11,** 224 (2009).

14.   Yeung Tsang, K., Wa Tsang, S., Chan, D. & Cheah, K. S. E. The chondrocytic journey in endochondral bone growth and skeletal dysplasia. *Birth Defects Res. Part C - Embryo Today Rev.* **102,** (2014).

15.   Gilbert, A. M., Bikker, J. A. & O'Neil, S. V. Advances in the development of novel aggrecanase inhibitors. *Expert Opin. Ther. Pat.* **21,** 1–12 (2011).

16.   Parks, W. C., Wilson, C. L. & López-Boado, Y. S. Matrix metalloproteinases as modulators

of inflammation and innate immunity. *Nat. Rev. Immunol.* **4,** 617–629 (2004).

17. Yoon, Y. M. *et al.* Epidermal growth factor negatively regulates chondrogenesis of mesenchymal cells by modulating the protein kinase C-alpha, Erk-1, and p38 MAPK signaling pathways. *J. Biol. Chem.* **275,** 12353–9 (2000).

18. Fortier Dvm, L. A., Barker, J. U., Strauss, E. J., Mccarrel, T. M. & Cole, B. J. SYMPOSIUM: CLINICALLY RELEVANT STRATEGIES FOR TREATING CARTILAGE The Role of Growth Factors in Cartilage Repair. doi:10.1007/s11999-011-1857-3

19. Van Der Kraan, P. M. Differential Role of Transforming Growth Factor-beta in an Osteoarthritic or a Healthy Joint. (2018). doi:10.11005/jbm.2018.25.2.65

20. Gamer, L. W. *et al.* The Role of *Bmp2* in the Maturation and Maintenance of the Murine Knee Joint. *J. Bone Miner. Res.* **33,** 1708–1717 (2018).

21. Wei, F.-Y. *et al. Correlation of insulin-like growth factor 1 and osteoarthritic cartilage degradation: a spontaneous osteoarthritis in guinea-pig HHS Public Access. Eur Rev Med Pharmacol Sci* **21,** (2017).

22. Appleton, C. T. G., Pitelka, V., Henry, J. & Beier, F. Global analyses of gene expression in early experimental osteoarthritis. *Arthritis Rheum.* **56,** 1854–1868 (2007).

23. Appleton, C. T. G., Usmani, S. E., Bernier, S. M., Aigner, T. & Beier, F. Transforming growth factor alpha suppression of articular chondrocyte phenotype and Sox9 expression in a rat model of osteoarthritis. *Arthritis Rheum.* **56,** 3693–705 (2007).

24. Usmani, S. E. *et al.* Transforming growth factor alpha controls the transition from hypertrophic cartilage to bone during endochondral bone growth. *Bone* **51,** 131–141 (2012).

25. Appleton, C. T. G. *et al.* Reduction in disease progression by inhibition of transforming growth factor α-CCL2 signaling in experimental posttraumatic osteoarthritis. *Arthritis Rheumatol. (Hoboken, N.J.)* **67,** 2691–701 (2015).

26. Usmani, S. E. *et al.* Context-specific protection of TGFα null mice from osteoarthritis. *Sci. Rep.* **6,** 30434 (2016).

27. Cui, G. *et al.* Association of Common Variants in TGFA with Increased Risk of Knee Osteoarthritis Susceptibility. *Genet. Test. Mol. Biomarkers* gtmb.2017.0045 (2017). doi:10.1089/gtmb.2017.0045

28. Zengini, E. *et al.* Genome-wide analyses using UK Biobank data provide insights into the genetic architecture of osteoarthritis. *Nat. Genet. 2018* 1 (2018). doi:10.1038/s41588-018-0079-y

29. Appleton, C. T. G., Usmani, S. E., Mort, J. S. & Beier, F. Rho/ROCK and MEK/ERK activation by transforming growth factor-alpha induces articular cartilage degradation. *Lab. Invest.* **90,** 20–30 (2010).

30. Wang, K., Yamamoto, H., Chin, J. R., Werb, Z. & Vu, T. H. Epidermal growth factor receptor-deficient mice have delayed primary endochondral ossification because of defective osteoclast recruitment. *J. Biol. Chem.* **279,** 53848–56 (2004).

31. Zhang, X. *et al.* The critical role of the epidermal growth factor receptor in endochondral ossification. *J. Bone Miner. Res.* **26,** 2622–33 (2011).

32. Jia, H. *et al.* EGFR signaling is critical for maintaining the superficial layer of articular cartilage and preventing osteoarthritis initiation. doi:10.1073/pnas.1608938113

33. Shepard, J. B., Jeong, J.-W., Maihle, N. J., O'Brien, S. & Dealy, C. N. Transient anabolic effects accompany epidermal growth factor receptor signal activation in articular cartilage in vivo. *Arthritis Res. Ther.* **15,** R60 (2013).

34. Zhang, X. *et al.* Reduced EGFR signaling enhances cartilage destruction in a mouse osteoarthritis model. *Bone Res.* **2,** 14015 (2014).

35. Qin, L. & Beier, F. EGFR Signaling: Friend or Foe for Cartilage? *JBMR Plus* **3,** e10177 (2019).

36. Jin, N., Gilbert, J. L., Broaddus, R. R., Demayo, F. J. & Jeong, J.-W. Generation of a Mig-6 conditional null allele. *Genesis* **45,** 716–21 (2007).

37. Frosi, Y. *et al.* A two-tiered mechanism of EGFR inhibition by RALT/MIG6 via kinase suppression and receptor degradation. *J. Cell Biol.* **189,** 557–71 (2010).

38. Zhang, Y.-W. *et al.* Targeted disruption of Mig-6 in the mouse genome leads to early onset degenerative joint disease. *Proc. Natl. Acad. Sci. U. S. A.* **102,** 11740–5 (2005).

39. Mateescu, R. G., Todhunter, R. J., Lust, G. & Burton-Wurster, N. Increased MIG-6 mRNA transcripts in osteoarthritic cartilage. *Biochem. Biophys. Res. Commun.* **332,** 482–6 (2005).

40. Joiner, D. M. *et al.* Accelerated and increased joint damage in young mice with global inactivation of mitogen-inducible gene 6 after ligament and meniscus injury. *Arthritis Res. Ther.* **16,** R81 (2014).

41. Pest, M. A., Russell, B. A., Zhang, Y.-W., Jeong, J.-W. & Beier, F. Disturbed cartilage and joint homeostasis resulting from a loss of mitogen-inducible gene 6 in a mouse model of joint dysfunction. *Arthritis Rheumatol. (Hoboken, N.J.)* **66,** 2816–27 (2014).

42. Shepard, J. B., Jeong, J.-W., Maihle, N. J., O'Brien, S. & Dealy, C. N. Transient anabolic effects accompany epidermal growth factor receptor signal activation in articular cartilage in vivo. *Arthritis Res. Ther.* **15,** R60 (2013).

43. Kim, T. H. *et al.* Mig-6 suppresses endometrial cancer associated with pten deficiency and ERK activation. *Cancer Res.* **74,** 7371–7382 (2014).

44. Terpstra, L. *et al.* Reduced chondrocyte proliferation and chondrodysplasia in mice lacking

the integrin-linked kinase in chondrocytes. *J. Cell Biol.* **162,** (2003).

45. Ratneswaran, A. *et al.* Nuclear receptors regulate lipid metabolism and oxidative stress markers in chondrocytes. *J. Mol. Med. (Berl).* **95,** 431–444 (2017).

46. Schneider, C. A., Rasband, W. S. & Eliceiri, K. W. NIH Image to ImageJ: 25 years of image analysis. *Nat. Methods* **9,** 671–675 (2012).

47. Beaucage, K. L., Pollmann, S. I., Sims, S. M., Dixon, S. J. & Holdsworth, D. W. Quantitative in vivo micro-computed tomography for assessment of age-dependent changes in murine whole-body composition. *Bone Reports* **5,** 70–80 (2016).

48. White, D. R. Tissue substitutes in experimental radiation physics. *Med. Phys.* **5,** 467–479 (1978).

49. Glasson, S. S., Chambers, M. G., Van Den Berg, W. B. & Little, C. B. The OARSI histopathology initiative – recommendations for histological assessments of osteoarthritis in the mouse. *Osteoarthr. Cartil.* **18,** S17–S23 (2010).

50. Ratneswaran, A. *et al.* Peroxisome proliferator-activated receptor δ promotes the progression of posttraumatic osteoarthritis in a mouse model. *Arthritis Rheumatol. (Hoboken, N.J.)* **67,** 454–64 (2015).

51. Zhang, M., Theleman, J. L., Lygrisse, K. A. & Wang, J. Experimental Section / Mini-Review Epigenetic Mechanisms Underlying the Aging of Articular Cartilage and Osteoarthritis. (2019). doi:10.1159/000496688

52. Lefebvre, V., Dvir-Ginzberg, M. & Hebrew, : SOX9 and the many facets of its regulation in the chondrocyte lineage HHS Public Access. *Connect Tissue Res* **58,** 2–14 (2017).

53. Waller, K. A. *et al.* Role of lubricin and boundary lubrication in the prevention of chondrocyte apoptosis. doi:10.1073/pnas.1219289110

54. Jia, H. *et al.* EGFR signaling is critical for maintaining the superficial layer of articular cartilage and preventing osteoarthritis initiation. *Proc. Natl. Acad. Sci. U. S. A.* 201608938 (2016). doi:10.1073/pnas.1608938113

55. Wang, M. *et al.* MMP13 is a critical target gene during the progression of osteoarthritis. *Arthritis Res. Ther.* **15,** R5 (2013).

56. Goumans, K. *et al.* Osteoarthritis in Humans and Mice Elevated MMP-13 Expression in Increase in ALK1/ALK5 Ratio as a Cause for. *J Immunol Ref.* **182,** 7937–7945 (2009).

57. Mariani, E., Pulsatelli, L. & Facchini, A. Signaling pathways in cartilage repair. *Int. J. Mol. Sci.* **15,** 8667–98 (2014).

58. Lee, A. *et al.* A Current Review of Molecular Mechanisms Regarding Osteoarthritis and Pain. *Gene* **527,** 440–447 (2013).

59. Bader, D. L., Salter, D. M. & Chowdhury, T. T. Biomechanical influence of cartilage homeostasis in health and disease. *Arthritis* **2011,** 979032 (2011).

60. Richmond, S. A. *et al.* Are Joint Injury, Sport Activity, Physical Activity, Obesity, or Occupational Activities Predictors for Osteoarthritis? A Systematic Review. *J. Orthop. Sport. Phys. Ther.* **43,** 515-B19 (2013).

61. Zhang, X. *et al.* Reduced EGFR signaling enhances cartilage destruction in a mouse osteoarthritis model. *Bone Res.* **2,** 14015 (2014).

62. Hackel, P. O., Gishizky, M. & Ullrich, A. Mig-6 Is a Negative Regulator of the Epidermal Growth Factor Receptor Signal. *Biol. Chem.* **382,** (2001).

63. Maity, T. K. *et al.* Loss of MIG6 Accelerates Initiation and Progression of Mutant Epidermal Growth Factor Receptor-Driven Lung Adenocarcinoma. *Cancer Discov.* **5,** 534–49 (2015).

64. Li, Z. *et al.* Downregulation of Mig-6 in nonsmall-cell lung cancer is associated with EGFR signaling. *Mol. Carcinog.* **51,** 522–34 (2012).

65. Zhang, Y.-W. *et al.* Evidence that MIG-6 is a tumor-suppressor gene. *Oncogene* **26,** 269–276 (2007).

66. Sasaki, M., Terabayashi, T., Weiss, S. M. & Ferby, I. The Tumor Suppressor MIG6 Controls Mitotic Progression and the G2/M DNA Damage Checkpoint by Stabilizing the WEE1 Kinase. *Cell Rep.* **24,** 1278–1289 (2018).

67. Zhang, X. *et al.* Epidermal growth factor receptor plays an anabolic role in bone metabolism in vivo. *J. Bone Miner. Res.* **26,** 1022–34 (2011).

68. Sibilia, M. *et al.* Correction: Mice humanised for the EGF receptor display hypomorphic phenotypes in skin, bone and heart. *Development* **143,** 4755–4755 (2017).

69. Zhang, X. *et al.* Epidermal Growth Factor Receptor (EGFR) Signaling Regulates Epiphyseal Cartilage Development through β-Catenin-dependent and -independent Pathways. *J. Biol. Chem.* **288,** 32229–32240 (2013).

70. Ma, H.-L. *et al.* Osteoarthritis severity is sex dependent in a surgical mouse model. *Osteoarthr. Cartil.* **15,** 695–700 (2007).

71. Appleton, C. T. G., Usmani, S. E., Bernier, S. M., Aigner, T. & Beier, F. Transforming growth factor α suppression of articular chondrocyte phenotype andSox9 expression in a rat model of osteoarthritis. *Arthritis Rheum.* **56,** 3693–3705 (2007).

72. Jiang, X. *et al.* Inhibition of Cdc42 is essential for Mig-6 suppression of cell migration induced by EGF. *Oncotarget* (2016). doi:10.18632/oncotarget.10205

73. Hopkins, S. *et al.* Mig6 is a sensor of EGF receptor inactivation that directly activates c-Abl to induce apoptosis during epithelial homeostasis. *Dev. Cell* **23,** 547–59 (2012).

74.   Pante, G. *et al.* Mitogen-inducible gene 6 is an endogenous inhibitor of HGF/Met-induced cell migration and neurite growth. *J. Cell Biol.* **171,** 337–48 (2005).

Chapter 3

3 Overexpression of Mig-6 In Limb Mesenchyme Leads to Accelerated Osteoarthritis In Mice

Bellini, Melina Rodrigues[1,2], Pest, Michael Andrew[1,2], Jae-Wook Jeong[4], Beier, Frank[1,2,3]

[1] Department of Physiology and Pharmacology, Western University, London, ON, Canada

[2] Western University Bone and Joint Institute, London, ON, Canada

[3] Children's Health Research Institute, London, ON, Canada

[4] Department of Obstetrics, Gynecology and Reproductive Biology, Michigan State University College of Human Medicine, Grand Rapids, Michigan.

Corresponding author: Dr. Frank Beier, Department of Physiology and Pharmacology, Western University, London, ON, Canada; Phone 519-661-2111 ext. 85344; email: fbeier@uwo.ca

The authors have no conflicts of interest to declare.

3.1   Abstract

Background: Mitogen-inducible gene 6 (Mig-6) is a tumour suppressor gene that is also associated with the development of osteoarthritis (OA)-like disorder. Recent evidence from our lab and others showed that cartilage-specific Mig-6 knockout (KO) mice develop chondro-osseous nodules, along with increased articular cartilage thickness and enhanced EGFR signaling in the articular cartilage. Here, we evaluate the phenotype of mice with skeletal-specific overexpression of Mig-6.

Methods: Synovial joint tissues of the knee were assessed in 12 and 36 weeks-old skeleton-specific *Mig-6* overexpressing (*Mig-6$^{over/over}$*) and control animals using histological stains, immunohistochemistry, semi-quantitative OARSI scoring, and microCT for skeletal morphometry. Measurement of articular cartilage and subchondral bone thickness were also performed using histomorphometry.

Results: Our results show only subtle developmental effects of Mig-6 overexpression. However, male *Mig-6$^{over/over}$* mice show accelerated cartilage degeneration at 36 weeks of age, in both medial and lateral compartments of the knee. Immunohistochemistry for SOX9 and PRG4 showed decreased staining in *Mig-6$^{over/over}$* mice relative to controls, providing potential molecular mechanisms for the observed effects.

Conclusion: Overexpression of *Mig-6* in articular cartilage causes no major developmental phenotype but results in accelerated development of OA during aging. These data demonstrate that precise regulation of the Mig-6/EGFR pathway is critical for joint homeostasis.

3.2   Introduction

Osteoarthritis (OA) is a failure of joint homeostasis and results in the whole-joint tissue degeneration (1). In fact, OA is a multifactorial disease affecting 630 million individuals worldwide, and the economic impact of OA treatment is estimated at 190 billion dollars in direct and indirect health care costs in North America annually (2,3). OA patients experience limits in daily activities and often suffer from co-morbidities including mental health disorders (4). Treatment for pain and inflammation (analgesics, non-steroidal anti-inflammatory drugs (NSAIDS) and targeted physiotherapy (5) are commonly used to address patients' symptoms, but no effective pharmacological therapy is currently available to delay disease progression. Future directions for effective OA management rely on better understanding of joint physiology and pathophysiological mechanism to develop disease-modifying therapies for OA patients.

Risk factors including aging, genetics, obesity, and trauma contribute to the dysfunction of joint structures in OA. During the early stages of OA, alteration in chondrocyte physiology including cluster formation and changes in the composition of extracellular matrix (ECM) lead to altered cartilage function (6–8). Gradual degeneration of the articular cartilage, subchondral bone sclerosis, osteophyte development, and synovial inflammation/hyperplasia all contribute to joint degeneration in OA (9–11). Expression of matrix metalloproteinases (MMPs) (i.e., MMP-1 and MMP-13) and aggrecanases (disintegrin and metalloproteinase with a thrombospondin type 1 motif (ADAMTS) (i.e., ADAMTS 1,4,5) is up-regulated in response to inflammatory factors and other signals (12–14). Importantly, the tissues of the whole joint work together to maintain joint homeostasis. Therefore, failure in one joint structure might lead to failure of the whole organ, such as the knee joint (15).

Over the past two decades, epidermal growth factor receptor (EGFR) signaling has been studied in several stages of cartilage development and homeostasis. These studies demonstrate both degenerative and protective roles of this pathway (16), with potential therapeutic implications for OA (17–26). EGFR signaling modulates many canonical signaling pathways including MEK/ERK that have been implicated in cellular proliferation and growth in cartilage and bone, as well as Jun N-terminal kinases (JNKs), PLC-PKC signaling and others (24,27,28). Mitogen inducible gene 6 (Mig-6) is well-known as a negative regulator for EGFR signaling (29). Two different mouse

strains with global deletion of *Mig-6* demonstrated bone erosion and spontaneous development of OA-like phenotypes (30,31). Cartilage-specific Mig-6 KO mice display normal early bone development, but show anabolic buildup of articular cartilage, and formation of chondro-osseous nodules at 12 and 36 weeks of age (32) . Another study using limb mesenchyme-specific deletion of *Mig-6* in mice (using the *Prx1-cre* driver line) demonstrated similar phenotypes as those observed in cartilage-specific knockout mice (33). Our laboratory has shown that cartilage-specific *Mig-6* overexpression in mice results in no major developmental abnormalities in articular cartilage, however, during aging (12 and 18 months) *Mig-6^{over/over}* mice show accelerated cartilage degeneration (34). To evaluate the contribution of Mig-6 in multiple joint tissues to joint homeostasis and OA pathogenesis, we used *Prx1* promoter-driven Cre recombinase to selectively overexpress *Mig-6* in all mesenchymal limb tissues in mice.

3.3   Methods

3.3.1   Animals

All animals and procedures were approved by the Council for Animal Care (CCAC) at Western University-Canada (Animal use permit:2015-031). *Mig-6* overexpression animals with the overexpression targeted to the Rosa26 locus (35) were backcrossed for 10 generations into a C57Bl/6 background. In these mice, transcription of *Mig-6* is under the control of a ubiquitously expressed chicken beta actin-cytomegalovirus hybrid (CAGGS) promoter, but blocked by a "Stop Cassette" flanked by LoxP sites (LSL) (35). *Mig-6* overexpression mice were bred to mice carrying the Cre recombinase gene under the control of the Prx1-Cre transgene (36) to induce recombination and removal of the Stop Cassette specifically in early limb bud mesenchyme. Animals with overexpression of Mig-6 from both alleles are termed *Mig-6 ^{over/over} (Mig-6 ^{over/over}Prx1-Cre^{+/-})*, while control mice are identical but without the Cre gene (denoted "control" for simplicity). Mice were group housed (2 or 4 mice per cage of littermate matched control and overexpression animals), on a standard 12 hour light/dark cycle, and with free access to mouse chow and water. Genotyping and assessment of genomic recombination was performed on DNA samples from ear tissue from mice surviving to at least 21 days of age. Standard polymerase chain reaction (PCR) was performed using primer set P1 and P2 can amplify a 300 bp fragment from the wild-type allele, whereas P1 and P3 can amplify a 450 bp fragment from the targeted ROSA26 locus allele (35)**.**

3.3.2 Histologic Assessment

The knee joints of mice were dissected and fixed in 4% paraformaldehyde in phosphate buffered saline (PBS, pH 7.0) for 24 hours at room temperature. The intact joints were then decalcified in 5% ethylenediaminetetraacetic acid (EDTA) in phosphate buffered saline (PBS), pH 7.0 for 10 – 12 days at room temperature. All joints were processed and embedded in paraffin in sagittal or frontal orientation, with serial sections taken at a thickness of 5 μm. Sections were stained with Toluidine Blue (0.04% toluidine blue in 0.2M acetate buffer, pH 4.0, for 10 minutes) for glycosaminoglycan content and general evaluation of articular cartilage.

Immunohistochemistry was performed on frontal sections of paraffin embedded knee joints as previously described (32,37). Primary antibodies against SOX9 (R&D Systems, AF3075), MMP13 (Protein Tech, Chicago, IL, USA, 18165-1-AP), and lubricin (Abcam, ab28484) were used and slides without primary antibody were used as control. Sections were incubated with primary antibody overnight at 4°C. After washing, sections were incubated with horseradish peroxidase (HRP)-conjugated donkey anti-goat or goat anti-rabbit secondary antibody (R&D system and Santa Cruz), before incubation with diaminobenzidine substrate as a chromogen (Dako, Canada). Finally, sections were counterstained with 0.5% methyl green (Sigma) and dehydrated in graded series of 70-100% ethanol in water, followed by 100% xylene, and mounted using xylene-based mounting media. All images were taken using a Leica DM1000 microscope with attached Leica DFC295 digital camera.

3.3.3 Histologic evaluation of articular cartilage and histopathology scoring

Articular cartilage thickness was determined from toluidine blue-stained frontal sections of knee joints by a blinded observer with regard to the tissue source. ImageJ Software (v.1.51) (38) was used to measure the cartilage thickness separately for the non-calcified articular cartilage (measured from the superficial tangential zone to the tidemark) and the calcified articular cartilage (measured from the subchondral bone to the tidemark) across three evenly spaced points from all four quadrants of the joint (medial/lateral tibia and femur), in 4 sections spanning at least 500 μm. For OARSI scoring, Toluidine blue-stained sections were evaluated by one to two blinded observers (MB, MAP) on the four quadrants of the knee: lateral femoral condyle (LFC), lateral tibial plateau (LTP), medial femoral condyle (MFC), and medial tibial plateau (MTP), according

to the Osteoarthritis Research Society International (OARSI) histopathologic scale (39). Subchondral bone area from the tibial plateau was traced by one observer (MB) using the Osteomeasure analysis software (OsteoMetrics, Decatur, GA, USA) for histomorphometry measurements using three sections spanning at least 500 µm from each animal.

3.3.4 Visualization of collagen fiber content

In order to analyze the collagen fibril content and network, Picrosirius Red Staining (0.1% Sirius red in saturated picric acid solution for 60 minutes, with 0.5% acetic acid washes) was performed (32). Stains were imaged under polarized light microscopy to visualize the organization and size of collagen fibrils. Light intensity and tissue angle (45°) relative to polarizing filter (Leica no. 11505087) and analyzer (Leica no. 11555045) were kept identical between samples as per (32)

3.3.5 Micro-Computerized Tomography (µCT)

Mice were euthanized and imaged using General Electric (GE) SpeCZT microCT machine (40) at a resolution of 50µm/voxel or 100µm/voxel in 12 and 36 week-old control and *Mig-6* $^{over/over}$ male and female mice. GE Healthcare MicroView software (v2.2) was used to generate 2D maximum intensity projection and 3D isosurface images to evaluate skeletal morphology (32,41). MicroView was used to create a line measurement tool in order to calculate the bone lengths; femurs lengths were calculated from the proximal point of the greater trochanter to the base of the lateral femoral condyle. Tibiae lengths were measured from the midpoint medial plateau to the medial malleolus. Humerus lengths were measured from the midpoint of the greater tubercle to the center of the olecranon fossa.

3.3.6 Statistical Analysis

All statistical analyses were performed using GraphPad Prism (v6.0). Differences between two groups were evaluated using Student's *t*-test, and Two-Way ANOVA was used to compare four groups followed by a Bonferroni multiple comparisons test. All *n* values represent the number of mice used in each group/genotyping.

3.4 Results

3.4.1 Overexpression of Mig-6 has minor effects on body weight during development

Mice with alleles for conditional overexpression of Mig-6 (35) were bred to mice expressing Cre recombinase under control of the Prx1 promoter, which is active in the mesenchyme of developing limb buds. Homozygote mice overexpressing Mig-6 in mesenchymal limb tissue from both Rosa26 alleles are referred to as *Mig-6 over/over* from here on. Control mice do not express Cre recombinase. Overexpressing mice were obtained at the expected Mendelian ratios (data not shown). Animal weights were significantly lower at 7, 12, and 13 weeks after birth in male mutant mice compared to control mice **(Fig. 3.1A)**, while female *Mig-6over/over* mice had similar weights as control mice **(Fig. 3.1B).** However, at 36 weeks of age mice there were no differences in weights of neither male nor female mutant mice compared to the control group **(Fig. 3.1C, D).**

Figure 3.1 Total body weight of male and female control and *Mig-6*$^{over/over}$ mice. Total body weight of 12-week-old male **(A)** and female **(B)** mice. Total body weights of 36-week-old male **(C)** and female **(D)** *Mig-6*$^{over/over}$ mice and controls did not show any statistically significant differences. Individual data points are presented with mean ± SEM (P<0.05). Data were analyzed by two tailed student t-tests from 8-10 mice per group (age/genotyping).
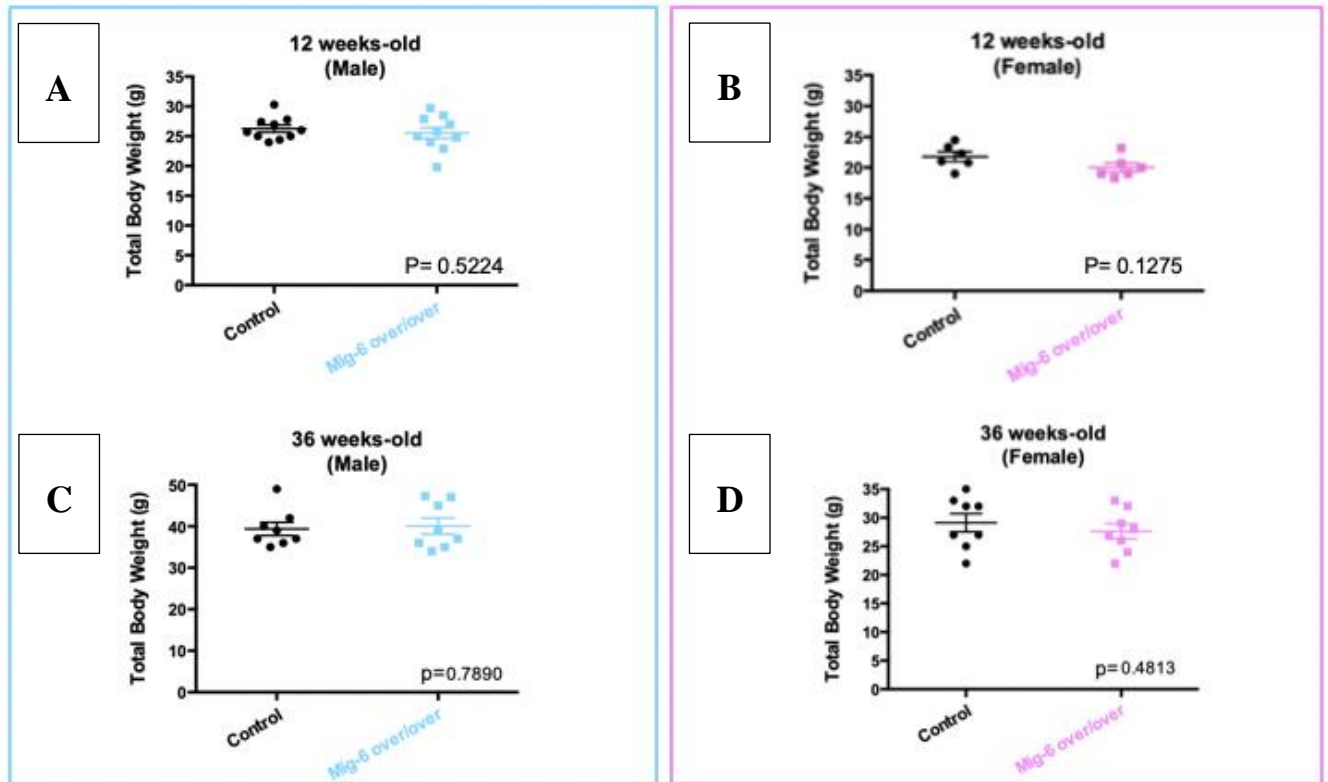
Figure 3.1 Total body weight of male and female control and *Mig-6^over/over* mice

3.4.2 Mig-6 overexpressing mice show no differences in bone length

Micro computed tomography (microCT) was used to investigate skeletal morphology and bone length. Whole body microCT scans of *Mig-6 over/over* male mice and their controls were taken post-mortem at 12 and 36 weeks of age to generate 3D isosurface reconstructions of 50μm/voxel μCT scans, in order to measure long bones lengths (femurs, humeri, and tibiae) in GE MicroView v2.2 software. Mutant male mice at 12 and 36 weeks did not show any difference in bone length compared to controls **(Fig. 3.2A-B)**. Moreover, no differences in gross skeletal morphology were detected **(Fig. 3.2C).**

Figure 3.2 Mig-6 overexpression does not affect bone length. The lengths of right femora, tibiae and humeri were measured on microCT scans of mice at 12 **(A)** and 36 **(B)** weeks of age using GE MicroView software. There were no statistically significant differences in any bones at either age. Individual data points are presented with mean ± SEM (P<0.05). Data were analyzed by two tailed student t-tests from 8 mice per group (age/gender). **(C)** shows a representative 3D isosurface reconstruction of a 100µm/voxel µCT scan.
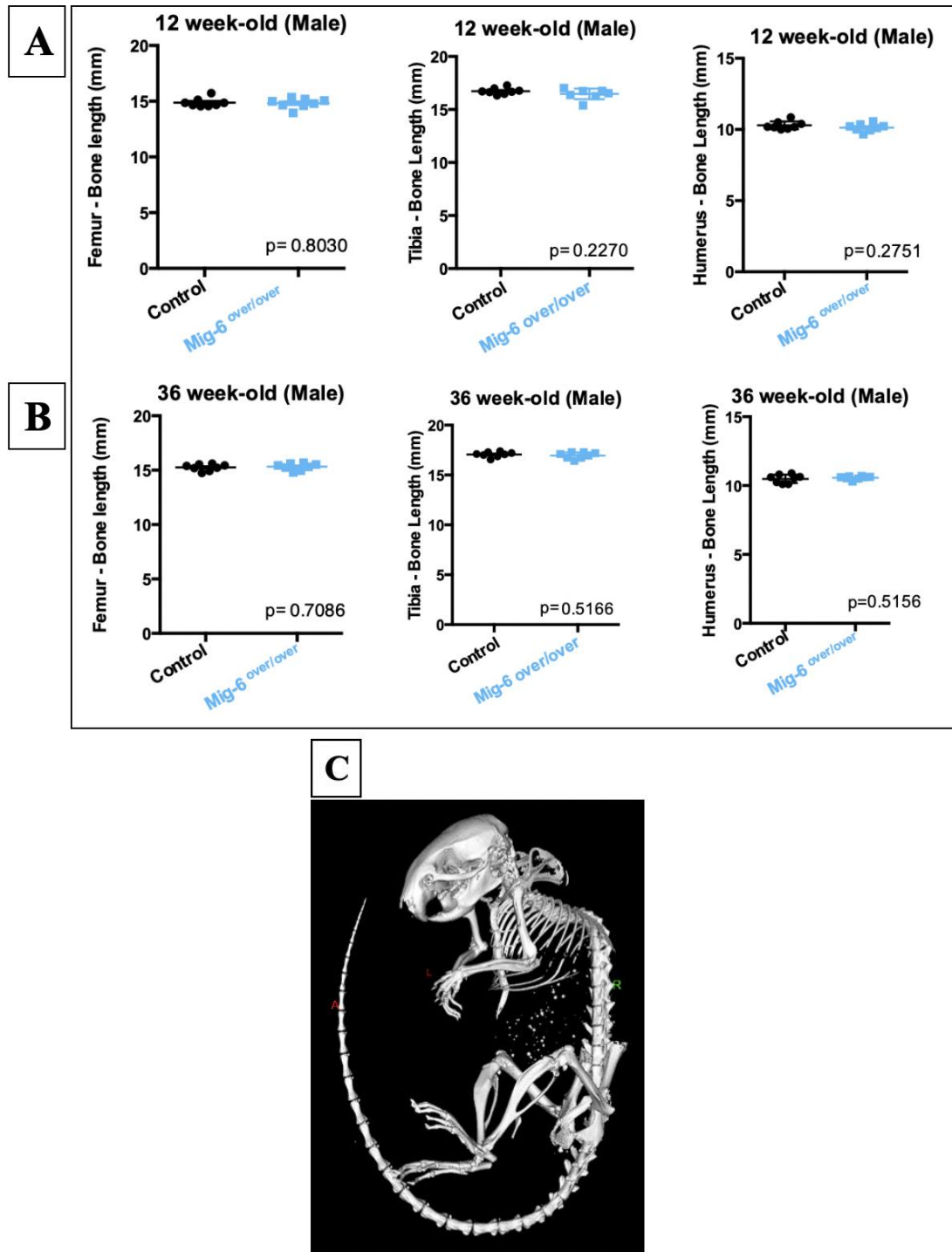
Figure 3.2 Mig-6 overexpression does not affect bone length

3.4.3 Specific overexpression of Mig-6 in limbs display healthy articular cartilage at skeletal mature

Histological analysis of knee sections was performed on 12-week-old mutant and control male mice using toluidine blue stained paraffin frontal knee sections **(Fig. 3.3A-B)**. No major differences in tissue architecture were seen between genotypes. However, the thickness of the calcified articular cartilage in the medial femoral condyle (MFC) and medial tibial plateau (MTP) of male *Mig-6* $^{over/over}$ mice was statistically significantly lower than in controls. Uncalcified cartilage did not show any differences between genotypes.

Figure 3.3 12-week-old *Mig-6$^{over/over}$* male mice show healthy articular cartilage.

Representative (n=5) toluidine blue-stained frontal sections of knee joints from 12-week-old control **(A, B)** and *Mig-6$^{over/over}$* **(C, D)** mice showed no apparent damage. Mig-6 overexpressing mice did show statistically significant differences in thickness of the calcified articular cartilage on the medial femoral condyle (MFC) and medial tibial plateau (MTP) **(E)** when compared to controls. However, no statistically significant differences were seen in the non-calcified articular cartilage **(F).** The lateral femoral condyle (LFC) and lateral tibial plateau (LTP) did not show any significant differences. Individual data points are presented with mean ± SEM. Data were analyzed by two-way ANOVA (95% CI) with Bonferroni post-hoc test. Scale bar = 100µm.
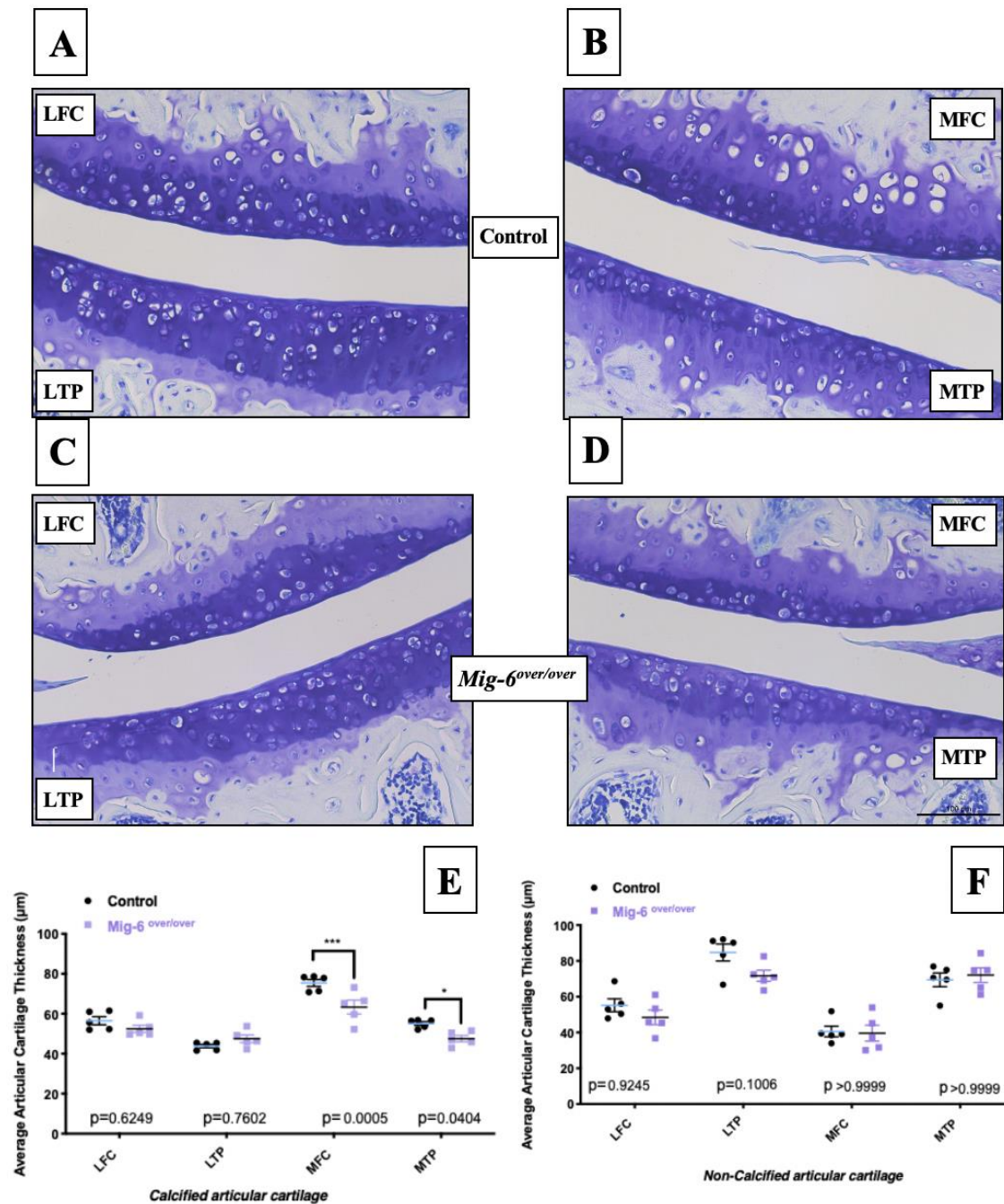
Figure 3.3 12-week-old *Mig-6^{over/over}* male mice show healthy articular cartilage

3.4.4 Mig-6 overexpressing male mice display articular cartilage damage at 36 weeks of age

We evaluated the knee joints of 36 weeks-old control and *Mig-6 over/over* male mice using toluidine blue staining and OARSI grading method (39). At this age, control mice exhibited little to no damage of articular cartilage (**Fig. 3.4A).** Conversely, three of seven *Mig-6 over/over* mice exhibited cartilage damage and erosion with significantly elevated scores in the medial compartment of the knee. Moreover, all seven *Mig-6 over/over* mice had OA in the lateral compartment of the knee (**Fig. 3.4B),** with fibrillation and fissure formation. Furthermore, two of six *Mig-6 over/over* female mice showed mild cartilage degeneration of the medial compartment **(Fig. 3.5B)**, in contrast to the control group where no cartilage damage was observed **(Fig. 3.5A).**

Figure 3.4 Cartilage damage in knee joints of 36-week-old male Mig-6 overexpressing mice. Toluidine blue staining demonstrated healthy knee joints and articular cartilage in all 36-week-old male control mice **(A)**, while many Mig-6-overexpressing mice showed clear damage to the articular surface **(B)**. OARSI histopathology scoring demonstrated that cartilage degeneration scores significantly increased in the MFC, MTP, LFC and LTP of Mig-6 overexpressing mice. **(C)** Data were analyzed by two-way ANOVA with Bonferroni's multiple comparisons test. Individual data points are presented with mean ± SEM. All scale bars =100 μm. N = 7 mice/group.
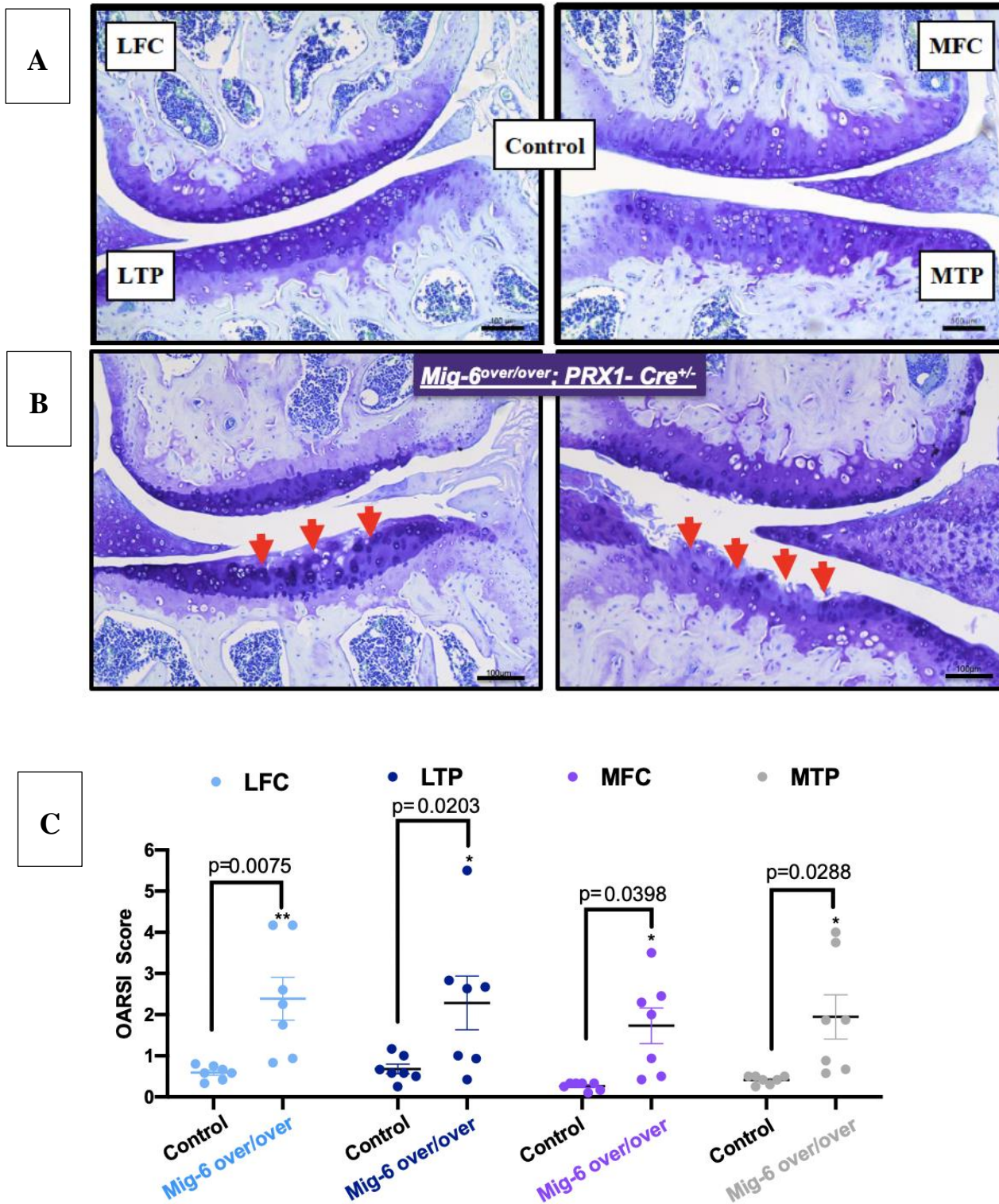
Figure 3.4 Cartilage damage in knee joints of 36 week-old male Mig-6 overexpressing mice

Figure 3.5 Minor damage in articular cartilage of 36-week-old female Mig-6 overexpressing mice. (A) Paraffin sections of knee joints from 36-week-old female control (A) and Mig-6 overexpressing **(B)** mice demonstrated healthy joints in controls and minor cartilage damage in some mutant mice, which was confirmed by OARSI histopathology scoring **(C).** Data were analyzed by two-way ANOVA with Bonferroni's multiple comparisons test. Individual data points are presented with mean ± SEM. All scale bars =100 μm. N = 7 mice/group.
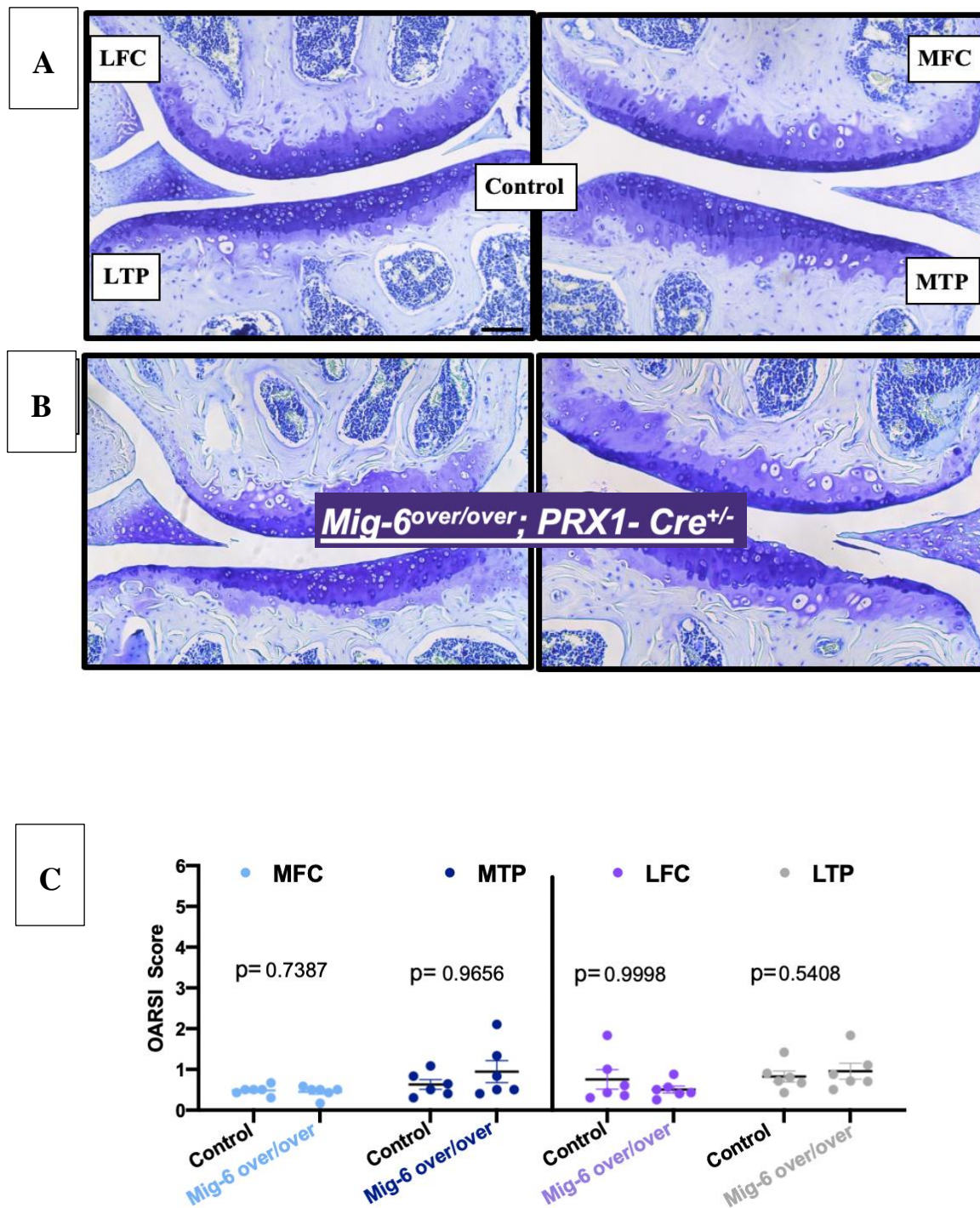
Figure 3.5 Minor damage in articular cartilage of 36-week-old female Mig-6 overexpressing mice

3.4.5 Specific overexpression of Mig-6 results in normal bone area

Bone structural alteration is related to knee osteoarthritis as an adaptive response to the loading distribution across joints (42). Measurement of the subchondral bone area from *Mig-6*$^{over/over}$ and controls male mice at 36 weeks-old across the entire joint did not reveal any significant differences between genotypes (**Fig. 3.6A-B**). Specific measurements of the lateral and medial tibia plateau did not show any significant differences either (data not shown).

Figure 3.6 No differences in the subchondral bone area upon overexpression of Mig-6. The subchondral bone area from 12-week-old male control and Mig-6 overexpressing **(A)** or 36-week-old male control and Mig-6 overexpressing **(B)** mice are shown. Representative images of the subchondral area selected using the OsteoMeasure bone histomorphometry system are shown in **(C)**. Individual data points are presented with mean ± SEM. Data were analyzed by one observer (MB). All scale bars =100 μm. N = 6-7 mice/group.
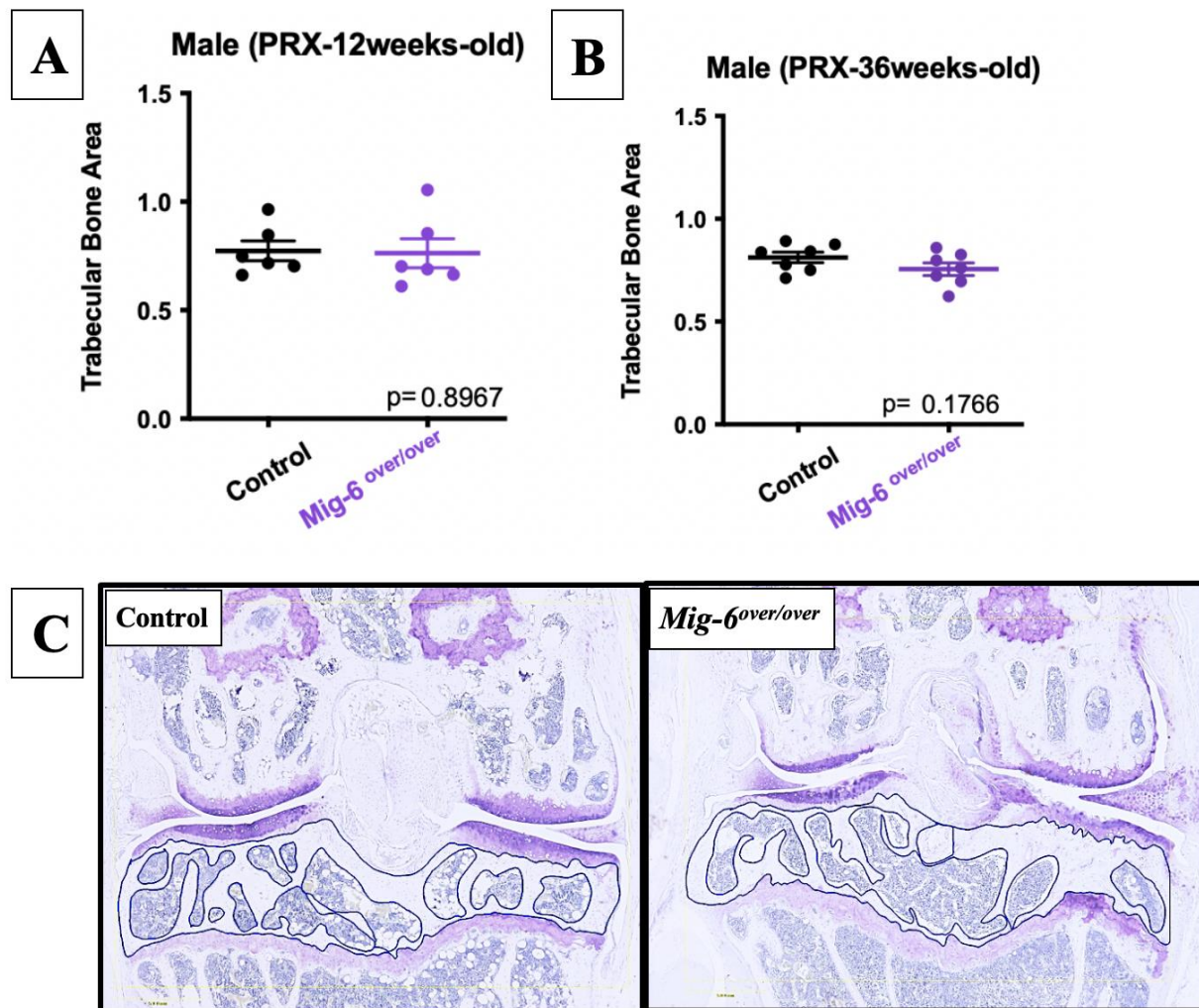
Figure 3.6 No differences in the subchondral bone area upon overexpression of Mig-6.

3.4.6 Mig-6 overexpressing mice display altered collagen fiber organization in articular cartilage

Frontal sections from 36 weeks-old male mice were stained with Picrosirius red to visualize the collagen network under polarized light microscope. In the control male mice, the collagen fibers in the articular cartilage exhibit greenish/yellow birefringence in the superficial and transitional zones, resulting from thin collagen fibers in these regions. In the deep and calcified cartilage, and in bone, red birefringent fibers are visualized, indicating larger fiber diameter in these regions. The articular cartilage of *Mig-6* $^{over/over}$ showed fewer green collagen fibers in the medial compartment of the knee, indicating a loss of normal collagen fibers (**Fig. 3.7A-B**).

Figure 3.7 Picrosirius Red Staining of control and Mig-6 overexpressing mice.

Representative paraffin sections of the medial and lateral compartment in 36-week-old male control **(A)** and Mig-6 overexpressing mice **(B)** were stained with picrosirius red (fibrillar collagen) and analyzed under polarized light to evaluate the collagen tissue organization and orientation in the articular cartilage. Cartilage in the medial compartment of *Mig-6$^{over/over}$* mice shows reduced collagen staining. N=5 mice/group; LFC = lateral femoral condyle, LTP = lateral tibial plateau, MFC = medial femoral condyle and MTP = medial tibial plateau. Scale bar = 100μm.
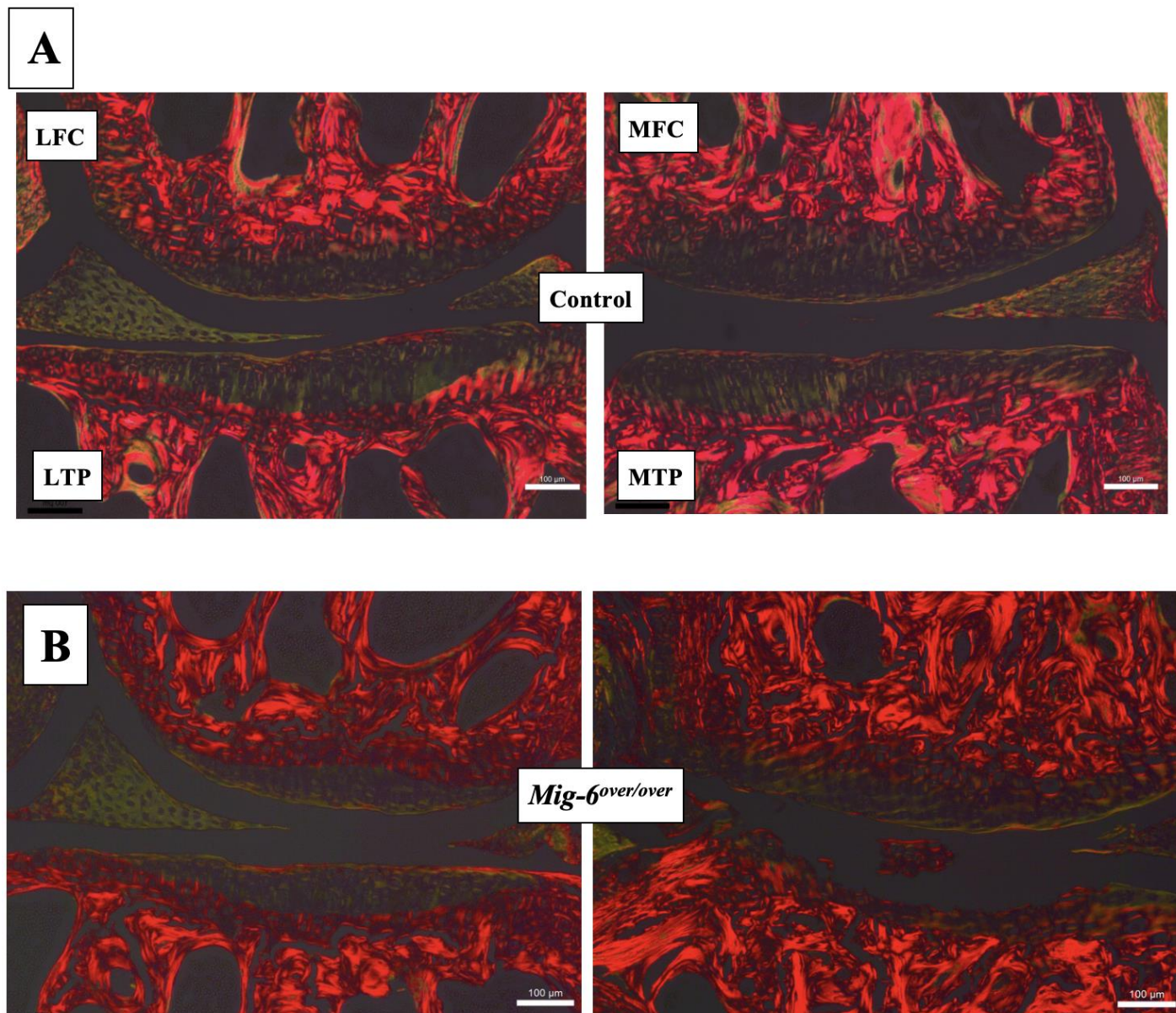
Figure 3.7 Picrosirius Red Staining of control and Mig-6 overexpressing mice

3.4.7 Overexpression of *Mig-6* decreases Sox9 expression

Studies have shown that expression of the transcription factor SRY (sex determining region Y)-box 9 [SOX9] was increased in articular cartilage upon both *Prx1-Cre 1*(43) and *Col2-Cre*-driven (32) deletion of *Mig-6*. SOX9 is an essential regulator of chondrogenesis and the maintenance of a chondrocyte-like phenotype (44). Frontal sections of paraffin embedded knees from 12- and 36-week-old male mice were used for SOX9 immunostaining. In 12-week-old control mice, nuclear SOX9 was abundantly present in the articular cartilage of the knee joints in all four quadrants. In contrast, *Mig-6 over/over* mice appear to have fewer cells staining positive in both lateral and medial compartments **(Fig. 3.8A, B).** 36-week-old *Mig-6 over/over* mice showed a further reduction in SOX9 immunostaining in the lateral quadrant, while the loss of cartilage in the medial compartment led to an absence of SOX9 staining **(Fig. 3.9A, B)**. For both ages, negative controls did not show staining in chondrocytes (data not shown).

Figure 3.8 Lower numbers of SOX9-positive cells in 12-week-old male Mig-6 overexpressing mice. Representative SOX9 immunostaining in knee joints of 12-week-old male control **(A)** or Mig-6 overexpressing **(B)** mice (n=5 mice/group). Ratio between the total cell number from control and *Mig-6 over/over* mice in 12-week-old male mice **(C).** Ratio between the percentage of Sox9 positive cells from control and *Mig-6 over/over* at 12-week-old male mice **(D).** Data analyzed by two-way ANOVA (95% CI) with Bonferroni post-hoc test. Individual data points presented with mean ± SEM; N= 5 mice/genotyping. LFC = lateral femoral condyle, LTP = lateral tibial plateau, MFC = medial femoral condyle and MTP = medial tibial plateau. Scale bar = 100µm.

Figure 3.8 Lower numbers of SOX9-positive cells in 12-week old male Mig-6 overexpressing mice.

Figure 3.9 Lower numbers of SOX9-positive cells in 36-week old male Mig-6 overexpressing mice. Representative SOX9 immunostaining in knee joints of 36-week-old male control **(A)** or Mig-6 overexpressing **(B)** mice (n=5 mice/group). Overexpressing mice showed reduced numbers of positive cells in the medial and lateral compartments. LFC = lateral femoral condyle, LTP = lateral tibial plateau, MFC = medial femoral condyle and MTP = medial tibial plateau. Scale bar = 100µm.

Figure 3.9 Lower numbers of SOX9-positive cells in 36-week old male Mig-6 overexpressing mice

3.4.8 Lubricin/PGR4 is decreased upon Mig-6 overexpression

Lubricin/proteoglycan 4 plays an important role as joint boundary lubricant and is produced by synoviocytes as well as superficial zone chondrocytes (45,46). In 12-week-old *Mig-6 $^{over/over}$* mice, lubricin was observed in superficial zone (SZ) and middle zone (MZ) chondrocytes, in a similar pattern as control mice, although intensity appeared reduced in *Mig-6 $^{over/over}$* mice **(Fig. 3.10 A-C).** 36-week-old control male mice show lubricin immunostaining in the SZ and MZ, however, less lubricin immunostaining is present in the SZ of the medial side of *Mig-6 $^{over/over}$* mice. Negative controls did not show staining in chondrocytes or articular cartilage at either age **(Fig. 3.10 A-C)**.

Figure 3.10 Lubricin immunostaining is slightly decreased in the articular cartilage of Mig-6 overexpressing mice at 12 weeks of age. Immunostaining of sections of the knee joint indicate the presence of Lubricin (*PRG4*) in the superficial zone chondrocytes of 12-week-old male control mice (**A**), with apparently reduced staining in Mig-6 overexpressing mice (**B**). Ratio between the total cell number from control and *Mig-6* $^{over/over}$ at 12-week-old male mice (**C**). Ratio between the percentage of Lubricin (*PRG4*) positive cells from control and *Mig-6* $^{over/over}$ mice at 12 weeks of age (**D**). Data analyzed by two-way ANOVA (95% CI) with Bonferroni post-hoc test. Individual data points presented with mean ± SEM; N= 5 mice/genotyping. LFC = lateral femoral condyle, LTP = lateral tibial plateau, MFC = medial femoral condyle and MTP = medial tibial plateau. Scale bar = 100µm.

Figure 3.10 Lubricin immunostaining is decreased in the articular cartilage of Mig-6 overexpressing mice at 12 weeks of age

3.4.9 MMP13 immunostaining is increased in Mig-6-overexpressing compared to control mice

Previous studies have shown that matrix metalloproteinase (MMP) 13 is the main collagenase associated with type II collagen destruction in OA. Frontal sections of knees from 36-week-old control and *Mig-6* $^{over/over}$ male mice were used for MMP13 immunohistochemistry. While some staining was seen in control mice, intensity of staining was increased in areas of damage on the medial side of *Mig-6* $^{over/over}$ mice. Negative controls did not show staining in cartilage or subchondral bone **(Fig. 3.11 A, B, and C).**

Figure 3.11 36-week-old Mig-6 overexpressing mice show increased MMP13 staining in cartilage. Representative immunohistochemistry of matrix metalloproteinase 13 (MMP13) in 36-week-old control **(A)** and Mig-6 overexpressing **(B)** mice show increased staining in the degrading cartilage of overexpressors. No primary antibody control is shown in **(C).** N=5 mice/genotyping. LFC = lateral femoral condyle, LTP = lateral tibial plateau, MFC = medial femoral condyle and MTP = medial tibial plateau. Scale bar = 100µm.
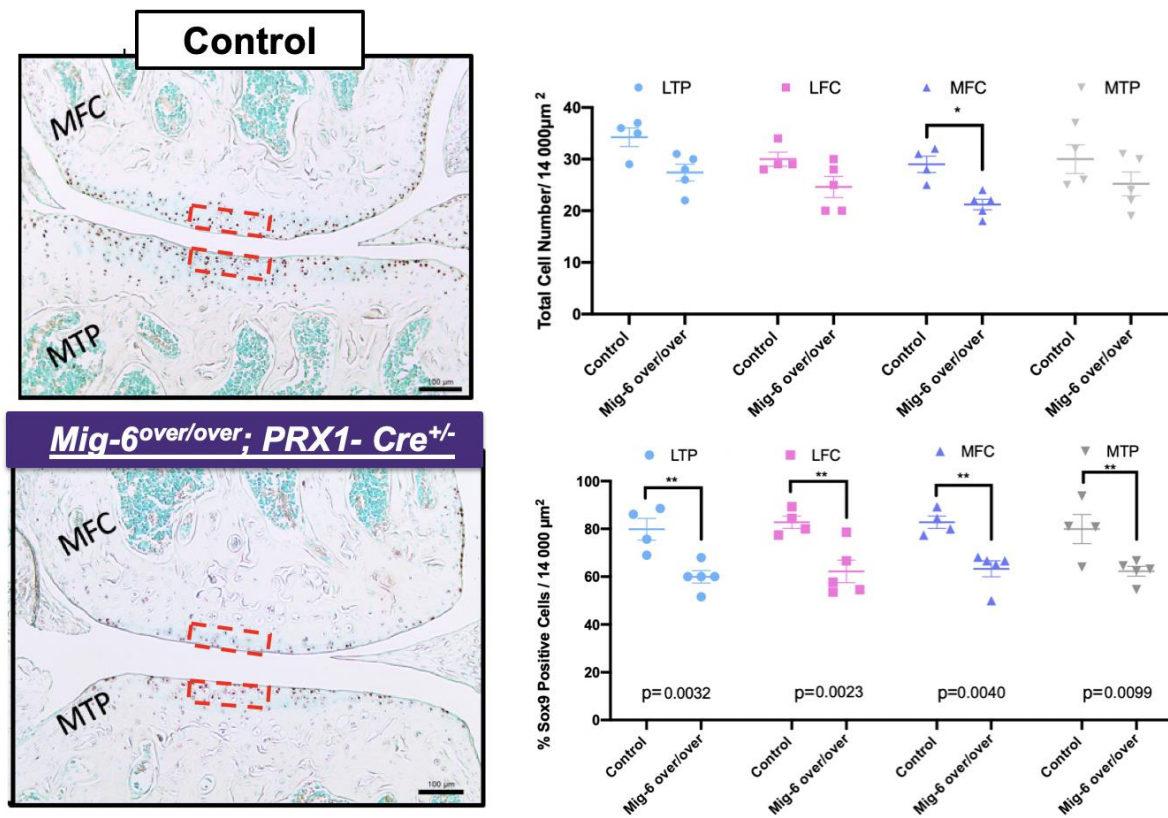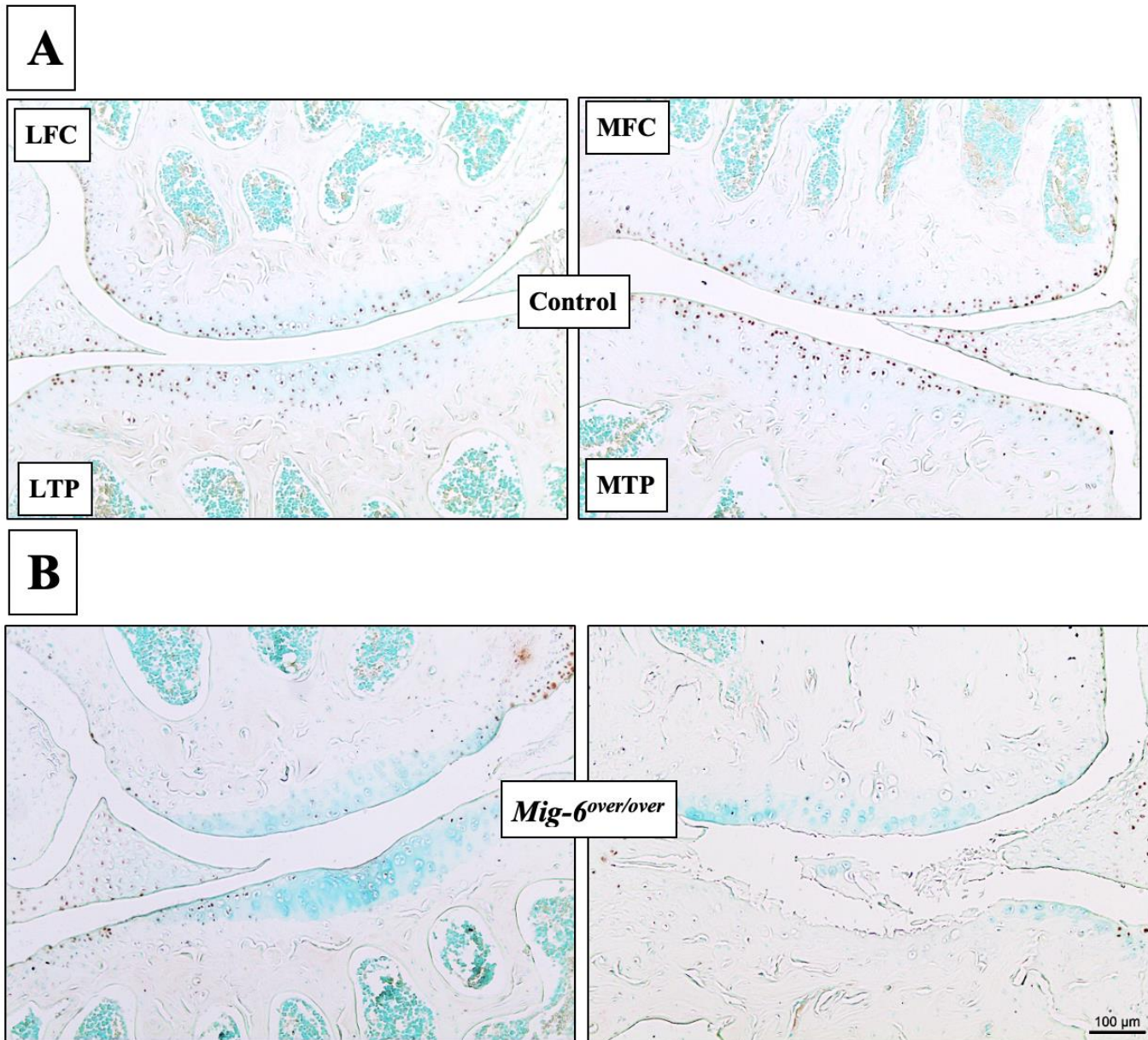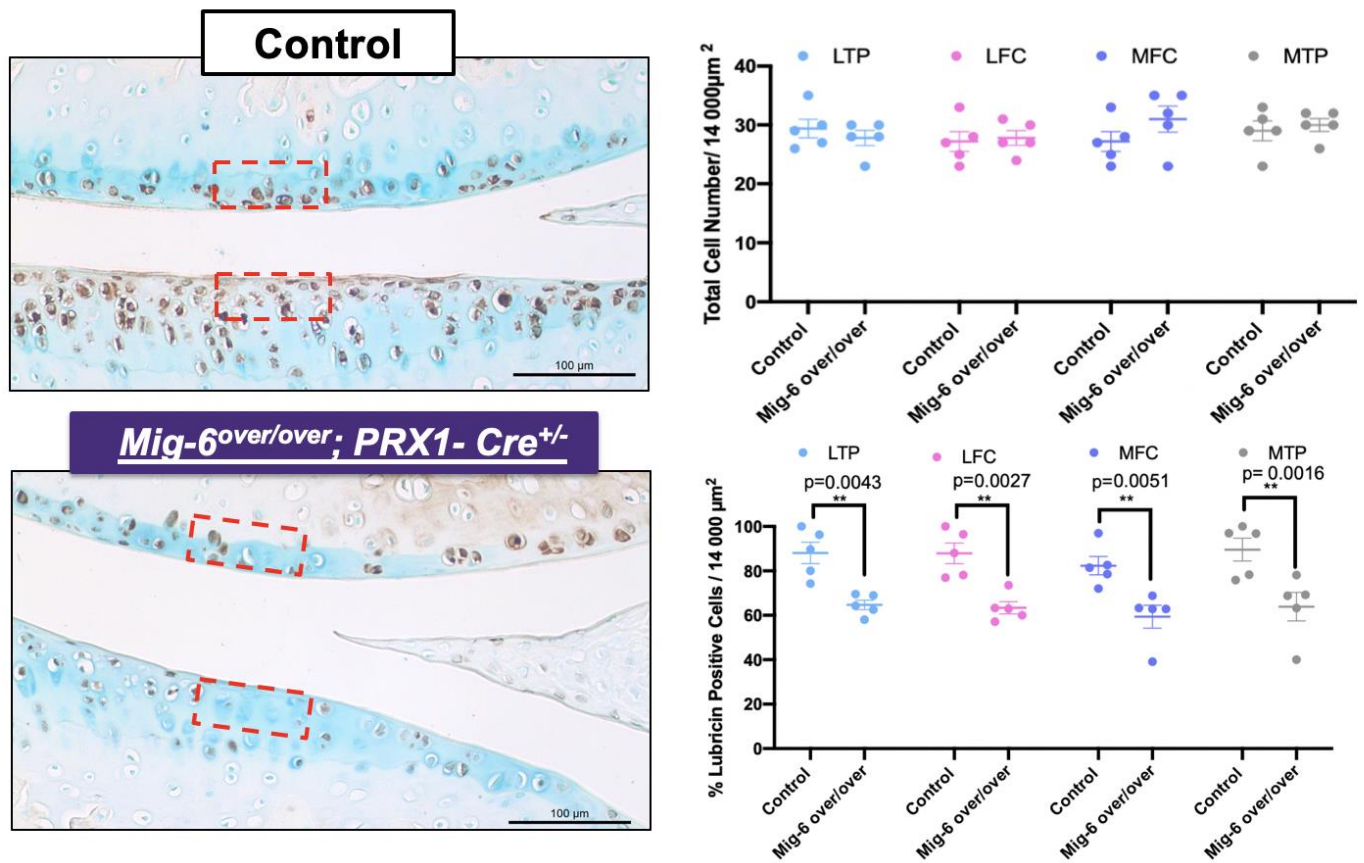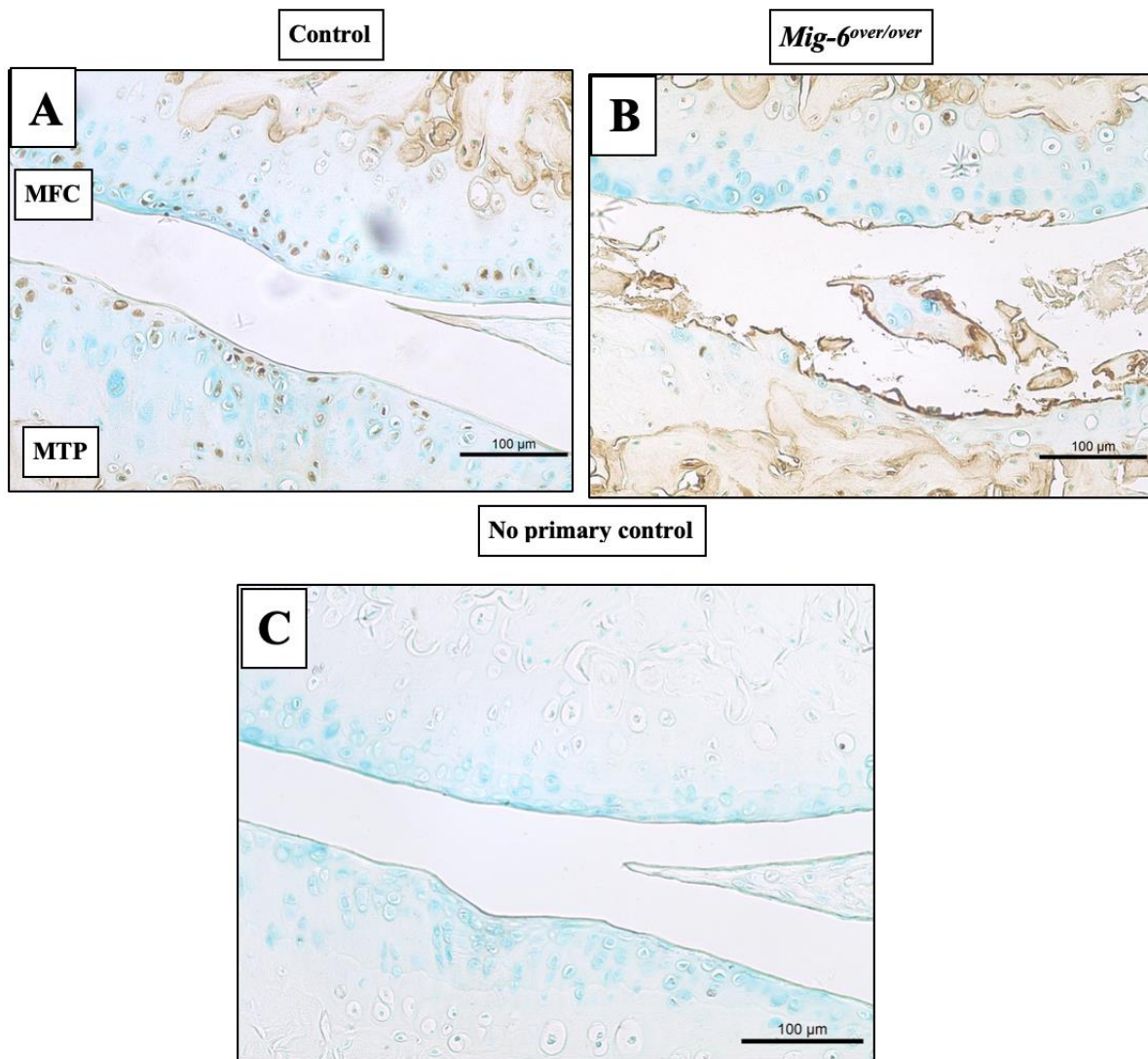
Figure 3.11 36-week-old Mig-6 overexpressing mice show increased MMP13 staining in cartilage

3.5   Discussion

Mig-6 has been studied in a variety of human diseases, including cancer and more recently OA progression(16,31–33,47). Many studies, including from our lab, also identified TGFα /EGFR signaling as a regulator of OA progression and cartilage homeostasis (21,24,48). Interestingly, cartilage-specific (Col2-Cre) deletion of *Mig-6* (Mig-6 KO) (32) results in increased proliferation of chondrocytes and a thicker layer of cartilage while skeletal-specific (Prx1-Cre) deletion of *Mig-6* results in transient anabolic buildup of cartilage followed by catabolic events such as cartilage degeneration at 16 weeks of age (33). In fact, global deletion of *Mig-6* in mice results in a complex set of phenotypes, including joint damage at relatively early time-points in a surgical mouse model (31,49,50). Previous research demonstrates that Mig-6 acts as a negative feedback inhibitor of EGFR signaling (51). Thus, Mig-6 has been suggested as a potential tumor suppressor, as a suppressor of EGFR signaling in human carcinomas (35,52–55). Recent work has revealed that overexpression of Mig-6 acts as a negative regulator of EGFR-ERK signalling in mouse uterus (35). In our study, we set out to evaluate the role of *Mig-6* in joint physiology by using skeletal-specific constitutive overexpression of *Mig-6*. In this study, we show no major effects of Mig-6 overexpression on bone length at the ages of 12 or 36 weeks. While male *Mig-6$^{over/over}$* mice did show slightly reduced body weight up to 12 weeks after birth, these differences were no longer present at 36 weeks of age.

Our results show that *Mig-6$^{over/over}$* (Prx1-Cre) male mice developed cartilage lesions at 36 weeks of age, where control mice show healthy cartilage. OARSI scores of *Mig-6$^{over/over}$* mice reveal significantly increased cartilage degeneration compared to control group. Surprisingly, it appeared that cartilage degeneration in *Mig-6$^{over/over}$* mice was not accompanied by any obvious changes in subchondral bone. However, the thickness of the calcified articular cartilage in *Mig-6$^{over/over}$* was significantly decreased at the 12-week time-point, at least in the medial compartment. It is currently unclear whether and how this is related to the subsequent degeneration of articular cartilage in these mice.

SOX9 is a transcription factor that is necessary for the formation of mesenchymal condensations as well as chondrocyte differentiation and proliferation (56,57). Our data suggest a lower number of SOX9-positive cells at the 12-week time point in mutant mice, preceding cartilage damage. The

number of SOX9-expressing cells is further reduced in 36-week-old mutant mice, although this is partially due to the loss of cartilage and chondrocytes. In agreement with these data, mice with cartilage- or limb mesenchyme-specific deletion of *Mig-6* showed increased expression of SOX9 in the articular cartilage (32,33).

Lubricin/*PRG4* is necessary for joint lubrication and to maintain healthy cartilage (58,59). Our results suggest a slight decrease in lubricin staining in 12 weeks-old male *Mig-6* *over/over* mice, compared to the control group. We also observed the same trend towards decreased staining in 36 weeks-old male Mig-6 over/over mice. Together, these data suggest that the decreased of SOX9 and lubricin in the articular cartilage could contribute to cartilage degeneration in our mutant mice.

We recently described mice with cartilage-specific (Col2-Cre-driven) overexpression of Mig-6 (34). Despite the differences in recombination patterns conferred by the two different Cre drivers, overall the phenotypes observed upon Mig-6 overexpression are quite similar. Both are characterised by no or only subtle developmental defects, followed by reduced SOX9 and lubricin expression, followed by cartilage degeneration. One unique feature of the Prx1-driven Mig6-overexpression described here is the stronger OA phenotype in the lateral compartment of 36-week-old mutant male mice. Future studies will need to investigate the underlying causes.

While Mig-6 had been identified as a negative regulator of EGFR signaling, it also interacts with a number of other potential candidate proteins that may contribute to the phenotype described here, such as Cdc42 (60), c-Abl (61), and the hepatocyte growth factor receptor c-Met (62). Therefore, additional work is necessary to elucidate the potential role of these proteins in the phenotype presented. In conclusion, in this study using limb mesenchyme-specific *Mig-6* overexpression we show a reduction of SOX9 and PRG4 expression, and accelerated cartilage damage. The data highlights the importance of more studies on the specific role of Mig-6 signaling in joint homeostasis and OA development.

3.6 Acknowledgements

3.7   References

1. Nuki, G. Osteoarthritis: a problem of joint failure. *Z. Rheumatol.* **58,** 142–7 (1999).

2. Badley, E. M. The effect of osteoarthritis on disability and health care use in Canada. *J. Rheumatol. Suppl.* **43,** 19–22 (1995).

3. Kotlarz, H., Gunnarsson, C. L., Fang, H. & Rizzo, J. A. Insurer and out-of-pocket costs of osteoarthritis in the US: Evidence from national survey data. *Arthritis Rheum.* **60,** 3546–3553 (2009).

4. Nazarinasab, M., Motamedfar, A. & Moqadam, A. E. Investigating mental health in patients with osteoarthritis and its relationship with some clinical and demographic factors. *Reumatologia* **55,** 183–188 (2017).

5. Berenbaum, F. New horizons and perspectives in the treatment of osteoarthritis. *Arthritis Res. Ther.* **10,** S1 (2008).

6. Carballo, C. B., Nakagawa, Y., Sekiya, I. & Rodeo, S. A. Basic Science of Articular Cartilage. *Clin. Sports Med.* **36,** 413–425 (2017).

7. Nam, J. *et al.* Sequential Alterations in Catabolic and Anabolic Gene Expression Parallel Pathological Changes during Progression of Monoiodoacetate-Induced Arthritis. *PLoS One* **6,** e24320 (2011).

8. Lorenzo, P., Bayliss, M. T. & Heinegård, D. Altered patterns and synthesis of extracellular matrix macromolecules in early osteoarthritis. *Matrix Biol.* **23,** 381–391 (2004).

9. Bush, J. R. & Beier, F. TGF-β and osteoarthritis—the good and the bad. *Nat. Med.* **19,** 667–669 (2013).

10. Blaney Davidson, E. N. *et al.* Inducible chondrocyte-specific overexpression of BMP2 in young mice results in severe aggravation of osteophyte formation in experimental OA without altering cartilage damage. *Ann. Rheum. Dis.* **74,** 1257–1264 (2015).

11. Goldring, M. B. *et al.* Cartilage homeostasis in health and rheumatic diseases. *Arthritis Res. Ther.* **11,** 224 (2009).

12. Kaspiris, A. *et al.* Subchondral cyst development and MMP-1 expression during progression of osteoarthritis: An immunohistochemical study. *Orthop. Traumatol. Surg. Res.* **99,** 523–529 (2013).

13. Liacini, A. *et al.* Induction of matrix metalloproteinase-13 gene expression by TNF-alpha is mediated by MAP kinases, AP-1, and NF-kappaB transcription factors in articular chondrocytes. *Exp. Cell Res.* **288,** 208–17 (2003).

14. Song, R.-H. *et al.* Aggrecan degradation in human articular cartilage explants is mediated by both ADAMTS-4 and ADAMTS-5. *Arthritis Rheum.* **56,** 575–585 (2007).

15. Kapoor, M., Martel-Pelletier, J., Lajeunesse, D., Pelletier, J.-P. & Fahmi, H. Role of proinflammatory cytokines in the pathophysiology of osteoarthritis. *Nat. Rev. Rheumatol.* **7,** 33–42 (2011).

16. Qin, L. & Beier, F. EGFR Signaling: Friend or Foe for Cartilage? *JBMR Plus* **3,** e10177 (2019).

17. Appleton, C. T. G., Pitelka, V., Henry, J. & Beier, F. Global analyses of gene expression in early experimental osteoarthritis. *Arthritis Rheum.* **56,** 1854–1868 (2007).

18. Appleton, C. T. G., Usmani, S. E., Bernier, S. M., Aigner, T. & Beier, F. Transforming growth factor α suppression of articular chondrocyte phenotype andSox9 expression in a rat model of osteoarthritis. *Arthritis Rheum.* **56,** 3693–3705 (2007).

19. Usmani, S. E. *et al.* Transforming growth factor alpha controls the transition from hypertrophic cartilage to bone during endochondral bone growth. *Bone* **51,** 131–141 (2012).

20. Appleton, C. T. G. *et al.* Reduction in disease progression by inhibition of transforming growth factor α-CCL2 signaling in experimental posttraumatic osteoarthritis. *Arthritis Rheumatol. (Hoboken, N.J.)* **67,** 2691–701 (2015).

21. Usmani, S. E. *et al.* Context-specific protection of TGFα null mice from osteoarthritis. *Sci. Rep.* **6,** 30434 (2016).

22. Cui, G. *et al.* Association of Common Variants in TGFA with Increased Risk of Knee Osteoarthritis Susceptibility. *Genet. Test. Mol. Biomarkers* gtmb.2017.0045 (2017). doi:10.1089/gtmb.2017.0045

23. Zengini, E. *et al.* Genome-wide analyses using UK Biobank data provide insights into the genetic architecture of osteoarthritis. *Nat. Genet. 2018* 1 (2018). doi:10.1038/s41588-018-0079-y

24. Appleton, C. T. G., Usmani, S. E., Mort, J. S. & Beier, F. Rho/ROCK and MEK/ERK activation by transforming growth factor-alpha induces articular cartilage degradation. *Lab. Invest.* **90,** 20–30 (2010).

25. Wang, K., Yamamoto, H., Chin, J. R., Werb, Z. & Vu, T. H. Epidermal growth factor receptor-deficient mice have delayed primary endochondral ossification because of defective osteoclast recruitment. *J. Biol. Chem.* **279,** 53848–56 (2004).

26. Jia, H. *et al.* EGFR signaling is critical for maintaining the superficial layer of articular cartilage and preventing osteoarthritis initiation. *Proc. Natl. Acad. Sci. U. S. A.* 201608938 (2016). doi:10.1073/pnas.1608938113

27. Schneider, M. R., Sibilia, M. & Erben, R. G. The EGFR network in bone biology and pathology. *Trends Endocrinol. Metab.* **20,** 517–524 (2009).

28. Mariani, E., Pulsatelli, L. & Facchini, A. Signaling pathways in cartilage repair. *Int. J. Mol. Sci.* **15,** 8667–98 (2014).

29. Frosi, Y. *et al.* A two-tiered mechanism of EGFR inhibition by RALT/MIG6 via kinase suppression and receptor degradation. *J. Cell Biol.* **189,** 557–71 (2010).

30. Ferby, I. *et al.* Mig6 is a negative regulator of EGF receptor–mediated skin morphogenesis and tumor formation. *Nat. Med.* **12,** 568–573 (2006).

31. Joiner, D. M. *et al.* Accelerated and increased joint damage in young mice with global inactivation of mitogen-inducible gene 6 after ligament and meniscus injury. *Arthritis Res. Ther.* **16,** R81 (2014).

32. Pest, M. A., Russell, B. A., Zhang, Y.-W., Jeong, J.-W. & Beier, F. Disturbed cartilage and joint homeostasis resulting from a loss of mitogen-inducible gene 6 in a mouse model of joint dysfunction. *Arthritis Rheumatol. (Hoboken, N.J.)* **66,** 2816–27 (2014).

33. Shepard, J. B., Jeong, J.-W., Maihle, N. J., O'Brien, S. & Dealy, C. N. Transient anabolic effects accompany epidermal growth factor receptor signal activation in articular cartilage in vivo. *Arthritis Res. Ther.* **15,** R60 (2013).

34. Bellini, M., Pest, M. A., Miranda-Rodrigues, M., Jeong, J. & Beier, F. Overexpression of mig-6 in cartilage induces an osteoarthritis-like phenotype in mice. *bioRxiv* 764142 (2019). doi:10.1101/764142

35. Kim, T. H. *et al.* Mig-6 suppresses endometrial cancer associated with pten deficiency and ERK activation. *Cancer Res.* **74,** 7371–7382 (2014).

36. Logan, M. *et al.* Expression of Cre recombinase in the developing mouse limb bud driven by aPrxl enhancer. *genesis* **33,** 77–80 (2002).

37. Ratneswaran, A. *et al.* Peroxisome proliferator-activated receptor δ promotes the progression of posttraumatic osteoarthritis in a mouse model. *Arthritis Rheumatol. (Hoboken, N.J.)* **67,** 454–64 (2015).

38. Schneider, C. A., Rasband, W. S. & Eliceiri, K. W. NIH Image to ImageJ: 25 years of image analysis. *Nat. Methods* **9,** 671–675 (2012).

39. Glasson, S. S., Chambers, M. G., Van Den Berg, W. B. & Little, C. B. The OARSI histopathology initiative – recommendations for histological assessments of osteoarthritis in the mouse. *Osteoarthr. Cartil.* **18,** S17–S23 (2010).

40. Beaucage, K. L., Pollmann, S. I., Sims, S. M., Dixon, S. J. & Holdsworth, D. W. Quantitative in vivo micro-computed tomography for assessment of age-dependent changes in murine whole-body composition. *Bone Reports* **5,** 70–80 (2016).

41. Dupuis, H. *et al.* Exposure to the RXR agonist SR11237 in early life causes disturbed skeletal morphogenesis in a rat model. *bioRxiv* 774851 (2019). doi:10.1101/774851

42. Lowitz, T. *et al.* Characterization of knee osteoarthritis-related changes in trabecular bone using texture parameters at various levels of spatial resolution-a simulation study. *Bonekey Rep.* **3,** 615 (2014).

43. Shepard, J. B., Jeong, J.-W., Maihle, N. J., O'Brien, S. & Dealy, C. N. Transient anabolic effects accompany epidermal growth factor receptor signal activation in articular cartilage in vivo. *Arthritis Res. Ther.* **15,** R60 (2013).

44. Akiyama, H., Chaboissier, M.-C., Martin, J. F., Schedl, A. & de Crombrugghe, B. The transcription factor Sox9 has essential roles in successive steps of the chondrocyte differentiation pathway and is required for expression of Sox5 and Sox6. *Genes Dev.* **16,** 2813–28 (2002).

45. Coles, J. M. *et al.* Loss of cartilage structure, stiffness, and frictional properties in mice lacking PRG4. *Arthritis Rheum.* **62,** 1666–1674 (2010).

46. Iqbal, S. M. *et al.* Lubricin/Proteoglycan 4 binds to and regulates the activity of Toll-Like Receptors In Vitro. *Sci. Rep.* **6,** 18910 (2016).

47. Zhang, Y.-W. & Vande Woude, G. F. Mig-6, Signal Transduction, Stress Response and Cancer. *Cell Cycle* **6,** 507–513 (2007).

48. Usmani, S. E., Appleton, C. T. G. & Beier, F. Transforming growth factor-alpha induces endothelin receptor A expression in osteoarthritis. *J. Orthop. Res.* **30,** 1391–7 (2012).

49. Zhang, Y.-W. *et al.* Targeted disruption of Mig-6 in the mouse genome leads to early onset degenerative joint disease. *Proc. Natl. Acad. Sci. U. S. A.* **102,** 11740–5 (2005).

50. Jin, N., Gilbert, J. L., Broaddus, R. R., Demayo, F. J. & Jeong, J.-W. Generation of a Mig-6 conditional null allele. *Genesis* **45,** 716–21 (2007).

51. Hackel, P. O., Gishizky, M. & Ullrich, A. Mig-6 Is a Negative Regulator of the Epidermal Growth Factor Receptor Signal. *Biol. Chem.* **382,** (2001).

52. Maity, T. K. *et al.* Loss of MIG6 Accelerates Initiation and Progression of Mutant Epidermal Growth Factor Receptor-Driven Lung Adenocarcinoma. *Cancer Discov.* **5,** 534–49 (2015).

53. Li, Z. *et al.* Downregulation of Mig-6 in nonsmall-cell lung cancer is associated with EGFR signaling. *Mol. Carcinog.* **51,** 522–34 (2012).

54. Zhang, Y.-W. *et al.* Evidence that MIG-6 is a tumor-suppressor gene. *Oncogene* **26,** 269–276 (2007).

55. Sasaki, M., Terabayashi, T., Weiss, S. M. & Ferby, I. The Tumor Suppressor MIG6 Controls Mitotic Progression and the G2/M DNA Damage Checkpoint by Stabilizing the WEE1 Kinase. *Cell Rep.* **24,** 1278–1289 (2018).

56. Kobayashi, T. & Kronenberg, H. Minireview: Transcriptional Regulation in Development of Bone. *Endocrinology* **146,** 1012–1017 (2005).

57. Akiyama, H. The transcription factor Sox9 has essential roles in successive steps of the chondrocyte differentiation pathway and is required for expression of Sox5 and Sox6. *Genes Dev.* **16,** 2813–2828 (2002).

58. Flannery, C. R. *et al.* Prevention of cartilage degeneration in a rat model of osteoarthritis by intraarticular treatment with recombinant lubricin. *Arthritis Rheum.* **60,** 840–847 (2009).

59. Ruan, M. Z. C. *et al.* Proteoglycan 4 Expression Protects Against the Development of Osteoarthritis. *Sci. Transl. Med.* **5,** 176ra34-176ra34 (2013).

60. Jiang, X. *et al.* Inhibition of Cdc42 is essential for Mig-6 suppression of cell migration induced by EGF. *Oncotarget* (2016). doi:10.18632/oncotarget.10205

61. Hopkins, S. *et al.* Mig6 is a sensor of EGF receptor inactivation that directly activates c-Abl to induce apoptosis during epithelial homeostasis. *Dev. Cell* **23,** 547–59 (2012).

62. Pante, G. *et al.* Mitogen-inducible gene 6 is an endogenous inhibitor of HGF/Met-induced cell migration and neurite growth. *J. Cell Biol.* **171,** 337–48 (2005).

Chapter 4

4 Cartilage-Specific Overexpression of Mig-6 Accelerates Post-Traumatic Osteoarthritis in Mice

These data are currently unpublished but will contribute to an original first author research paper to be submitted for publication.

Bellini, Melina Rodrigues[1,2], Bali, Supinder Kour[1,2], Pest, Michael Andrew[1,2], Dawn-Marie Bryce[1,2], Jae-Wook Jeong[4], Beier, Frank[1,2,3]

[1] Department of Physiology and Pharmacology, Western University, London, ON, Canada

[2] Western University Bone and Joint Institute, London, ON, Canada

[3] Children's Health Research Institute, London, ON, Canada

[4] Department of Obstetrics, Gynecology and Reproductive Biology, Michigan State University College of Human Medicine, Grand Rapids, Michigan.

Corresponding author: Dr. Frank Beier, Department of Physiology and Pharmacology, Western University, London, ON, Canada; Phone 519-661-02111 ext 85344; email: fbeier@uwo.ca

The authors have no conflicts of interest to declare.

4.1 Abstract

Background: Osteoarthritis (OA) is a chronic degenerative disease characterised by cartilage loss and changes in the whole joint (e.g. subchondral bone sclerosis, osteophyte formation, synovitis). Moreover, OA leads to pain, loss of joint function as well as a decrease in quality of life. Currently, there is no cure for OA. Several studies have shown that molecular derangement is involved in the disruption of joint homeostasis and imbalance between catabolic and anabolic signals. Mitogen-inducible gene 6 (Mig-6) has been identified as a potential regulator of cartilage physiology. Our lab has demonstrated that cartilage-specific Mig-6 knockout (KO) mice develop osteophyte-like chondro-osseous nodules in the knee joints and anabolic increase in articular cartilage thickness. Recently, our previous study showed that cartilage- or limb mesenchyme-specific *Mig-6* overexpression in mice results in cartilage degeneration during aging. Here we examine the effects of cartilage-specific Mig-6 overexpression on post-traumatic OA in the DMM model.

Methods: Cartilage-specific *Mig-6* overexpressing (*Mig-6$^{over/over}$*) and control mice underwent destabilization on medial meniscus (DMM) to induce PTOA at 16 weeks of age. Mice were sacrificed 8 weeks after surgery. Behavioural outcomes were analyzed through Open Field Testing prior to sacrifice. Joint pathology was examined using histopathological scoring (semi-quantitative OARSI scoring) using Toluidine Blue staining of paraffin sections of knee joints.

Results: Mice undergoing DMM surgery exhibited behavioral changes (less movement and vertical activity) between genotypes. Control and *Mig-6$^{over/over}$* DMM operated mice show significant cartilage degeneration compared to sham operated using OARSI scoring of cartilage.

Conclusion: Surgical-induced OA mice with overexpression of *Mig-6* in articular cartilage significantly aggravated the destruction of articular cartilage. However, *Mig-6$^{over/over}$* did not significantly exhibited behaviour changes. These results suggested that *Mig-6$^{over/over}$* indicate to alter disease progression of OA.

4.2   Introduction

Mitogen-inducible gene 6 (Mig-6) has been implicated in a variety of human diseases such as lung cancer, including squamous cell carcinoma, non-small cell lung cancer, and osteoarthritis (1–5). Biochemically, Mig-6 has been identified as a negative regulator of Epidermal Growth Factor Receptor (EGFR) signaling (6–8), which regulates many aspects of cell physiology, such as proliferation and differentiation (9,10). Cartilage- or limb mesenchyme-specific *Mig-6* overexpression (in *Mig-6 over/over* mice) results in accelerated cartilage degeneration during aging (12 and 18 months) (11,12). In contrast, cartilage-specific Mig-6 knockout (KO) mice show increased articular cartilage thickness but also ectopic chondro-osseous nodules in their knee joints (13). Limb mesenchyme-specific *Mig-6* deletion (using *Prx1-cre*) drive resulted in similar transient anabolic phenotype including cartilage thickening that was followed by catabolic effects such as matrix degradation (14). However, global deletion of *Mig-6* led to early-onset osteoarthritis (OA) such as formation of bone cysts and degradation of articular cartilage (2). Therefore, numerous studies have shown that Mig-6 plays an important role in articular cartilage homeostasis and maintenance.

OA is the most highly prevalent degenerative joint disease in humans (15–17). OA pathogenesis is a complex process that leads to alteration in the whole joint and its different structures including articular cartilage, menisci, ligaments, subchondral bone, and synovium (18,19). OA has multifactorial causes including systemic and local factors such as genetic susceptibility, trauma (posttraumatic OA/PTOA), female sex, obesity, muscle weakness, all of which can lead to early-onset OA (20). Currently the treatments options available for OA are pharmacological, non-pharmacological, and alternative medicine, but none of these address the cause of the disease or slow disease progression (21). Furthermore, surgical OA treatment (e.g. joint replacement) is a last resort, based on OA stage, patient's age and comorbidities, and physical examination/activity (22). In this study, we evaluated the effects of cartilage-specific *Mig-6* overexpressing (*Mig-6over/over*) on the development of osteoarthritis following surgical destabilization of medical meniscus (DMM). DMM is a widely accepted and well validated model of posttraumatic OA (23).

4.3 Methods

4.3.1 Animals

All mice were bred and housed in accordance with Council for Animal Care (CCAC) guidelines at The University of Western Ontario. Male mice were group housed (2 or 4 mice per cage, matched control and overexpressing animals), on a standard 12 hour light/dark cycle, and with free access to mouse chow and water. Mice were separated to double housing post-surgery. To conditionally overexpress Mig-6 in chondrocytes, *Mig-6* overexpression animals were bred with Col2-Cre mice as described (11,24). Genotyping was performed on DNA samples from ear tissue of mice at 21 days of age. Standard polymerase chain reaction (PCR) was performed using primer set P1 and P2 that amplify a 300 bp fragment from the wild-type allele, whereas P1 and P3 can amplify a 450 bp fragment from the targeted ROSA26 locus allele (24).

Post-traumatic OA was induced at 16 weeks of age by performing DMM surgery on the right hind limb of male *Mig-6 over/over* and control littermates mice, as described (23,25). DMM or Sham surgery was performed by Dr. Supinder K. Bali. 34 mice were used for this surgical trial, 16 control (9DMM, 7sham) and 18 *Mig-6 over/over* mice (9 DMM, 9 sham). Isofluorane was used as surgical anesthetic. Buprenorphine (dose: 1.0mg/ml) was administered subcutaneously as an analgesic, and ampicillin (dose: 0.1ml) was administered subcutaneously as a prophylactic antibiotic. 1 week after surgery, running wheels were added to the cages of all experimental animals, and they had free access for the remainder of the trial. All mice were sacrificed 8 weeks following surgery by CO_2 asphyxiation and operated right limbs were harvested.

4.3.2 Histologic Assessment

Knee joints of mice were harvested 8 weeks following surgeries and fixed in 4% paraformaldehyde in phosphate buffered saline (PBS, pH 7.0) for 24 hours at room temperature. The intact joints were then decalcified in 5% ethylenediaminetetraacetic acid (EDTA) in phosphate buffered saline (PBS), pH 7.0 for 10 – 12 days at room temperature. All joints were processed and embedded in paraffin in sagittal or frontal orientation, with serial sections taken at a thickness of 5 μm. Sections were stained with Toluidine Blue (0.04% toluidine blue in 0.2M acetate buffer, pH 4.0, for 10 minutes) for glycosaminoglycan content and general evaluation of articular cartilage. Sections through the entire joint were scored according to the Osteoarthritis Research Society International

(OARSI) histopathologic scale (26) by one blinded observer. Scores from 0-6 represent OA severity, with 0 referring to healthy cartilage and 6 denoting erosion of more than 75% of articular cartilage. Individual scores are averaged across the four quadrants of the knee: lateral femoral condyle (LFC), lateral tibial plateau (LTP), medial femoral condyle (MFC), and medial tibial plateau (MTP) from each animal/group.

4.3.3   Behavioural Testing

Exploratory behaviour and motor activity in mice were assessed using mouse open field activity monitors (AccuScan Instruments, Omnitech Electronic, Columbus, OH) with a transparent Plexiglas cage (height = 40cm, width = 20cm, and length = 20cm). Mice were placed in an Open Field Tester for 30 minutes, prior to sacrifice. Rest, movement, ambulation, and vertical activity time and incidence were measured and analyzed using the Fusion Software provided by the manufacturer.

4.3.4   Statistical Analysis

All statistical analyses were performed using GraphPad Prism (v8.0). Behavioural measures were analyzed by two-way analysis of variance (ANOVA) followed by Turkey's multiple comparisons test. OARSI scores were compared using a two-way ANOVA followed by Turkey's multiple comparisons test.

4.4   Results

4.4.1   Overexpression of Mig-6 in cartilage increases severity of DMM-induced osteoarthritis

Male *Mig-6 over/over* and control mice received either SHAM or DMM surgery. At 8 weeks post-surgery, mice were euthanized, and their joints were harvested for histopathologic analyses to evaluate the effect of *Mig-6* overexpression on the progression of OA. Serial frontal sections per mice were assessed semi-quantitatively by 1 blinded observer using the OARSI recommendation (26). SHAM-operated mice displayed healthy joints, as expected, with only very minor damage in a few cases. Histologically, varying degrees of cartilage damage in the medial compartment was seen in all 9 control and all 9 *Mig-6 over/over* DMM-operated animals. Four of nine control mice showed mild cartilage degeneration, with focal, full thickness cartilage lesions spanning limited

areas through the joint. One of nine control mice showed extensive cartilage erosion, spanning 50-100% of the articular surface across the entire medial compartment. In *Mig-6 over/over* mice, five of nine DMM operated mice showed full thickness cartilage erosion spanning 75% to 50% of the articular surface across the entire width of the joint. However, four of nine DMM operated mice showed milder phenotypes, with cartilage erosion spanning 50% to 25% of the articular surface across the entire medial compartment **(Fig 4.1A-B).** Semi-quantitative OARSI scoring of the medial compartment confirmed that *Mig-6 over/over* mice had significantly higher damage after DMM surgery than control mice after the same surgery **(Fig. 4.2A-B).** As expected, lateral compartments showed very little damage and no significant differences between all groups **(Fig. 4.3A-B** and **Fig. 4.4A-B**).

Figure 4.1 Overexpression of Mig-6 in cartilage increases severity of surgically induced osteoarthritis. Male *Mig-6 over/over* and control mice received either SHAM or DMM surgery. 8 weeks after surgery, animals were sacrificed, and OA was assessed by Toluidine Blue staining on serial frontal sections. SHAM operated control or mutant mice show healthy cartilage, subchondral bone and menisci **(A).** Control mice showed moderate cartilage damage after DMM surgery **(B).** However, *Mig-6 over/over* mice showed cartilage erosion and full thickness defects after DMM surgery. All scale bars =100 μm. N=7-9 per group.

Medial Compartment
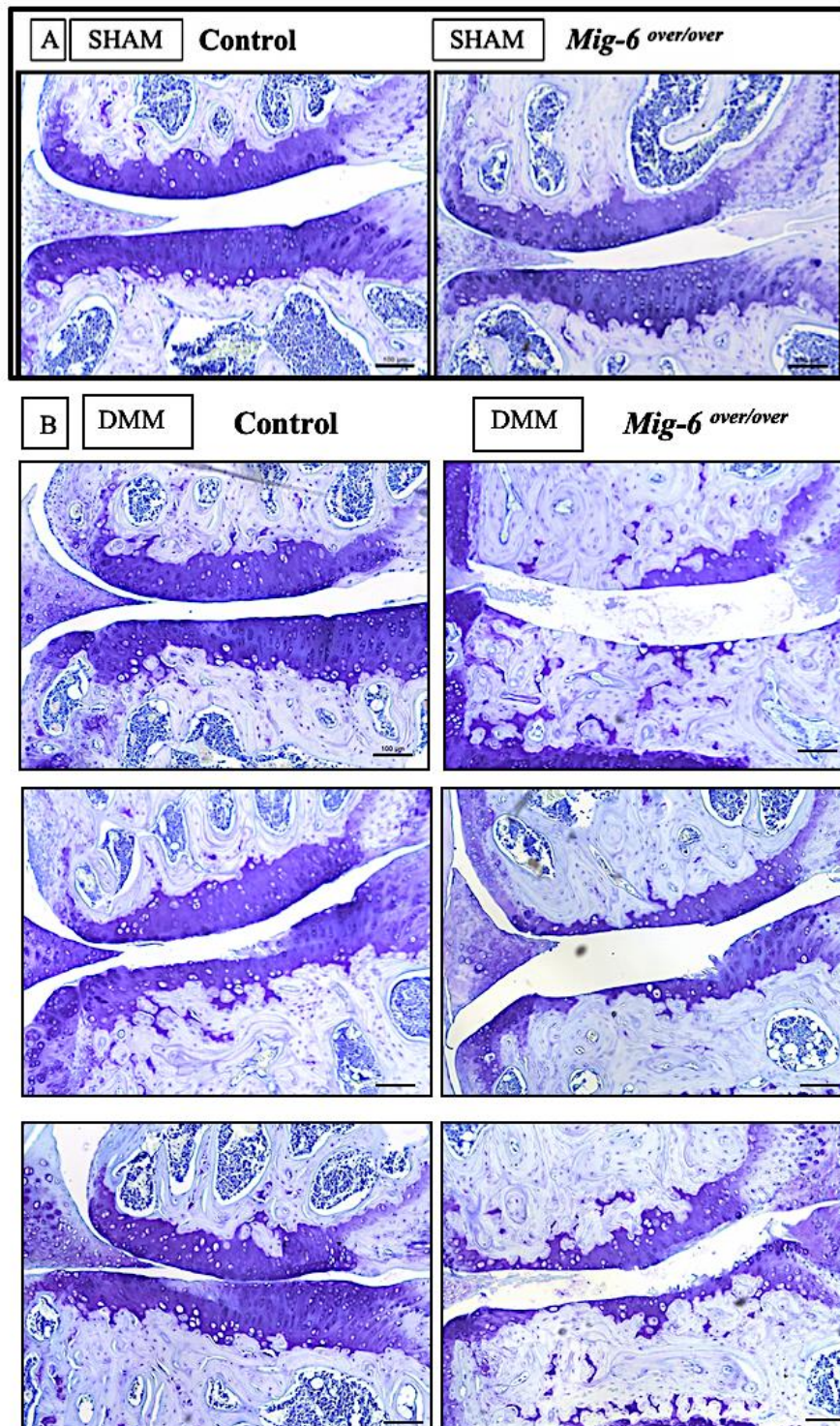
Figure 4.1 Overexpression of Mig-6 in cartilage increases severity of surgically induced osteoarthritis

Figure 4.2 Semi-quantitative assessment of knee joint histopathology after surgical induction of PTOA. Structural progression of OA was semi-quantitatively assessed via OARSI scoring for cartilage degeneration. Control SHAM operated mice show articular cartilage with regular proteoglycan staining **(A).** *Mig-6* $^{over/over}$ DMM operated mice had significantly more cartilage damage in either quadrant of the medial side versus control DMM operated animals. N=7-9 per group, data shown are mean ± SEM, p<0.05.
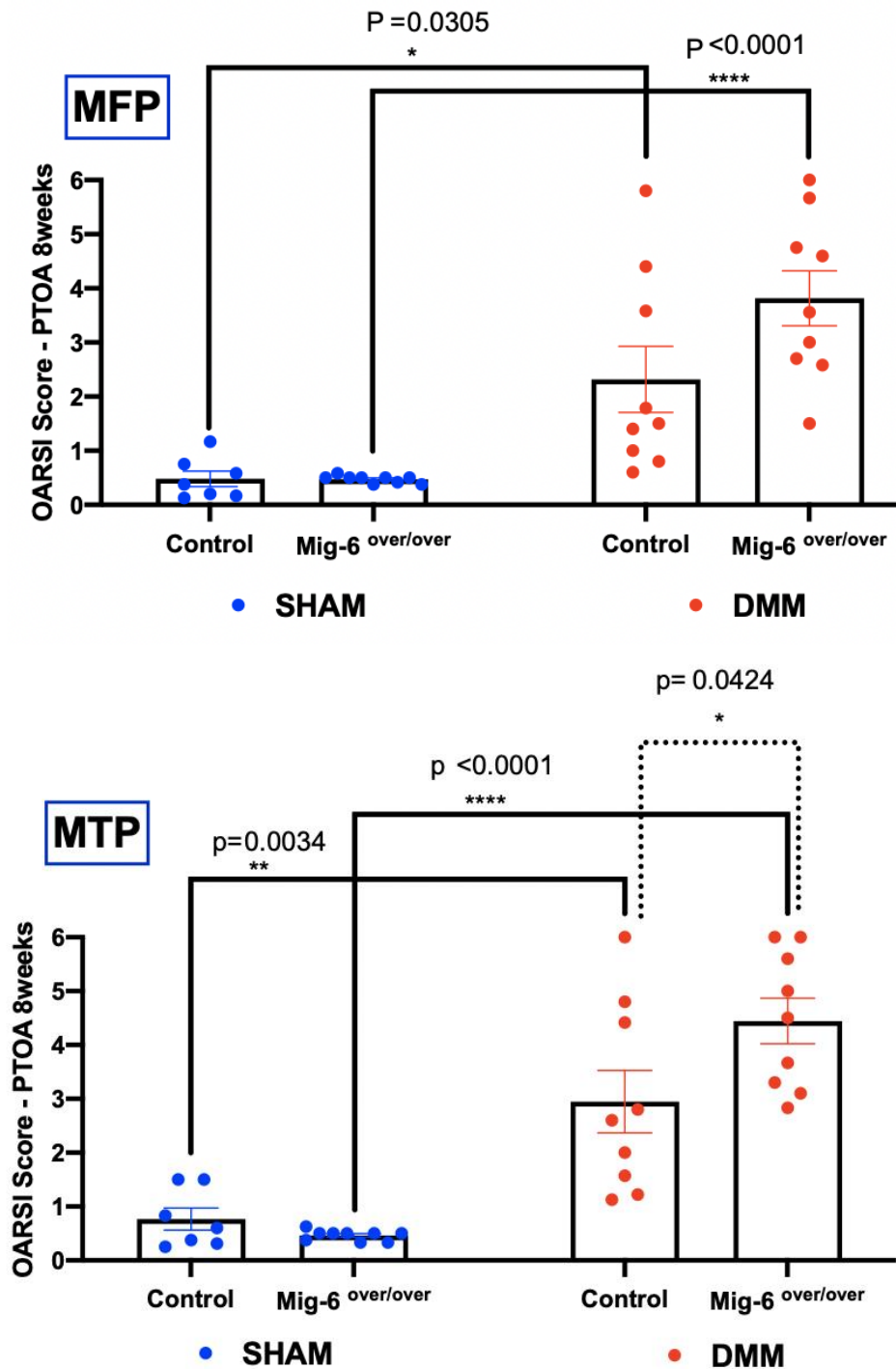
Figure 4.2 Semi-quantitative assessment of knee joint histopathology after surgical induction of PTOA

Figure 4.3 Overexpression of Mig-6 in cartilage show healthy articular cartilage on lateral compartment of the knee. SHAM control or mutant mice show healthy cartilage, subchondral bone and menisci **(A).** DMM control and mutant mice reveal little proteoglycan loss or articular cartilage damage in the lateral femoral condyle and lateral tibial plateau 8 weeks post-surgery **(B).** All scale bars =100 μm. N=7-9 per group.

Lateral Compartment
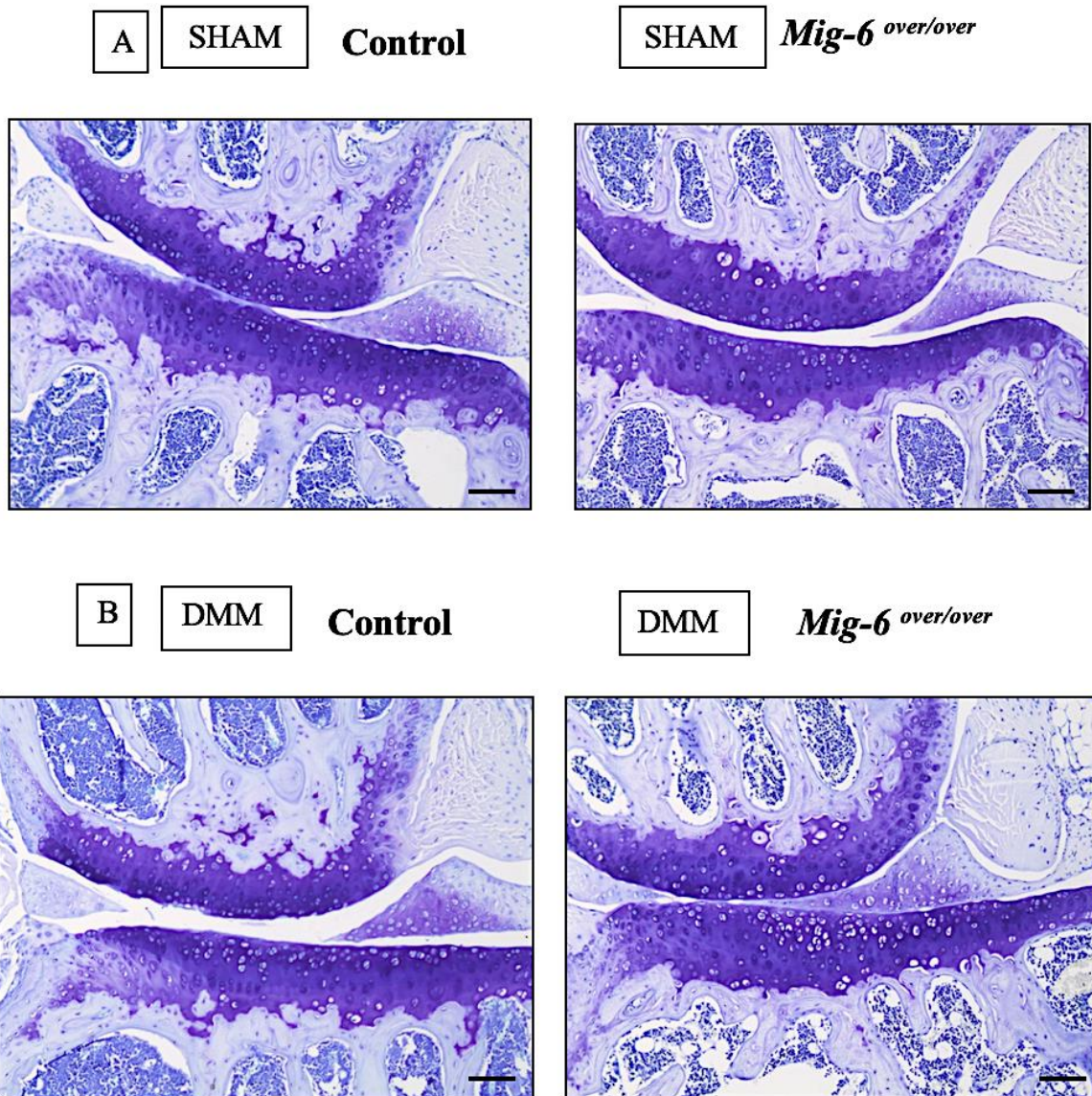
A | SHAM | **Control**   SHAM | *Mig-6* ^{over/over}

B | DMM | **Control**   DMM | *Mig-6* ^{over/over}

Figure 4.3 Overexpression of Mig-6 in cartilage show healthy articular cartilage on lateral compartment of the knee

Figure 4.4 OARSI scoring does not indicate differences in lateral compartments of the knee after SHAM or DMM surgery. OARSI scores of the Lateral Femoral Condyle and the Lateral Tibial Plateau indicate minimal damage to the articular surfaces across genotypes and surgical conditions of the lateral knee. N=7-9 per group, data shown are mean ± SEM, p≤0.05.
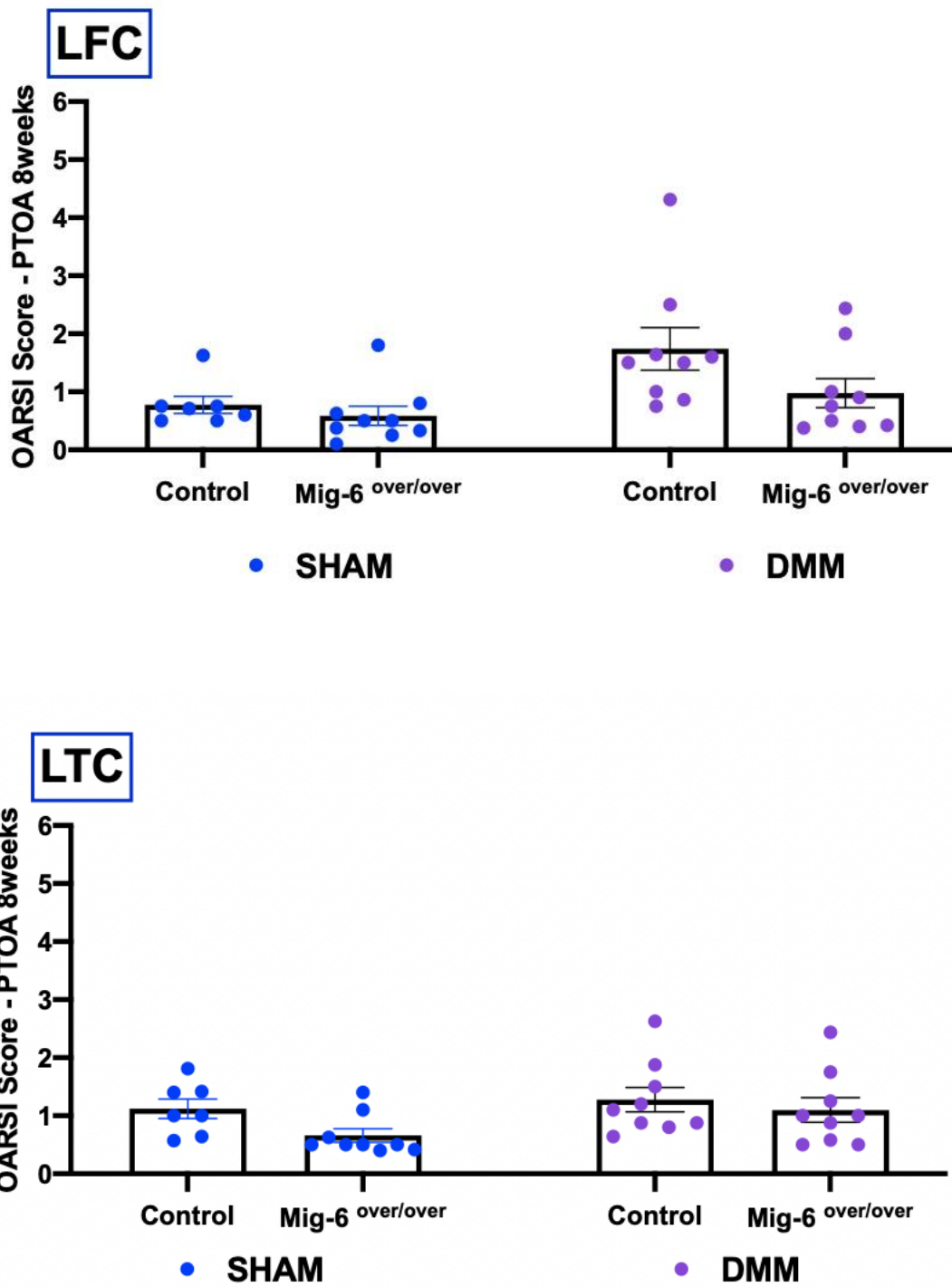
Figure 4.4 OARSI scoring does not indicate differences in lateral compartments of the knee after SHAM or DMM surgery

4.4.2 Mig-6 overexpressing male mice show minor alterations in behaviour post-surgery

To evaluate changes in behaviour that could be indicative of pain, mice were examined through Open Field Testing to measure changes in spontaneous locomotor activity. 8 weeks post-surgery, most parameters examined (including distance travelled, horizontal activity, rest time etc.) did not show any statistically significant differences in response to either DMM surgery or genotype. However, vertical activity count was reduced in *Mig-6* $^{over/over}$ mice in both SHAM and DMM groups **(Fig. 4.5).**

Figure 4.5 Mig-6 overexpressing mice show reduced vertical activity. Open Field Testing 8 weeks after DMM surgery demonstrates no changes in most spontaneous locomotor activities. However, Mig-6 overexpression reduces vertical activity count compared to control mice, independent of the type of surgery. N=7-9 per group, data shown are mean ± 95%CI; p≤0.05.

30 minutes
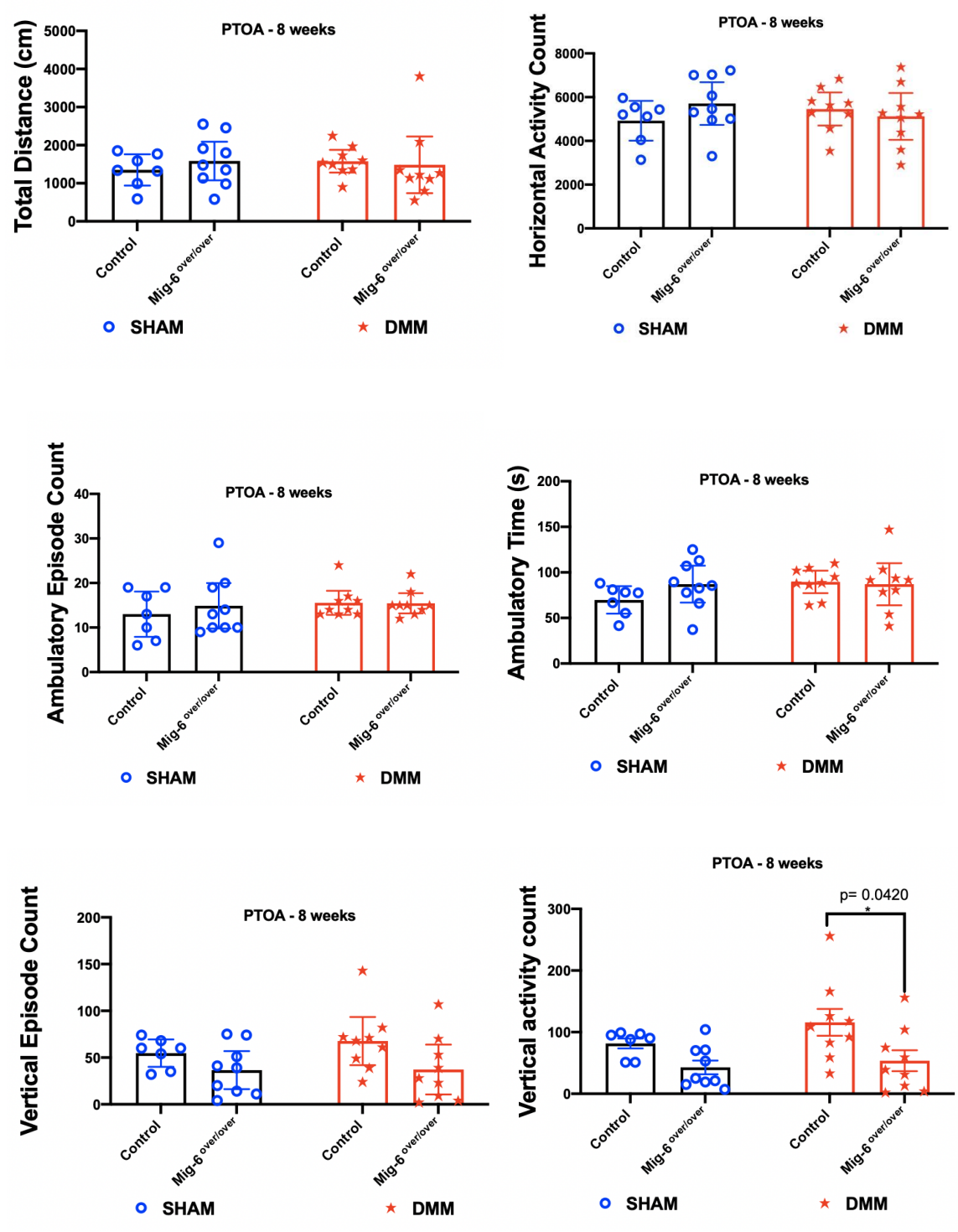
Figure 4.5 Mig-6 overexpressing mice show reduced vertical activity.

4.5   Discussion

Recently, we have shown that cartilage-specific overexpression of the gene encoding Mitogen-Inducible gene 6 (*Mig-6*) develop accelerated cartilage degeneration during aging (11). A similar phenotype was seen when *Mig-6* was overexpressed using the limb mesenchyme-specific Prx1 promoter (12). However, there is increasing evidence that OA is a heterogeneous disease, with multiple phenotypes potentially progressing through different processes (27–29). Therefore, results from our aging studies cannot be extrapolated to other forms of OA. Here, we analyze the role of *Mig-6* in a mouse model of post-traumatic OA. Using mice with cartilage-specific constitutive overexpression of *Mig-6*, initially characterised by our lab (11), in comparison to control mice, we utilized DMM surgery to induce knee OA. Histological analysis and OARSI scores revealed that Mig-6 overexpression resulted in an increased catabolic response to DMM surgery at 8 weeks-post surgery. Damage was largely limited to the medial joint compartment, as is usually seen in the DMM model. Importantly, SHAM-operated mice showed little to no damage (with a few exceptions in both genotypes). Thus, *Mig-6* overexpression does not induce cartilage damage on its own at the age of 6 months (the age of sacrifice for these mice), but accelerates development of post-traumatic damage. The combination of genetic manipulation and surgery-induced mechanical stress appears to accelerate cartilage degeneration, in line with the reported upregulation of endogenous Mig-6 expression after cartilage impact in a dog model (30–32).

In our previous study we had demonstrated accelerated OA in the same cartilage-specific *Mig-6* overexpressing mice at 12 months of age (11). In conjunction with the phenotypes of our SHAM-operated mice described here, these data indicate that primary OA pathogenesis begins between 6 and 12 months of age in these mice. Future studies will need to address the molecular pathways involved; for example, our results (11) suggest that down-regulation of Sox9 expression precedes cartilage degeneration. This is, to our knowledge, the first study to analyze exploratory motor behaviour using open field testing in mice with induced post-traumatic knee OA. Our findings indicate that most parameters were not changed by either DMM surgery or *Mig-6* overexpression. However, Mig-6 overexpression decreased vertical activity (rearing). Rearing had been shown to be affected by DMM surgery using the LABORAS behavioral platform (33), which appears logical since it involves increased loading on the hind limbs, including the DMM-operated knee. However, in our study, DMM surgery itself did not affect vertical activity in either genotype.

Instead, we found Mig-6 overexpression to decrease this activity both after SHAM and after DMM surgeries. The underlying cause is unclear at this point. It should be noted that changes in these open field tests are not necessarily related to OA pain, but could be caused by effects in other tissues (e.g. muscle weakness), or by anxiety or depression. Given that our animals are cartilage-specific transgenic mice, and that there is no apparent histological defect in SHAM-operated animals (that demonstrate reduced vertical activity), such effects appear less likely, but cannot be ruled out completely. Direct analyses of pain, for example through von Frey filaments or hot plate assays, could provide a more direct readout of whether increased histological OA damage in Mig-6-overexpressing mice correlates with increased pain. In addition, later time points after surgery could result in clearer effects on pain and activity. A limitation of this study is the focus on male mice only. This was done since the DMM model progresses more rapid in males (23), and since Mig-6 overexpression had more severe effects during aging in males (11). Nevertheless, future studies should include female Mig-6-overexpressing mice. Additional future studies should examine more time points (e.g. 4, 12, and possibly 16 weeks after surgery) as well as underlying molecular changes.

Altogether, our studies indicate that *Mig-6* overexpression not only accelerates the development of primary OA during aging, but may also worsen posttraumatic OA pathogenesis in the DMM model. Since Mig-6 primarily acts through down-regulation of EGFR activity, these data indicate a requirement for EGFR signaling in protecting from DMM-induced damage, in line with recent studies (34–36). This is in contrast to the protective effects observed upon genetic deletion of the gene for TGFα, an EGFR ligand, in the DMM model (37) and to the effects of a small molecule EGFR inhibitor in a rat model of PTOA (38). However, the context-specific roles of this pathway in OA have been recognized and discussed recently (39). This study provides further insight into the complex role of this pathway in OA.

4.6   Acknowledgements

4.7   References

1.   Tseng, R.-C. *et al.* Genomewide loss of heterozygosity and its clinical associations in non small cell lung cancer. *Int. J. Cancer* **117,** 241–247 (2005).

2.   Zhang, Y.-W. *et al.* Targeted disruption of Mig-6 in the mouse genome leads to early onset degenerative joint disease. *Proc. Natl. Acad. Sci. U. S. A.* **102,** 11740–5 (2005).

3.   Mateescu, R. G., Todhunter, R. J., Lust, G. & Burton-Wurster, N. Increased MIG-6 mRNA transcripts in osteoarthritic cartilage. *Biochem. Biophys. Res. Commun.* **332,** 482–6 (2005).

4.   Jin, N., Gilbert, J. L., Broaddus, R. R., DeMayo, F. J. & Jeong, J.-W. Generation of a Mig-6 conditional null allele. *genesis* **45,** 716–721 (2007).

5.   Velasquillo, C. *et al.* Expression of MIG-6, WNT-9A, and WNT-7B during osteoarthritis. *Ann. N. Y. Acad. Sci.* **1117,** 175–80 (2007).

6.   Hackel, P. O., Gishizky, M. & Ullrich, A. Mig-6 Is a Negative Regulator of the Epidermal Growth Factor Receptor Signal. *Biol. Chem.* **382,** (2001).

7.   Ferby, I. *et al.* Mig6 is a negative regulator of EGF receptor–mediated skin morphogenesis and tumor formation. *Nat. Med.* **12,** 568–573 (2006).

8.   Zhang, Y.-W. & Vande Woude, G. F. in *Futur. Asp. Tumor Suppressor Gene* (InTech, 2013). doi:10.5772/54393

9.   Anastasi, S., Castellani, L., Alemà, S. & Segatto, O. A pervasive role for MIG6 in restraining cell proliferation. *Cell Death Differ.* **21,** 345–347 (2013).

10.   Zhang, X., Gureasko, J., Shen, K., Cole, P. A. & Kuriyan, J. An Allosteric Mechanism for Activation of the Kinase Domain of Epidermal Growth Factor Receptor. *Cell* **125,** 1137–1149 (2006).

11.   Bellini, M., Pest, M. A., Miranda-Rodrigues, M., Jeong, J. & Beier, F. Overexpression of mig-6 in cartilage induces an osteoarthritis-like phenotype in mice. *bioRxiv* 764142 (2019). doi:10.1101/764142

12.   Bellini, M. R., Pest, M. A., Jeong, J.-W. & Beier, F. Overexpression Of Mig-6 In Limb Mesenchyme Leads To Accelerated Osteoarthritis In Mice. *bioRxiv* 871350 (2019). doi:10.1101/871350

13.   Pest, M. A., Russell, B. A., Zhang, Y.-W., Jeong, J.-W. & Beier, F. Disturbed cartilage and joint homeostasis resulting from a loss of mitogen-inducible gene 6 in a mouse model of joint dysfunction. *Arthritis Rheumatol. (Hoboken, N.J.)* **66,** 2816–27 (2014).

14.   Shepard, J. B., Jeong, J.-W., Maihle, N. J., O'Brien, S. & Dealy, C. N. Transient anabolic effects accompany epidermal growth factor receptor signal activation in articular cartilage

in vivo. *Arthritis Res. Ther.* **15,** R60 (2013).

15. Centers for Disease Control and Prevention (CDC). Prevalence of doctor-diagnosed arthritis and arthritis-attributable activity limitation --- United States, 2007-2009. *MMWR. Morb. Mortal. Wkly. Rep.* **59,** 1261–5 (2010).

16. McDonough, C. M. & Jette, A. M. The Contribution of Osteoarthritis to Functional Limitations and Disability. *Clin. Geriatr. Med.* **26,** 387–399 (2010).

17. McCurry, S. M. *et al.* Frequency of comorbid insomnia, pain, and depression in older adults with osteoarthritis: Predictors of enrollment in a randomized treatment trial. *J. Psychosom. Res.* **71,** 296–299 (2011).

18. Gs, M. & Mologhianu G. *Osteoarthritis pathogenesis-a complex process that involves the entire joint*. *J. Med. Life* **7,**

19. Loeser, R. F., Goldring, S. R., Scanzello, C. R. & Goldring, M. B. Osteoarthritis: A disease of the joint as an organ. *Arthritis Rheum.* **64,** 1697–1707 (2012).

20. Blagojevic, M., Jinks, C., Jeffery, A. & Jordan, K. P. Risk factors for onset of osteoarthritis of the knee in older adults: a systematic review and meta-analysis. *Osteoarthr. Cartil.* **18,** 24–33 (2010).

21. Vaishya, R., Pariyo, G. B., Agarwal, A. K. & Vijay, V. Non-operative management of osteoarthritis of the knee joint. *J. Clin. Orthop. trauma* **7,** 170–6 (2016).

22. Rönn, K., Reischl, N., Gautier, E. & Jacobi, M. Current surgical treatment of knee osteoarthritis. *Arthritis* **2011,** 454873 (2011).

23. Glasson, S. S., Blanchet, T. J. & Morris, E. A. The surgical destabilization of the medial meniscus (DMM) model of osteoarthritis in the 129/SvEv mouse. *Osteoarthr. Cartil.* **15,** 1061–1069 (2007).

24. Kim, T. H. *et al.* Mig-6 suppresses endometrial cancer associated with pten deficiency and ERK activation. *Cancer Res.* **74,** 7371–7382 (2014).

25. Welch, I. D., Cowan, M. F., Beier, F. & Underhill, T. M. The retinoic acid binding protein CRABP2 is increased in murine models of degenerative joint disease. *Arthritis Res. Ther.* **11,** R14 (2009).

26. Glasson, S. S., Chambers, M. G., Van Den Berg, W. B. & Little, C. B. The OARSI histopathology initiative – recommendations for histological assessments of osteoarthritis in the mouse. *Osteoarthr. Cartil.* **18,** S17–S23 (2010).

27. Driban, J. B., Sitler, M. R., Barbe, M. F. & Balasubramanian, E. Is osteoarthritis a heterogeneous disease that can be stratified into subsets? doi:10.1007/s10067-009-1301-1

28. Dell'Isola, A., Allan, R., Smith, S. L., Marreiros, S. S. P. & Steultjens, M. Identification of

clinical phenotypes in knee osteoarthritis: a systematic review of the literature. *BMC Musculoskelet. Disord.* **17,** 425 (2016).

29.   Chen, D. *et al.* Osteoarthritis: toward a comprehensive understanding of pathological mechanism. *Nat. Publ. Gr.* **5,** (2016).

30.   Guilak, F. Biomechanical factors in osteoarthritis. *Best Pract. Res. Clin. Rheumatol.* **25,** 815–23 (2011).

31.   Feng, X. Chemical and Biochemical Basis of Cell-Bone Matrix Interaction in Health and Disease. *Curr. Chem. Biol.* **3,** 189–196 (2009).

32.   Bader, D. L., Salter, D. M. & Chowdhury, T. T. Biomechanical influence of cartilage homeostasis in health and disease. *Arthritis* **2011,** 979032 (2011).

33.   Miller, R. E. *et al.* CCR2 chemokine receptor signaling mediates pain in experimental osteoarthritis. *Proc. Natl. Acad. Sci. U. S. A.* **109,** 20602–20607 (2012).

34.   Jia, H. *et al.* EGFR signaling is critical for maintaining the superficial layer of articular cartilage and preventing osteoarthritis initiation. *Proc. Natl. Acad. Sci. U. S. A.* 201608938 (2016). doi:10.1073/pnas.1608938113

35.   Jia, H. *et al.* Subchondral bone plate sclerosis during late osteoarthritis is causedby loading-induced reduction in Sclerostin. *Arthritis Rheumatol. (Hoboken, N.J.)* **70,** 230 (2018).

36.   Zhang, X. *et al.* Reduced EGFR signaling enhances cartilage destruction in a mouse osteoarthritis model. *Bone Res.* **2,** 14015 (2014).

37.   Usmani, S. E. *et al.* Context-specific protection of TGFα null mice from osteoarthritis. *Sci. Rep.* **6,** 30434 (2016).

38.   Appleton, C. T. G. *et al.* Reduction in Disease Progression by Inhibition of Transforming Growth Factor α-CCL2 Signaling in Experimental Posttraumatic Osteoarthritis. *Arthritis Rheumatol.* **67,** 2691–2701 (2015).

39.   Qin, L. & Beier, F. EGFR Signaling: Friend or Foe for Cartilage? *JBMR Plus* **3,** e10177 (2019).

Chapter 5

5 Discussion

5.1 Overview

The overall objective of my thesis was to examine the role of mitogen inducible gene 6 (*Mig-6*) in cartilage biology and osteoarthritis (OA). Initially, our laboratory identified transforming growth factor alpha (TGFα), which is a ligand for epidermal growth factor receptor (EGFR), in microarray studies from cartilage isolated from a surgical rat model of OA (1,2). Our studies have shown that TGFα mRNA levels were almost 4-fold enhanced in the OA animals (2). Additional studies demonstrated that TGFα was amongst the genetic loci most strongly linked to hip OA and cartilage thickness in two genome-wide association studies (GWAS) (3,4). Based on these findings, our laboratory decided to investigate the role of EGFR signaling in cartilage development, homeostasis, and disease in detail (5–7). The next logical step was to investigate a negative regulator of EGFR signaling named Mig-6 (encoded by the gene *Errfi1)* (8,9).

Our and other previous data supports the hypothesis that Mig-6 plays a key role in cartilage homeostasis. Global *Mig-6* mouse knockout (KO) lines had demonstrated progressive cartilage degeneration similar to that seen in OA (10,11). Furthermore, cartilage-specific deletion of *Mig-6* resulted in anabolic and catabolic phenotypes similar to previous studies using whole body *Mig-6* KO models, such as increased articular cartilage thickness and formation of osteochondral nodules in their knee joints and spine (12). Mig-6 KO mice demonstrated activation of EGFR and increased expression of SOX9 and PCNA, both in nodule cells and in articular cartilage. Previous research demonstrates that Mig-6 overexpression acts as a negative feedback regulator of EGFR/ERK signaling (13), but these studies did not yet analyze joint tissues.

The first study in my thesis, I generated mice with cartilage-specific Mig-6 overexpression (14). Mice with conditional ('over') *Mig-6* alleles (*Mig-6$^{over/over}$)* were bred to mice expressing Cre recombinase under the control of the Collagen 2 promoter and overexpressing mice were obtained at the expected Mendelian ratios. I began by examining *Mig-6 $^{over/over}$* mice during early postnatal development and comparing them to control mice. I examined skeletal development and cartilage development at post-natal day 0 (P0), 6 weeks-old, 11 weeks-old, 12 and 18 months

of age and I observed no obvious gross malformations or growth plate alterations in *Mig-6^{over/over}* mice at developmental stages. However, long bones of *Mig-6^{over/over}* mice were significantly shorter than those of control mice at the ages of 6 and 11 weeks as well as at 12 and 18 months. Furthermore, articular cartilage from 6 and 11 weeks-old male and female mice appeared healthy during skeletal maturity. However, examination of the knee joints of *Mig-6^{over/over}* did show increased cartilage loss relative to controls at the ages of 12 and 18 months.

Therefore, overexpression of Mig-6 resulted in early OA-like pathology, in particular in male mice. Interestingly, immunostaining for SOX9, phosphoEGFR and lubricin (PRG4) was decreased in articular cartilage of *Mig-6^{over/over}* mice whereas MMP13 staining was increased in areas of cartilage degeneration. Importantly, reduced SOX9 staining preceded histological cartilage degeneration, suggesting a potential mechanism for OA progression in our mutant mice. Taken together, this led me to conclude that *Mig-6* plays an important role for initiating the OA-phenotype onset, likely through the activation of the EGFR pathway.

Second, we utilized *Prx-1 Cre* to drive the overexpression of *Mig-6* in the entire limb mesenchyme with the same *Mig-6^{over/over}* line (14) used in my previous study. My rationale was that overexpression in multiple joint tissues might have additional effects, in comparison to overexpression in cartilage only. *Mig-6^{over/over}* mice displayed minor differences in body weight in comparison to controls. Surprisingly, these mice showed similar bone length at 12 and 36 weeks-old, despite earlier and more widespread Cre activity compared to the Col2 Cre driver. However, the thickness of the calcified articular cartilage in the medial femoral condyle (MFC) and medial tibial plateau (MTP) of male *Mig-6^{over/over}* mice was statistically significantly lower than in controls. I evaluated the knee joints of 36 weeks-old *Mig-6^{over/over}* male mice that displayed increased articular cartilage damage in comparison to the control group. Again, male mice showed a stronger and more consistent phenotype than the female group. Interestingly, use of the Prx-1 Cre resulted in more damage on the lateral side of the knee joint compared to Col2-Cre, possibly due to overexpression of Mig-6 in additional joint structures. Measurement of the subchondral bone area in male *Mig-6^{over/over}* and control mice showed no differences. However, examination of picrosirius red staining under polarized light showed that the structure of the articular cartilage ECM in *Mig-6^{over/over}* was altered compared to that of control mice. The articular cartilage of control animals showed greenish/yellow birefringence, while that from *Mig-*

6 *over/over* animals showed fewer green collagen fibers, indicating a loss of normal collagen fiber organization. The resulting collagen network alterations may have an influence on the structural integrity of the cartilage and lead to degenerative pathologies (15). Immunohistochemistry for SOX9 and PRG4 showed decreased staining in *Mig-6over/over* mice relative to controls, providing potential molecular mechanisms for the observed effects. Moreover, MMP13 immunostaining appeared increased in *Mig-6over/over* mice in the areas of damage on the medial side.

Lastly, we surgically induced OA in cartilage-specific Mig-6 overexpressing male mice at 16 weeks of age through destabilization of medial meniscus surgery (DMM). This surgery is the most accepted and a widely surgical OA model in mice in order to induce secondary OA that develops gradually in the medial compartment (16). Our results showed that cartilage degeneration is more severe in Mig-6 overexpressing mice than in control littermates 8 weeks post surgery). Interestingly, while both surgery and Mig-6 overexpression did not affect most parameters assessed in Open Field testing, Mig-6 overexpression did reduce vertical activity (rearing) both after SHAM and DMM surgery.

5.2   Contribution to the Field of Osteoarthritis

Through this thesis, I characterise for the first time the role of *Mig-6* overexpression on joint health. In Chapter 2 and 3, I present work where I discovered that *Mig-6over/over* mice did not have major effects on cartilage development and bone growth. However, *Mig-6over/over* disrupts normal cartilage maintenance and homeostasis. For both of these chapters, I employed an aging model of OA by analyzing spontaneous joint disease.

In chapter 2, I used chondrocyte-specific overexpression of *Mig-6*. Prior to our investigation, systemic deletion of Mig-6 had been implicated in progressive joint disease with chondro-osseous growths in the ankle, temporomandibular joint (TMJ) and knee (11,17). Moreover, studies utilizing *Col2a1-Cre* to drive deletion of *Mig-6* in chondrocytes have shown increased articular cartilage thickness and invasive chondro-osseous nodules with overactive EGFR signaling and induction of SOX9 immunostaining (12,18). Additionally, in chapter 3, I investigate the role of *Mig-6* overexpression utilizing Prx1-Cre to drive overexpression of Mig-6 in the entire limb mesenchyme. Furthermore, SOX9 and PRG4 immunostaining seems to be

decreased in articular cartilage of 12-week-old mice and even more in 36-week-old mice when cartilage shows signs of degeneration. Chapter 4 provides the first report on the effect of chondrocyte-specific overexpression of *Mig-6* on post-traumatic OA. Our data demonstrated that Mig-6 overexpression worsened cartilage degeneration after DMM surgery.

Collectively, my data provide strong evidence that Mig-6 overexpression accelerates OA both during aging (primary OA) and after injury (secondary/post-traumatic OA). These effects are most likely due to decreased activation of EGFR signaling, as they resemble effects seen upon genetic inactivation of EGFR (19,20). Lastly, my findings from this thesis further emphasize that the Mig-6/EGFR network is a major regulator of cartilage homeostasis and OA, but many aspects of its action in cartilage are still not well understood (see next section).

5.3   Limitations of Research

5.3.1   Limitations of *in-vivo* models

The use of small animal model such as rodent models gives us the opportunity to study the role of a protein/gene using transgenic and knockout strains in a disease model. While we can control many variables in these studies, some are outside our control such as litter size and certain aspects of behavior. I tried to minimize the effects of these variations and to keep transgenic mice and controls under identical conditions. For example, I co-housed the control animals with their respective Mig-6 overexpressing littermates wherever possible. These models have allowed us to evaluate the function of Mig-6 in cartilage and the whole joint. In chapters 2 and 4, I used the collagen II promoter to drive Cr expression and activation of Mig-6 overexpression. This Cre line is not fully cartilage specific since recombination can occur in other joint cells as well as osteoblasts and osteocytes that develop from trans-differentiation of chondrocytes (21,22). In addition, this Cre driver becomes activated during development (before birth); thus, it can be difficult to distinguish developmental defects from OA-specific effects in adult articular cartilage. One way to overcome this in the future is the use of an inducible Cre-driver, such as the Aggrecan CreER and postnatal tamoxifen injection (23). Similar concerns and solutions apply to the Prx1 Cre driver used in chapter 3.

Currently, studies in chapters 2 and 3 use partially different time points/ages for analyses. For example, the eldest animals analyzed in chapter 2 were 18 months, while maximum age was 9 months in chapter 3. This limitation was due to different breeding schedules between the two lines, but future studies should aim to align time courses for both to allow direct comparison of the effects of the two different Cre drivers. Ideally, validation of results in a different genetic background would strengthen the conclusions. For feasibility, PTOA studies in chapter 4 were only done in male mice; ideally these should be done in female mice. Additional time points (4,12, and 16 weeks after surgery) should also be included into this study, as well as analyses of additional tissues (subchondral bone, synovium etc.).

5.3.2   Limitations of outcome measures

One major limitation of our analyses is the absence of a reliable Mig-6 antibody that would allow us to 1) quantify the level of Mig-6 protein overexpression; and 2) to localize where in the joint Mig-6 protein is expressed. However, none of the antibodies we tested were specific enough (e.g. they all gave strong signals from confirmed Mig-6 KO tissues). Other molecular techniques including qPCR, Western Blotting, etc. also could be used in the future. to provide more insights into the molecular mechanisms mediating Mig-6 effects in cartilage and other joint tissues. Imaging modalities such as high resolution microCT could be included to allow more quantitative, three-dimensional analyses of bony changes in our animals. Mechanical testing, for example by atomic force microscopy, could provide another readout of high physiological relevance. Our Open Field studies demonstrated minimal changes between groups in chapter 4, and none that could be attributed to DMM surgery. Additional measures that more directly examine pain (such as von Frey filaments or hot/cold plate assays) could be considered in the future to establish a more direct link between structural damage and pain.

5.4   Future Directions

My results implicate the need for several follow-up studies. In addition to those already mentioned in the last section (such as more time points and inclusion of female mice in DMM studies, additional molecular analyses and pain assays etc.), several larger questions should be tackled. My studies demonstrated that overexpression of Mig-6 accelerates both primary and

secondary OA and implicated reduced EGFR signaling and downregulation of SOX9 expression as potential mechanisms. However, detailed mechanistic studies are required to characterise the molecular pathways involved. We have proposed that the phenotypes seen in our Mig-6 overexpressing mice are due to reduced EGFR signaling. Downstream pathways mediating these activities, such as ERK1/2 or PI3K, should be investigated in detail using biochemical and cell biological assays. However, since Mig-6 interacts with a number of other potential candidates, e.g. the other EGFR family receptors (ErbB1-4), cMET, c-Abl and Cdc42 (24,25), we should also investigate whether any of these pathways are deregulated and contribute to the observed phenotypes. This might include the generation of double mutant mice to determine whether manipulation of these factors can rescue the phenotypes of the Mig-6 overexpressing mice (or the Mig-6 KO mice).

Aging-associated OA and post-traumatic OA are only two of several osteoarthritis subtypes. Both Mig-6 KO and overexpressing mice should also be tested in models of metabolic OA (e.g. on a high fat or western diet), and overuse-induced OA (e.g. treadmill running), both of which are established in our laboratory. Moreover, Mig-6 function should be examined in human samples, through knockdown and/or overexpression studies in isolated joint cells. While there are currently no drugs that directly affect Mig-6 activity, genetic strategies to inhibit its expression (shRNA or CRISPR/Cas9) could be attempted in the future. Any such attempts would have to be very tightly controlled both spatially and temporarily, because of the dual catabolic and anabolic role of EGFR signaling in the joint (5). This dual role, where EGFR has been shown to both protect from and promote OA dependent on the context, remains poorly understood. My studies clearly suggest a protective role of the pathway – if we inhibit EGFR signaling by overexpressing Mig-6, we see an acceleration in OA progression. However, strong evidence for a catabolic role of the same pathways has been provided by our lab and others (6,19,26–28). Understanding the basis of this dual role will likely require detailed mechanistic studies at the biochemical level, as well as more in vivo studies using crosses of multiple mouse lines, along with the use of tamoxifen-inducible Cre drivers that allow for precise activation or inactivation of genes.

5.5   References

1.   Appleton, C. T. G., Pitelka, V., Henry, J. & Beier, F. Global analyses of gene expression in early experimental osteoarthritis. *Arthritis Rheum.* **56,** 1854–1868 (2007).

2.   Appleton, C. T. G., McErlain, D. D., Henry, J. L., Holdsworth, D. W. & Beier, F. Molecular and histological analysis of a new rat model of experimental knee osteoarthritis. *Ann. N. Y. Acad. Sci.* **1117,** 165–174 (2007).

3.   Cui, G. *et al.* Association of Common Variants in TGFA with Increased Risk of Knee Osteoarthritis Susceptibility. *Genet. Test. Mol. Biomarkers* gtmb.2017.0045 (2017). doi:10.1089/gtmb.2017.0045

4.   Li, H. *et al. Association between EN1 rs4144782 and susceptibility of knee osteoarthritis: A case-control study.* (2017). at <www.impactjournals.com/oncotarget>

5.   Qin, L. & Beier, F. EGFR Signaling: Friend or Foe for Cartilage? *JBMR Plus* **3,** e10177 (2019).

6.   Sun, H. *et al.* Gefitinib for Epidermal Growth Factor Receptor Activated Osteoarthritis Subpopulation Treatment. *EBioMedicine* **32,** 223–233 (2018).

7.   Jia, H. *et al.* EGFR signaling is critical for maintaining the superficial layer of articular cartilage and preventing osteoarthritis initiation. doi:10.1073/pnas.1608938113

8.   Hackel, P. O., Gishizky, M. & Ullrich, A. Mig-6 Is a Negative Regulator of the Epidermal Growth Factor Receptor Signal. *Biol. Chem.* **382,** 1649–62 (2001).

9.   Jin, N. *et al.* Mig-6 is required for appropriate lung development and to ensure normal adult lung homeostasis. *Development* **136,** 3347–56 (2009).

10. Zhang, Y.-W. *et al.* Targeted disruption of Mig-6 in the mouse genome leads to early onset degenerative joint disease. *Proc. Natl. Acad. Sci. U. S. A.* **102,** 11740–5 (2005).

11. Jin, N., Gilbert, J. L., Broaddus, R. R., DeMayo, F. J. & Jeong, J.-W. Generation of aMig-6 conditional null allele. *genesis* **45,** 716–721 (2007).

12. Pest, M. A., Russell, B. A., Zhang, Y.-W., Jeong, J.-W. & Beier, F. Disturbed cartilage and joint homeostasis resulting from a loss of mitogen-inducible gene 6 in a mouse model of joint dysfunction. *Arthritis Rheumatol. (Hoboken, N.J.)* **66,** 2816–27 (2014).

13. Kim, T. H. *et al.* Mig-6 suppresses endometrial cancer associated with pten deficiency and ERK activation. *Cancer Res.* **74,** 7371–7382 (2014).

14. Bellini, M., Pest, M. A., Miranda-Rodrigues, M., Jeong, J. & Beier, F. Overexpression of mig-6 in cartilage induces an osteoarthritis-like phenotype in mice. *bioRxiv* 764142 (2019). doi:10.1101/764142

15. Lattouf, R. *et al.* Picrosirius Red Staining. *J. Histochem. Cytochem.* **62,** 751–758 (2014).

16. Glasson, S. S., Blanchet, T. J. & Morris, E. A. The surgical destabilization of the medial meniscus (DMM) model of osteoarthritis in the 129/SvEv mouse. *Osteoarthr. Cartil.* **15,** 1061–1069 (2007).

17. Joiner, D. M. *et al.* Accelerated and increased joint damage in young mice with global inactivation of mitogen-inducible gene 6 after ligament and meniscus injury. *Arthritis Res. Ther.* **16,** R81 (2014).

18. Shepard, J. B., Jeong, J.-W., Maihle, N. J., O'Brien, S. & Dealy, C. N. Transient anabolic effects accompany epidermal growth factor receptor signal activation in articular cartilage in vivo. *Arthritis Res. Ther.* **15,** R60 (2013).

19. Jia, H. *et al.* EGFR signaling is critical for maintaining the superficial layer of articular cartilage and preventing osteoarthritis initiation. *Proc. Natl. Acad. Sci. U. S. A.* 201608938 (2016). doi:10.1073/pnas.1608938113

20. Zhang, X. *et al.* Reduced EGFR signaling enhances cartilage destruction in a mouse osteoarthritis model. *Bone Res.* **2,** 14015 (2014).

21. Pest, M. A. & Beier, F. Is there such a thing as a cartilage-specific knockout mouse? *Nat. Rev. Rheumatol.* **10,** 702–704 (2014).

22. Fosang, A. J., Golub, S. B., East, C. J. & Rogerson, F. M. Abundant LacZ activity in the absence of Cre expression in the normal and inflamed synovium of adult Col2a1-Cre; ROSA26RLacZ reporter mice. *Osteoarthr. Cartil.* **21,** 401–404 (2013).

23. Henry, S. P. *et al.* Generation of aggrecan-CreERT2 knockin mice for inducible Cre activity in adult cartilage. *Genesis* **47,** 805–814 (2009).

24. Zhang, Y.-W. & Vande Woude, G. F. Mig-6, Signal Transduction, Stress Response and Cancer. *Cell Cycle* **6,** 507–513 (2007).

25. Zhang, Y.-W. & Vande Woude, G. F. in *Futur. Asp. Tumor Suppressor Gene* (InTech, 2013). doi:10.5772/54393

26. Appleton, C. T. G., Usmani, S. E., Mort, J. S. & Beier, F. Rho/ROCK and MEK/ERK activation by transforming growth factor-α induces articular cartilage degradation. *Lab. Investig.* **90,** 20 (2009).

27. Appleton, C. T. G., Usmani, S. E., Bernier, S. M., Aigner, T. & Beier, F. Transforming growth factor alpha suppression of articular chondrocyte phenotype and Sox9 expression in a rat model of osteoarthritis. *Arthritis Rheum.* **56,** 3693–705 (2007).

28. Zhang, X. *et al.* Epidermal Growth Factor Receptor (EGFR) Signaling Regulates Epiphyseal Cartilage Development through β-Catenin-dependent and -independent Pathways. *J. Biol. Chem.* **288,** 32229–32240 (2013).

Appendices

Appendix A: Animal Use Protocol

Western

AUP Number: 2019-035
PI Name: Beier, Frank
AUP Title: The Regulation of Endochondral Bone Growth by Hormones
Approval Date: 06/01/2019
Official Notice of Animal Care Committee (ACC) Approval:
Your new Animal Use Protocol (AUP) 2019-035:1: entitled " The Regulation of Endochondral Bone Growth by Hormones"
has been APPROVED by the Animal Care Committee of the University Council on Animal Care. This approval, although valid for up to four years, is subject to annual Protocol Renewal.

Prior to commencing animal work, please review your AUP with your research team to ensure full understanding by everyone listed within this AUP.

As per your declaration within this approved AUP, you are obligated to ensure that:
　　1) Animals used in this research project will be cared for in alignment with:
　　　　a) Western's Senate MAPPs 7.12, 7.10, and 7.15
　　　　http://www.uwo.ca/univsec/policies_procedures/research.html
　　　　b) University Council on Animal Care Policies and related Animal Care Committee procedures
　　　　http://uwo.ca/research/services/animalethics/animal_care_and_use_policies.htm
　　2) As per UCAC's Animal Use Protocols Policy,
　　　　a) this AUP accurately represents intended animal use;
　　　　b) external approvals associated with this AUP, including permits and scientific/departmental peer approvals, are complete and accurate;
　　　　c) any divergence from this AUP will not be undertaken until the related Protocol Modification is approved by the ACC; and
　　　　d) AUP form submissions - Annual Protocol Renewals and Full AUP Renewals - will be submitted and attended to within timeframes outlined by the ACC.
　　　　e) http://uwo.ca/research/services/animalethics/animal_use_protocols.html
　　3) As per MAPP 7.10 all individuals listed within this AUP as having any hands-on animal contact will
　　　　a) be made familiar with and have direct access to this AUP;
　　　　b) complete all required CCAC mandatory training (training@uwo.ca); and
　　　　c) be overseen by me to ensure appropriate care and use of animals.
　　4) As per MAPP 7.15,
　　　　a) Practice will align with approved AUP elements;
　　　　b) Unrestricted access to all animal areas will be given to ACVS Veterinarians and ACC Leaders;
　　　　c) UCAC policies and related ACC procedures will be followed, including but not limited to:
　　　　　　i) Research Animal Procurement
　　　　　　ii) Animal Care and Use Records
　　　　　　iii) Sick Animal Response
　　　　　　iv) Continuing Care Visits
　　5) As per institutional OH&S policies, all individuals listed within this AUP who will be using or potentially exposed to hazardous materials will have completed in advance the appropriate institutional OH&S training, facility-level training, and reviewed related (M)SDS Sheets, http://www.uwo.ca/hr/learning/required/index.html

Submitted by: Copeman, Laura
on behalf of the Animal Care Committee
University Council on Animal Care

Dr Timothy Regnault,
Animal Care Committee Chair
The University of Western Ontario Animal Care Committee / University Council on Animal Care
London, Ontario Canada N6A 5C1

Western

AUP Number: 2019-036
PI Name: Beier, Frank
AUP Title: Regulation of Endochondral Bone Growth by Hormones- Destabilization of Medial Meniscus Surgery
Approval Date: 06/01/2019
Official Notice of Animal Care Committee (ACC) Approval:
Your new Animal Use Protocol (AUP) 2019-036:1: entitled " Regulation of Endochondral Bone Growth by Hormones- Destabilization of Medial Meniscus Surgery"
has been APPROVED by the Animal Care Committee of the University Council on Animal Care. This approval, although valid for up to four years, is subject to annual Protocol Renewal.

Prior to commencing animal work, please review your AUP with your research team to ensure full understanding by everyone listed within this AUP.

As per your declaration within this approved AUP, you are obligated to ensure that:
    1) Animals used in this research project will be cared for in alignment with:
        a) Western's Senate MAPPs 7.12, 7.10, and 7.15
        http://www.uwo.ca/univsec/policies_procedures/research.html
        b) University Council on Animal Care Policies and related Animal Care Committee procedures
        http://uwo.ca/research/services/animalethics/animal_care_and_use_policies.htm
    2) As per UCAC's Animal Use Protocols Policy,
        a) this AUP accurately represents intended animal use;
        b) external approvals associated with this AUP, including permits and scientific/departmental peer approvals, are complete and accurate;
        c) any divergence from this AUP will not be undertaken until the related Protocol Modification is approved by the ACC; and
        d) AUP form submissions - Annual Protocol Renewals and Full AUP Renewals - will be submitted and attended to within timeframes outlined by the ACC.
        e) http://uwo.ca/research/services/animalethics/animal_use_protocols.html
    3) As per MAPP 7.10 all individuals listed within this AUP as having any hands-on animal contact will
        a) be made familiar with and have direct access to this AUP;
        b) complete all required CCAC mandatory training (training@uwo.ca); and
        c) be overseen by me to ensure appropriate care and use of animals.
    4) As per MAPP 7.15,
        a) Practice will align with approved AUP elements;
        b) Unrestricted access to all animal areas will be given to ACVS Veterinarians and ACC Leaders;
        c) UCAC policies and related ACC procedures will be followed, including but not limited to:
            i) Research Animal Procurement
            ii) Animal Care and Use Records
            iii) Sick Animal Response
            iv) Continuing Care Visits
    5) As per institutional OH&S policies, all individuals listed within this AUP who will be using or potentially exposed to hazardous materials will have completed in advance the appropriate institutional OH&S training, facility-level training, and reviewed related (M)SDS Sheets, http://www.uwo.ca/hr/learning/required/index.html

Submitted by: Copeman, Laura
on behalf of the Animal Care Committee
University Council on Animal Care

Dr.Timothy Regnault,
Animal Care Committee Chair
The University of Western Ontario Animal Care Committee / University Council on Animal Care
London, Ontario Canada N6A 5C1

Appendix B: Curriculum Vitae

<u>Melina Rodrigues Bellini</u>

Education:

2015- Present: The University of Western Ontario

London, Ontario, Canada

Ph.D. Candidate

2011 – 2013:   University of Sao Paulo

Bauru, Sao Paulo, Brazil

M.Sc. in Oral Biology

2007- 2010:   University of Sagrado Coração

Bauru, Sao Paulo, Brazil

Biological Sciences (BSc.)

Publications

1. **<u>Bellini, M</u>**, Pest, MA, Miranda-Rodrigues, M, Jeong JW, Beier F. Overexpression of Mig-6 in cartilage induces an osteoarthritis-like phenotype in mice. *BioRxiv. https://doi.org/10.1101/764142. (in preparation).*

2. **<u>Bellini, M</u>**, Pest, MA, Jeong JW, Beier F. Overexpression of Mig-6 in Limb Mesenchyme Leads to Accelerated Osteoarthritis in Mice. *BioRxiv https://doi.org/10.1101/871350. (in preparation).*

3. **<u>Bellini, M</u>**, Bali, SK, Pest, MA, Bryce, DM, Jeong JW, Beier F. Cartilage-Specific Overexpression of Mig-6 Accelerates Post-Traumatic Osteoarthritis in Mice. *(in preparation).*

4. Pest MA, Pest CA, **<u>Bellini MR</u>**, Beier F. Deletion of Dual Specificity Phosphatase 1 Does Not Predispose Mice to Increased Spontaneous Osteoarthritis. PLOS ONE.

Honours and Scholarships:

- **Science without Borders – Brazil (2015-2018):** Full Ph.D. Scholarship at the Western University. Period: 2015- 2018

- **Research Internships Abroad (BEPE).** Bauru School of Dentistry – University of Sao Paulo / Schulich School of Medicine & Dentistry (Western University, Canada). Period: 2012-2013.

- **Graduate Student Research, Scholarship from the Sao Paulo Research Foundation (FAPESP).** Brazil. Period: 2011 – 2013.

- **Undergraduate Student Research Scholarship, Scientific Initiation Program: Scholarship from the Sao Paulo Research Foundation (FAPESP).** Brazil. Period: 2009 – 2010.

Teaching and Supervision

- **Teaching Assistant –** Physiology 4530: Skeletal Physiology

- Jan. 2018 – April 2019 - Western University – Canada, London, Ont.
  - Training of one Undergraduate Honours Thesis Students, 2017-2018

Presentations at Scientific Meetings

2019   OARSI World Congress on Osteoarthritis, Toronto, Ontario, Canada

2018   Canadian Connective Tissue Society, Toronto, Ontario Canada

2018   3rd Biennial Canadian Bone and Joint Conference, London, Canada

2018   OARSI World Congress on Osteoarthritis, Liverpool, United Kingdom

2017   OARSI World Congress on Osteoarthritis, Las Vegas, NV, United States